2. Mathematical Model Analysis

2-1 Object and method of analysis

(1) Analysis objective

As different water volumes need to be distributed evenly and accurately to seven main canals by five regulators in the NDGRs, an analysis of flow conditions is conducted using a mathematical model to verify whether the NDGRs can demonstrate their necessary functions.

The concurrent operations of the gates, overflow and underflow, and the trends in sediment movement around the regulators are analyzed based on the results of the flow conditions analysis around the NDGRs. Then, the scouring and sedimentation phenomena upstream and downstream of the regulators are evaluated.

The analysis of the flow conditions around the NDGRs has two objectives, as described above:

1. In the flow analysis: the accurate recreation of the effects of mathematical flow conditions around the existing and new regulators and the changes in flow conditions due to multi-directional diversion.
2. In the riverbed variation analysis: A quasi three-dimension (Q3D) mathematical model shall be used in the flow condition analysis, taking into consideration the suspended sediment concentration and non-equilibrium of changes in water depth.

The results of the physical hydraulic model test conducted by HRI will be separately verified and reflected in the design. The same values of the physical hydraulic model test are applied-as far as possible-to the basic conditions for analyzing the topography, discharge, etc. in the flow analysis.

And, in the riverbed variation analysis, it was carried out using existing data. However, since sufficient accuracy has not been obtained to grasp the annual sediment volume, the result of the accuracy required for examining the countermeasure work has not been obtained. Here, it shows analysis results using existing data.

(2) Target of the analysis

The target of the analysis is the same area shown in the plane survey in Figure 2-1.1, including the DGRs and the NDGRs.

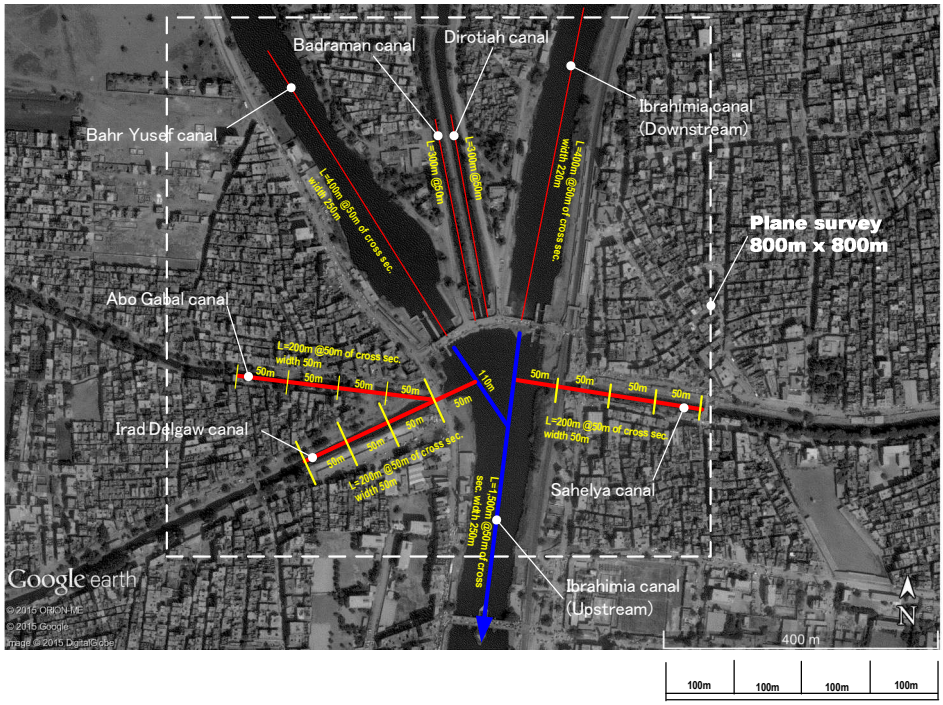

Figure 2-1.1 Scope of analysis

(3) Analysis method

a) Flow Analysis

1) Selection of applicable mathematical model

Mathematical hydraulic analysis of the NDGRs requires not only the evaluation of the flow in the downflow and transverse directions of the canal, but also the evaluation of the depth direction. For this reason, it is necessary to adopt either a Q3D (plane two-dimensional multilayer) calculation model or a three-dimensional calculation model.

As a result of comparing and reviewing the features of mathematical models, the Q3D calculation model was adopted for its ability to evaluate flow in the depth direction with the same accuracy as the three-dimensional calculation model, while requiring less input data and computation time than the three-dimensional calculation model.

Table 2-1.1 Comparison of mathematical models

Item	Q3D Model	3D Model	Remarks
1. Calculable items			
Flow velocity in downflow direction (u)	Available		
Flow velocity in transverse direction (v)	Available		
Flow velocity in depth direction (w)	Available		
2. No. of input data	Few (Good)	Many (Acceptable)	
3. Accuracy of calculation results	Almost the same		
4. Computation time (*)	1 (Good)	10 (Not good)	Relative ratio when computation time of quasi-3D model is taken as 1
5. Expression of results	Almost the same		
Overall evaluation	Excellent	Acceptable	

(*): Ottevanger, W, Uijttewaal, WSJ & Blanckaert, KJF (2012). Quasi-3D modelling of bed shear stresses at high curvature. In R Murillo Munoz (Ed.), River Flow 2012: Proceedings of the sixth edition of the international conference on fluvial hydraulics (pp. 775-782). London: Taylor & Francis Group.

2) Basic equations of analysis model

The Q3D model is a technique developed to obtain the same results as a three-dimensional model by applying approximate solutions in order to ease the computational load experienced in three-dimensional models.

The basic equations applied are described below in i-iv.

i) Features of analysis model

The features of the analysis model are shown in Table 2-1.2.

Table 2-1.2 Features of analysis model

Item	Features
Calculation variables	Flow velocity and water level are calculated
Calculation dimension	Water body is calculated in three dimensions
Hydrostatic approximation	As the water body is extensive in the horizontal direction and the vertical flow velocity is very small compared with the horizontal flow velocity, only hydrostatic pressure is taken into consideration
Viscosity and diffusion terms	Horizontal direction: SGS model is applied Vertical direction: Mellor & Yamada 2.5-order turbulence model is applied
Coordinate system	To fully reflect the complex and irregular topographical conditions, orthogonal curvilinear coordinate system is adopted in the horizontal direction, and σ-transformation is used to appropriately evaluate free water surface variation in the vertical direction.

ii) Basic equations

The basic equations are shown below. There are four equations in two types:

1. Continuity equation

$$\frac{\partial u}{\partial x}+\frac{\partial v}{\partial y}+\frac{\partial w}{\partial z}=0$$

2. Navier-Stokes (N-S) equations

$$\frac{\partial u}{\partial t}+u\frac{\partial u}{\partial x}+v\frac{\partial u}{\partial y}+w\frac{\partial u}{\partial z}-fv=-\frac{1}{\rho}\frac{\partial P}{\partial x}+\frac{\partial}{\partial x}\left(\upsilon_x\frac{\partial u}{\partial x}\right)+\frac{\partial}{\partial x}\left(\upsilon_y\frac{\partial u}{\partial y}\right)+\frac{\partial}{\partial x}\left(\upsilon_z\frac{\partial u}{\partial z}\right)$$

$$\frac{\partial v}{\partial t}+u\frac{\partial v}{\partial x}+v\frac{\partial v}{\partial y}+w\frac{\partial v}{\partial z}-fu=-\frac{1}{\rho}\frac{\partial P}{\partial x}+\frac{\partial}{\partial x}\left(\upsilon_x\frac{\partial v}{\partial x}\right)+\frac{\partial}{\partial x}\left(\upsilon_y\frac{\partial v}{\partial y}\right)+\frac{\partial}{\partial x}\left(\upsilon_z\frac{\partial v}{\partial z}\right)$$

$$\frac{\partial w}{\partial t}+u\frac{\partial w}{\partial x}+v\frac{\partial w}{\partial y}+w\frac{\partial w}{\partial z}=-\frac{1}{\rho}\frac{\partial P}{\partial x}+\frac{\partial}{\partial x}\left(\upsilon_x\frac{\partial w}{\partial x}\right)+\frac{\partial}{\partial x}\left(\upsilon_y\frac{\partial w}{\partial y}\right)+\frac{\partial}{\partial x}\left(\upsilon_z\frac{\partial w}{\partial z}\right)-g$$

Where,

u, v, w: Flow velocities (m/s) in x, y, z directions

P : Pressure (Pa)

g : Gravitational acceleration (m/s^2)

f : Coriolis parameter (rad/s)

υ_x, υ_y, υ_z : Turbulent eddy viscosity coefficient (m^2/s)

The turbulent eddy viscosity coefficient and eddy diffusion coefficient are given by the turbulence model described later.

iii) Coordinate system

The boundary-fitted orthogonal curvilinear coordinate system (Figure 2-1.2) is used for the horizontal coordinate system. σ-transformation is used (Figure 2-1.3) for the vertical coordinate system. The topography of curved river channels and coastlines can be expressed by orthogonal curvilinear coordinates. σ-transformation is a coordinate system where σ = 1 at the water surface and σ = 0 at the bottom. Expanding and contracting the vertical coordinates to suit the topography, enables complex topography to be expressed more naturally.

Conversion from Cartesian coordinates to σ-coordinates is defined by the following equation.

$$\sigma = \frac{z - \eta}{h + \eta}$$

Where,

x, y, z : Coordinates in the Cartesian coordinate system

$H \equiv h + \eta$

$h(x, y)$: Coordinates for the bottom

$\eta(x, y, z)$: Surface variation

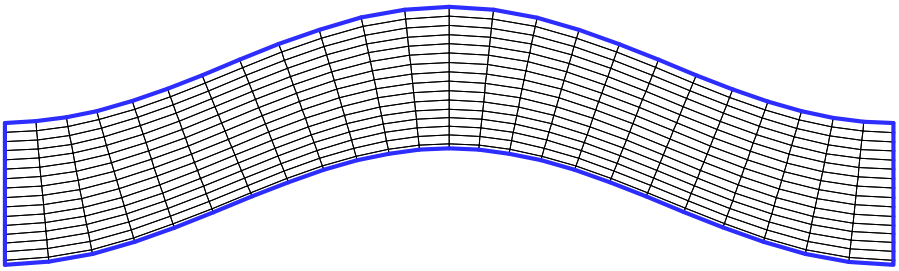

Figure 2-1.2 Orthogonal curvilinear coordinate system

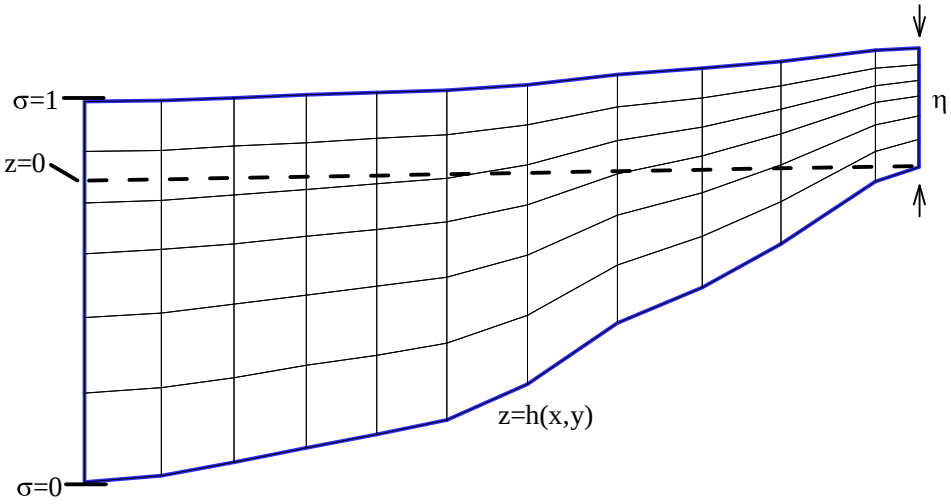

Figure 2-1.3 σ-coordinate system

iv) Turbulence model

The vertical turbulent eddy viscosity coefficient and vertical diffusion coefficient are obtained by the level 2.5 anisotropic second-order turbulence closure model. The stratification in the vertical direction and its effect on diffusion can be expressed in detail by the vertical turbulent eddy viscosity coefficient and vertical diffusion coefficient modeling.

3) Analysis conditions

i) Calculation meshes

Calculation meshes were created to appropriately express the shape of the distributing part and the regulator group.

The calculation mesh size in the longitudinal and transverse direction was set from 0.5m to 2.5m to enable detailed study of the flow fields especially around the newly constructed regulators.

To reduce the computational load, the calculation mesh size in the longitudinal direction was changed to between 2.5m and 10m for the upstream and downstream river channels.

As for the mesh division in the vertical direction, the channel was divided into five parts; from the deepest part to the water surface.

The meshes were deployed in line with the canal shape to recreate the Bahr Yusef, Ibrahimia, Abo Gabal, Irad Delgaw, and Sahelyia canals.

There are 218 meshes in total in the longitudinal direction x, 182 in the transverse direction x, and 5 in the vertical direction. These are 198,380 in total. The calculation mesh size of the entire area is roughly 4m in the longitudinal direction x, and 2.5m in the transverse direction.

The created calculation meshes are shown in Figure 2-1.4.

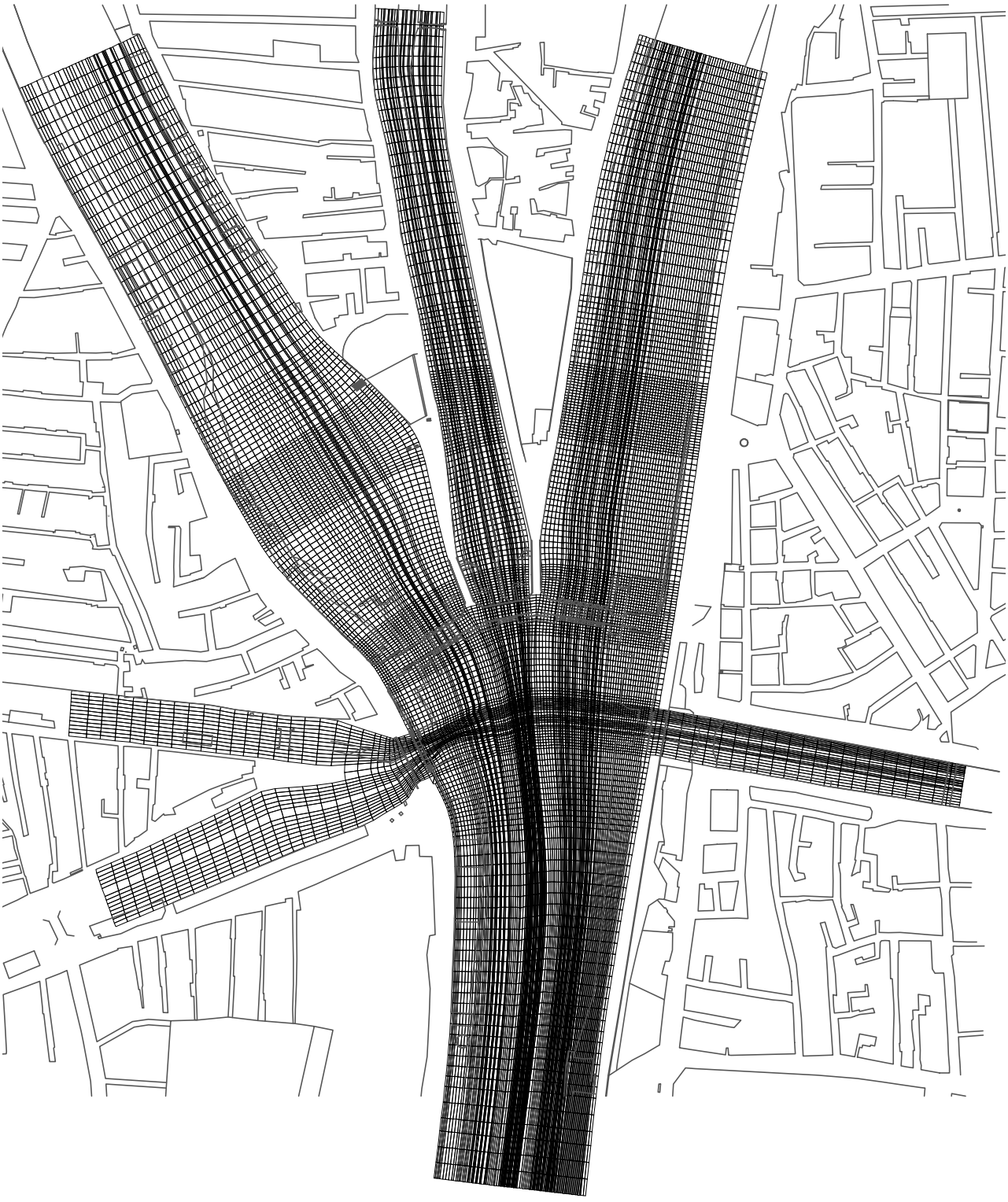

Figure 2-1.4 Canal meshes

ii) Topography

The following two topographies were used.

1. Topography surveyed in August 2015: The same calibration data as the physical hydraulic model test conducted by the HRI was used to verify the flow analysis.
2. Topography surveyed in January 2016: The topographic map after sediment removal was used in the design of the NDGRs and to evaluate the impact of constructing the regulators.

The created two-dimensional topographic plans are shown in Figure 2-1.5 and Figure 2-1.6.

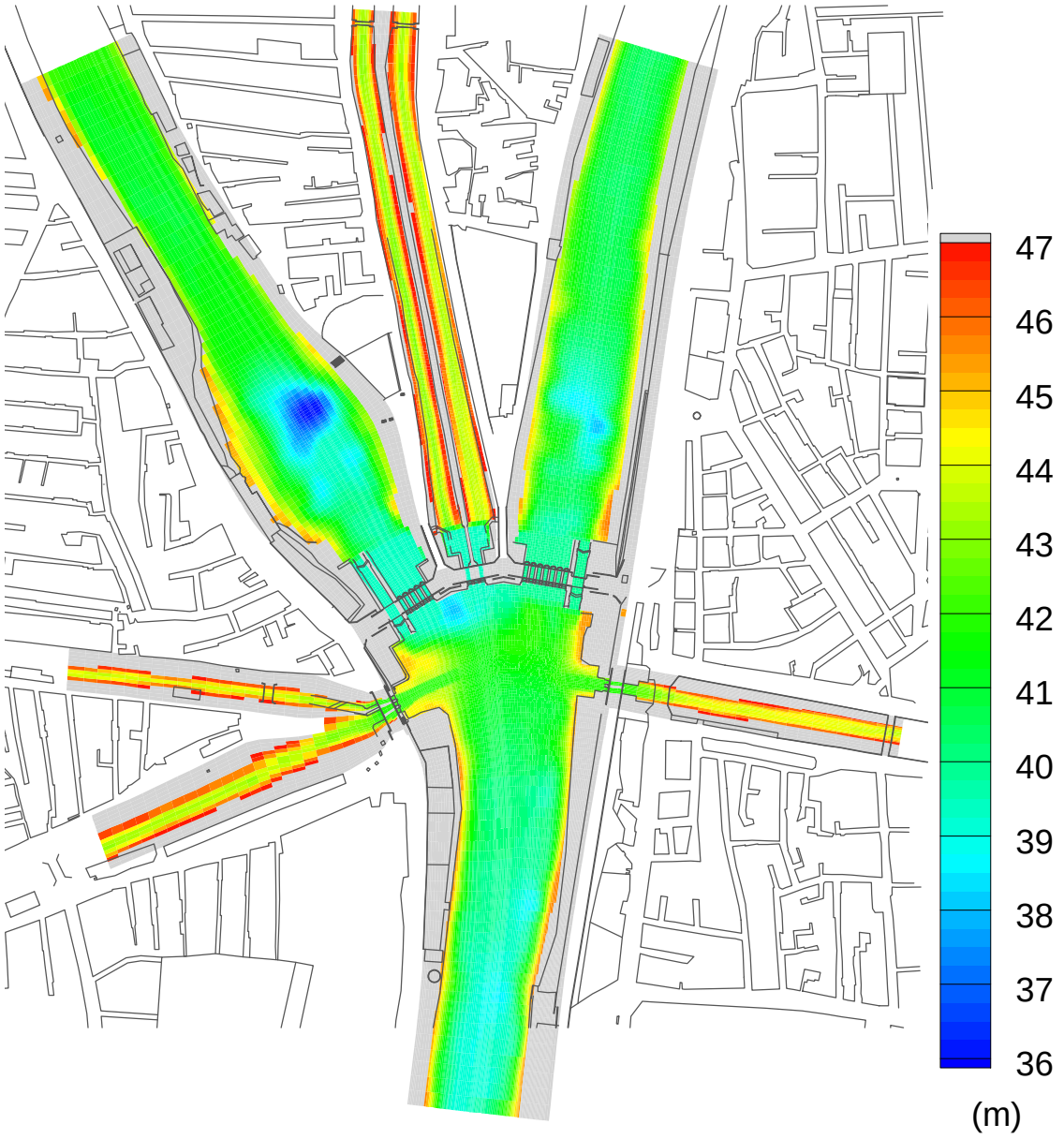

Figure 2-1.5 Contour map of canal bed (surveyed in August 2015)

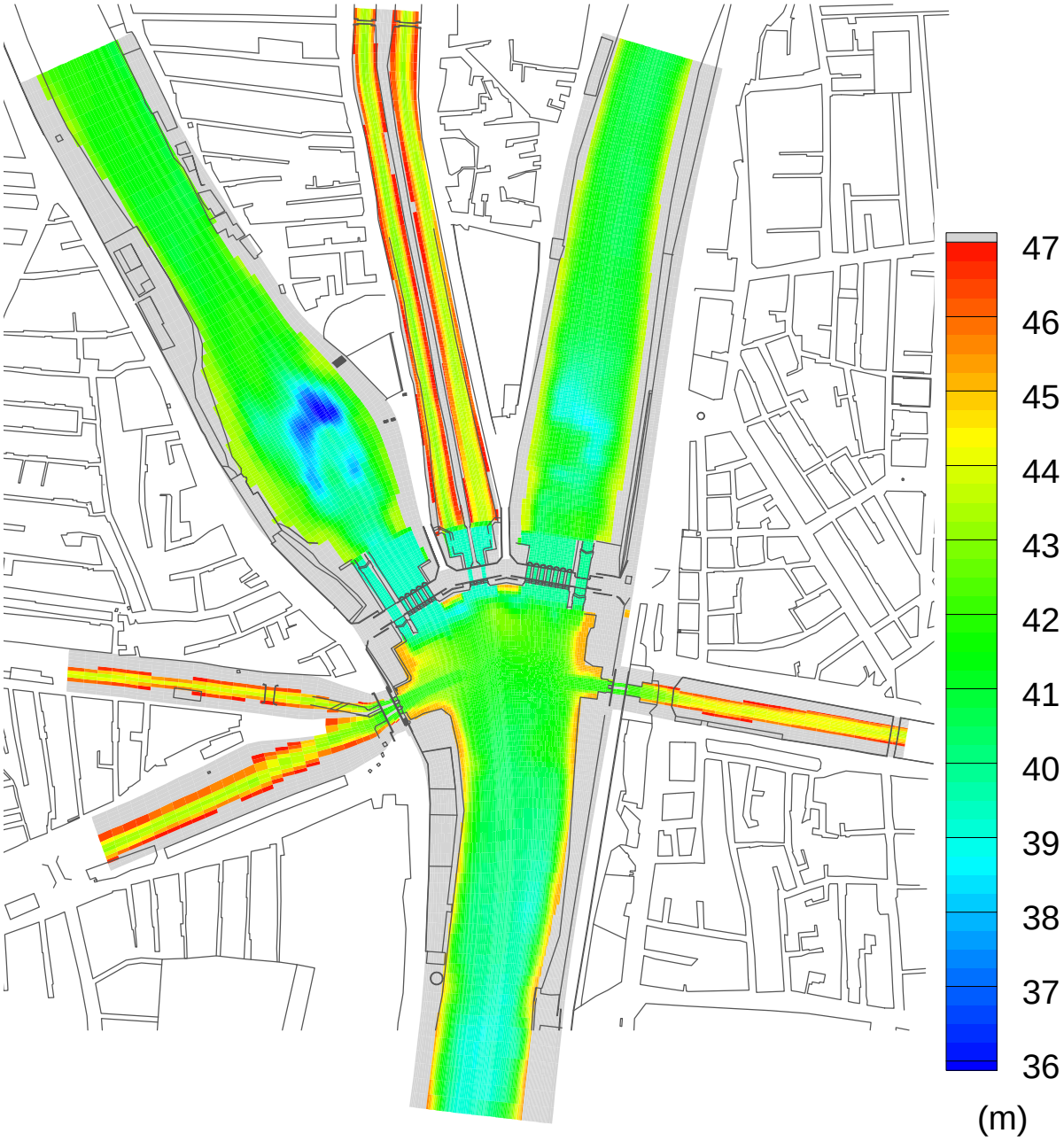

Figure 2-1.6 Contour map of canal bed (surveyed in January 2016)

Current dimensions of DGRs is shown in the following table.

Table 2-1.3 Current dimensions of DGRs

Name of canal at DGR		Structural dimensions		Gate dimensions
Downstream side of DGR	Bahr Yusef	No. of gate Pier Mid. apron Foundation Lock	5 vents 4 units & width 1.80~2.25m L=43.25m, thickness 3m limestone partially concrete width 8.5m	3m width x 5 vents Total height 7.5m 3 leaves of gate Bottom elevation 39.50m Operational high water level 46.00m
	Ibrahimia	No. of gate Pier Mid. apron Foundation Lock	7 vents 6 units & width 1.80~2.25m L=39.70m, thickness 3m limestone partially concrete width 8.5m	3m wide x 7 vents Total height 7.5m 3 leaves of gate Bottom elevation 39.81m Operational high water level 46.00m
	Badraman & Dirotiah	No. of gate Pier Mid. apron Foundation	2 vents (1 vent closed) 2 units & width 1.80~2.25m L=38.65m, limestone, t=unknown	3m wide x 2 vents total height 7.5m 3 leaves of gate Bottom elevation 39.30 m Operational high water level 46.00m
Upstream side of DGR	Abo Gabal & Irad Delgaw (left bank)	No. of gate Pier Mid. apron Foundation	3 vents 2 units & width 1.80~2.25m L=28.60m limestone, t=unknown	3m wide x 3 vents Total height 5.5m 1 leaves of gate Bottom elevation 42.00 m Operational high water level 46.00m
	Sahelyia (right bank)	No. of gate Pier Mid. apron Foundation	2 vents 1 unit & width 1.80~2.25m L=18.90m, Limestone, t=unknown	3m wide x 2 vents Total height 5.5m 1 leaves of gate Bottom elevation 41.80 m Operational high water level 46.00m

iii) Outflow from regulators

The outflow from the DGRs was adjusted so that the measured water level and outflow matched the water level and diversion discharge of the analysis model for each canal. The adjustments were based on values calculated by the following overflow discharge equation, which itself was applied to the physical hydraulic model test conducted by the HRI.

$$Q = \frac{2}{3} C_1 \sqrt{2g} B (H_1^{3/2} - H_2^{3/2})$$

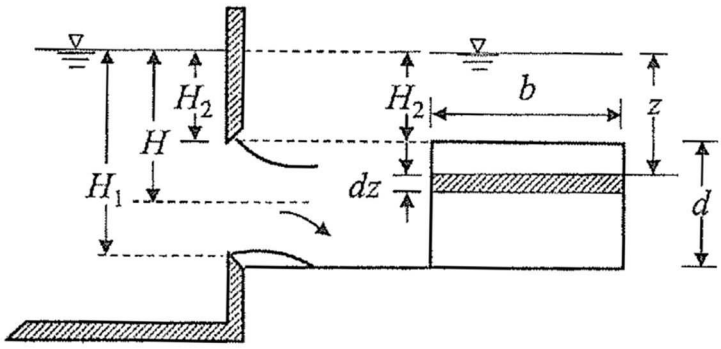

Where,

Q = Outflow (m^3/s)

C = Flow coefficient = 0.64

B = Regulator width (m)

g = Gravitational acceleration 9.8 (m^2/s)

H_1 H_2 = Water depth at the upstream and downstream of the orifice (m)

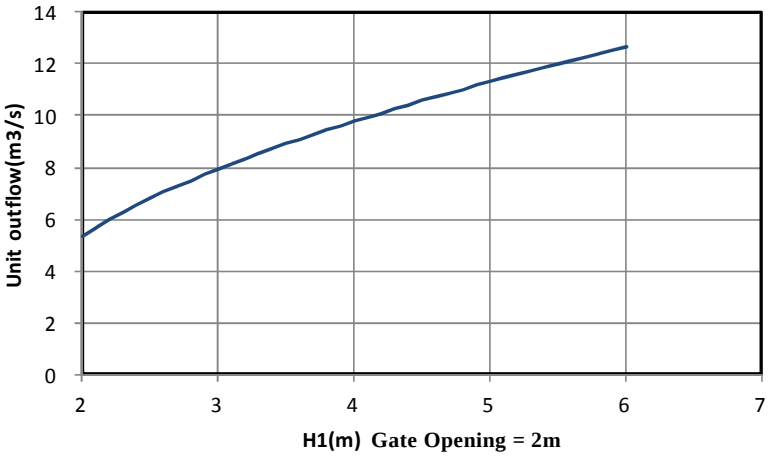

Figure 2-1.7 Rating curve of DGRs

The outflow from the NDGRs was adjusted so that the specified water level and outflow matched the water level and outflow of the analysis model for each canal. The adjustments were based on overflow values calculated by the overflow equation and underflow values calculated by the orifice equation.

Overflow equation

$Q=C*B*H^{3/2}$

Where:

Q = Outflow (m^3/s)

C = Flow coefficient

B = Regulator width (m)

H = the head over the gate (m)

Orifice equation (Underflow equation)

$$Q=\frac{2}{3}C_1\sqrt{2g}B(H_1^{3/2}-H_2^{3/2})$$

Where:

Q = Outflow (m^3/s)

C = Flow coefficient

B = Regulator width (m)

g = Gravitational acceleration 9.8 (m^2/s)

H_1 H_2 = Water depth at the upstream and downstream of the orifice (m)

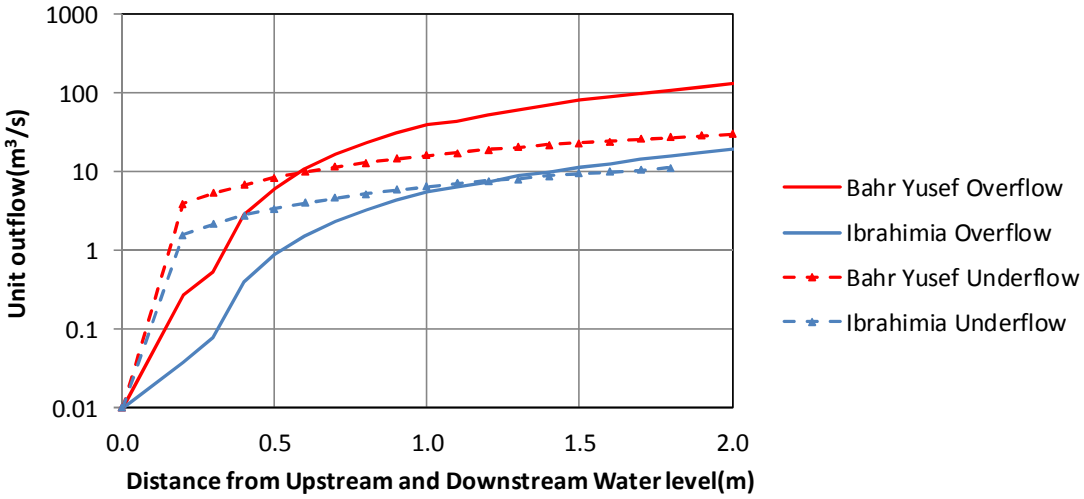

Figure 2-1.8 Rating curves of NDGRs (large regulators)

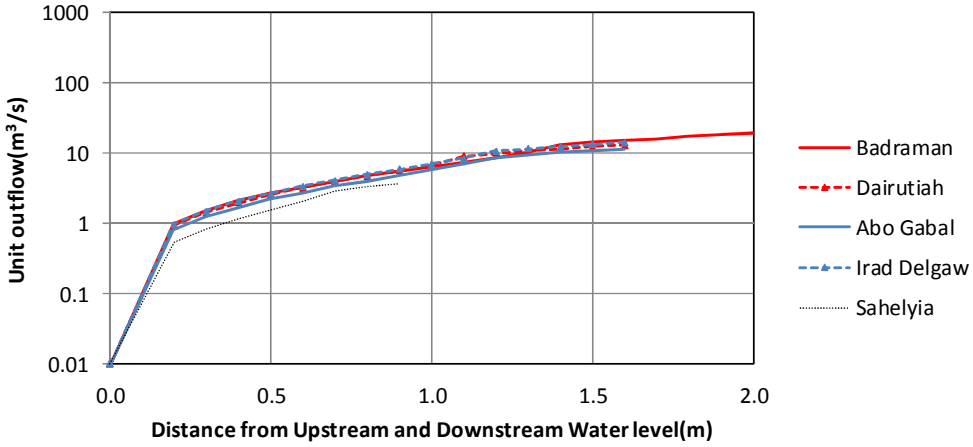

Figure 2-1.9 Rating curves of NDGRs (small regulators)

4) Boundary conditions

The outflow boundary at the upstream end of the Ibrahimia canal and the downstream ends of each of the canals were taken to be the water level boundaries.

5) Analysis cases

As shown in Table 2-1.4, the case analysis occurs in three stages: calibration, present state analysis, and planning.

1. At the calibration stage, the same topography, water level, and outflow values are measured against the results of the physical hydraulic model test conducted by the HRI.
2. Since the latest topographic data is applied to the design of the regulators in the present state and planning stages, the latest topographic data is applied to flow analysis.
3. At the planning stage, the gate discharge systems are analyzed to compare the differences in flow conditions at overflow and underflow.

The measured values (water level and discharge) obtained from the HRI (HRI surveyed and confirmed this data on 30th June 2015) are used for the model calibration. The design discharge is used at the present state and planning stages.

Table 2-1.4 Analysis cases

Analysis Case	Analysis Stage	Riverbed Condition	Facilities	Outflow(m^3/s)		Remarks
				Measured 355m^3/s	Design 455m^3/s	
Calibration	Calibration Stage	(1)	Existing (DGRs)	○		The same values as HRI are used for the water level and outflow.
Pesent State	Present state stage	(2)	Existing (DGRs)		○	
Planning 1	Planning stage	(2)	New Regulators (NDGRs) Gate:UnderFlow		○	
Planning 2			New Regulators (NDGRs) Gate:OverFlow		○	
Remarks	Reverbed Condition (survey data) (1):Aug,2015(HRI),(2):Jan,2016(D/D,HRI)(After Dredging)					

6) Water level, outflow, and gate opening by analysis case

The water level and outflow by analysis case are shown in Table 2-1.5, and the gate openings of calibration stage are shown in Table 2-1.6 and Figure 2-1.10.

Table 2-1.5 Water level and outflow by analysis case

Case	Outflow Condition	Upstream of Regulators		Downstream of Regulators						
		Ibrahimia		Bahr Yusef	Ibrahimia	Badraman	Dairutiah	Abo Gabal	Irad Delgaw	Saheleya
		Outflow (m^3/s)	Water Level (m)	Water Level (m)						
Calibration Stage	Calibration Outflow	355	46.02	45.82	45.05	45.68	45.88	45.73	44.79	45.72
Present State Stage	Design Outflow	455	46.30	45.82	45.13	45.90	45.90	45.90	45.90	45.90
Planning Stage	Desig Outflow	455	46.30	45.82	45.13	45.90	45.90	45.90	45.90	45.90

Table 2-1.6 Gate opening of calibration stage

Regulator		Gate Opening (m)							
		Gate Position	1	2	3	4	5	6	7
Bahr Yusef		Upper	N/A	N/A	N/A	N/A	N/A		
		Middle	2.25	2.25	2.25	2.25	2.25		
		Lower	0	0	0	0	0		
Ibrahimia		Upper	N/A	N/A	N/A	N/A	N/A	N/A	N/A
		Middle	2.00	2.00	2.00	2.00	2.00	2.00	2.00
		Lower	0	0	0	0	0	0	0
Badraman	Badraman	Upper	N/A						
		Middle	1.30						
		Lower	0						
	Dairutiah	Upper	N/A						
		Middle	0.875						
		Lower	0						
Abo Gabal	Abo Gabal		0.625						
	Irad Delgaw		0.15	0.15					
Sahelyia			0.10	0.10					

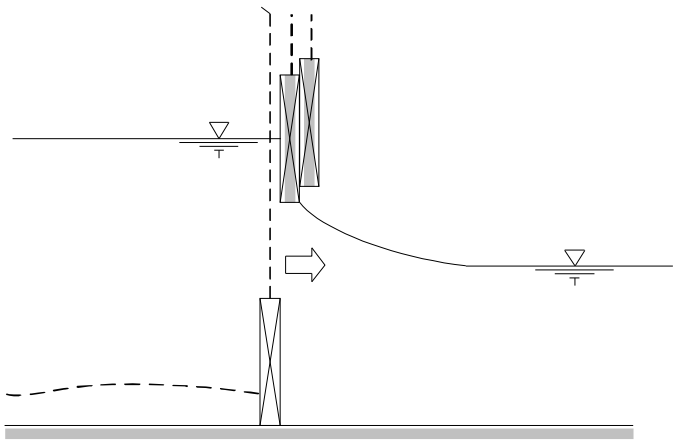

Figure 2-1.10 Gate opening at calibration stage at Bahr Yusef and Ibrahimia regulators

b) Riverbed variation analysis

1) Outline of riverbed variation analysis

As shown in Figure 2-1.11, riverbed variation analysis of the NDGRs is broadly divided into:

1. Flow calculation,
2. Calculation of riverbed variation and grain size distribution.

The mathematical hydraulic analysis model is applied to flow calculation.

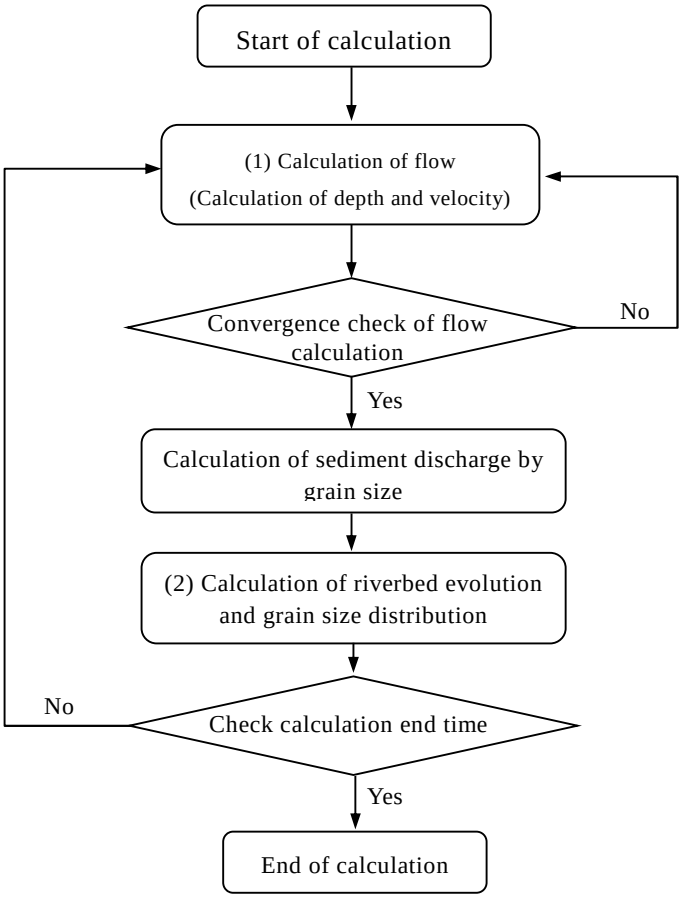

Figure 2-1.11 Calculation flow of riverbed variation analysis

2) Basic equations of riverbed variation analysis

The basic equations for riverbed variation analysis, and those for calculating riverbed variation and grain size distribution, are described below in i-iii.

i) Calculation of riverbed variation

Riverbed variation is calculated using the equation below.

Bed load transport rate is calculated by the local change in bed load caused by the change in bed flow and also by the difference in suspended and settled bed material. The value of suspended bed material is calculated by solving the advection-diffusion equation shown later.

$$\frac{\partial z_b}{\partial t} = \frac{-1}{(1-\lambda)} \sum_k \left\{ \frac{\partial q_{bxk}}{\partial x} + \frac{\partial q_{byk}}{\partial y} + (E_{sk} - D_{sk}) \right\} \tag{1-1}$$

Where,

z_b : Elevation of riverbed

q_{bxk} : Bed load discharge of grain size k per unit width of x direction

q_{byk} : Bed load discharge of grain size k per unit width of y direction

E_{sk}, D_{sk} : Rising and falling fluxes of the suspended load with grain size k

ii) Calculation of grain size distribution

The content of bed material at each grain size in the riverbed surface (transition layer) changes with riverbed fluctuations. It is calculated using the following equation.

$$\frac{\partial P_{bk}}{\partial t} - \frac{1}{E_m}\frac{\partial z_{bk}}{\partial t} + \frac{1}{E_m}\frac{\partial z_b}{\partial t}(\eta P_{bk} + (1-\eta)P_{bko}) = 0 \tag{2-2}$$

Where,

λ : Porosity of the bed material

P_{bk} : Percentage of D_k the grain in transition layer (also called the mixed layer)

P_{bko} : Percentage of D_k the grain in the bottom layer of the transition layer

E_m : Thickness of the transition layer

η : Identification factor with η = 0 in the case of erosion, η = 1 in the case of deposition, as shown in the following.

$$\eta = \begin{cases} 1 & \partial z_b / \partial t > 0 \\ 0 & \partial z_b / \partial t < 0 \end{cases} \tag{2-3}$$

The configuration of the riverbed is shown below in Figure 2-1.12. It is vertically divided into

a number of layers from the reference plane z_o to the riverbed surface z_b. The top layer is a mixed layer with thickness E_m. The layer immediately below that is a transition layer with thickness E_t. The other layers are 'deposited layers,' all with the same thickness E_d.

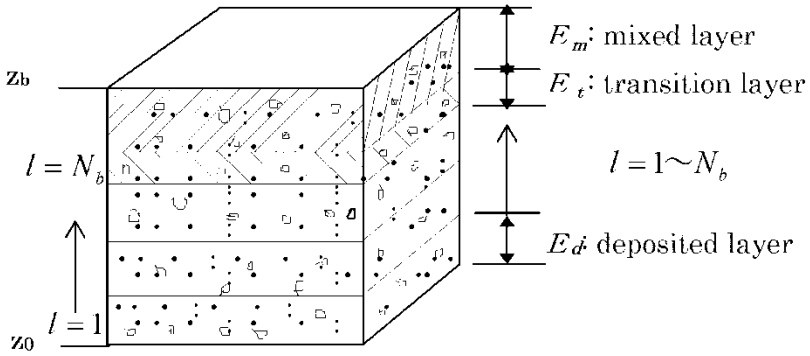

Figure 2-1.12 Riverbed formation

iii) Advection-diffusion equation

The advection-diffusion equation is shown below.

[Advection-diffusion equation: Suspended sediment concentration]

$$\frac{\partial C}{\partial t}+\frac{\partial uC}{\partial x}+\frac{\partial vC}{\partial y}+\frac{\partial wC}{\partial z}=$$
$$\frac{\partial}{\partial x}(D_{Ch}\frac{\partial C}{\partial x})+\frac{\partial}{\partial y}(D_{Ch}\frac{\partial C}{\partial y})+\frac{\partial}{\partial z}(D_{Cz}\frac{\partial C}{\partial z})$$

Where,

C : Suspended sediment concentration (by grain size)

u, v, w : x, y, z-direction flow velocities

D_{Ch}, D_{Cz} : Effective (molecule + eddy) diffusion coefficient of water quality in horizontal and vertical directions

3) Analysis conditions

i) Mesh sizes

The mesh sizes are the same as those in the flow analysis.

ii) Computation period, water level, and discharge

Taking the riverbed in January 2016 to be the initial riverbed for calibration, calculations are made in November 2016, after 11 months of deposition. The riverbed surveyed in November 2015 is assumed to correspond to the riverbed after deposition in November 2016, and the calculation results are verified against the deposition and erosion trends in the surveyed riverbed from November 2015 to November 2016. Analysis of the water level and discharge is

conducted using the average monthly values calculated from the measured values.

The actual discharges and water levels of the Bahr Yusef canal and the Ibrahimia canal for this period, were available. As Badraman, Diroutiah, Abo Gabal, Irad Delgaw, and Sahelyia canals are not monitored and the information unavailable, the discharge of each canal was computed using a percentage of the discharge and planned discharge of the Bahr Yusef and Ibrahimia canals mentioned above. The water level at the downstream end of each canal was given by the H-Q (Height-Discharge) relationship. The discharge is shown in Table 2-1.7 and Figure 2-1.13, and the water level is shown in Table 2-1.8 and Figure 2-1.14.

Taking the riverbed in January 2016 to be the initial riverbed for the calculation of predicted water levels and discharge, analysis was conducted with the given typical flow conditions for one year.

The average monthly discharge for 16 years from 1999 to 2014 was calculated to give the inflow, which was then distributed in proportion to the planned discharge. The discharge was calculated at the downstream end of each canal, and the water level at the downstream end of each canal was given by the H-Q relationship. The discharge is shown in Table 2-1.9 and Figure 2-1.15, and the water level is shown in Table 2-1.10 and Figure 2-1.16.

Table 2-1.7 Discharge used for calibration (January-November 2015)

Discharge(m^3/s)	Jan	Feb	Mar	Apr	May	June	July	Aug	Sep	Oct	Nov
Ibrahimia canal U/S	150.8	277.4	314.4	320.4	358.6	396.0	399.7	395.2	317.3	308.3	275.4
Bahr-Yusef canal	81.9	148.4	171.5	164.5	188.3	200.3	201.2	202.3	164.8	165.4	140.4
Ibrahimia canal D/S	52.6	99.1	109.0	121.4	131.6	153.0	155.4	150.3	118.3	109.7	105.3
Badraman canal	3.4	6.3	7.2	7.3	8.2	9.0	9.1	9.0	7.2	7.0	6.3
Diroutiah canal	4.6	8.4	9.6	9.8	10.9	12.1	12.2	12.0	9.7	9.4	8.4
Abo Gabal canal	2.7	4.9	5.6	5.7	6.4	7.1	7.1	7.1	5.7	5.5	4.9
Irad Delgaw canal	3.5	6.5	7.4	7.5	8.4	9.3	9.4	9.3	7.4	7.2	6.5
Saheleya canal	2.0	3.7	4.2	4.3	4.8	5.3	5.3	5.3	4.2	4.1	3.7

Table 2-1.8 Water level used for calibration (January-November 2015)

D/S Water level(m)	Jan	Feb	Mar	Apr	May	June	July	Aug	Sep	Oct	Nov
Ibrahimia canal U/S	44.2	45.5	45.7	45.7	45.8	46.0	46.0	46.0	45.7	45.6	45.6
Bahr-Yusef canal	42.2	44.9	45.3	45.2	45.6	45.8	45.8	45.8	45.2	45.2	44.7
Ibrahimia canal D/S	43.0	44.1	44.2	44.4	44.6	45.0	45.0	44.9	44.4	44.2	44.2
Badraman canal	44.1	45.5	45.5	45.5	45.6	45.6	45.7	45.7	45.5	45.4	45.5
Diroutiah canal	44.1	45.2	45.5	45.5	45.6	45.8	45.7	45.8	45.5	45.4	45.5
Abo Gabal canal	44.1	45.3	45.4	45.5	45.6	45.7	45.7	45.7	45.5	45.5	45.6
Irad Delgaw canal	44.1	44.6	44.6	44.7	44.7	44.8	44.8	44.7	44.6	44.5	44.6
Saheleya canal	44.1	45.4	45.6	45.5	45.6	45.8	45.7	45.8	45.5	45.5	45.6

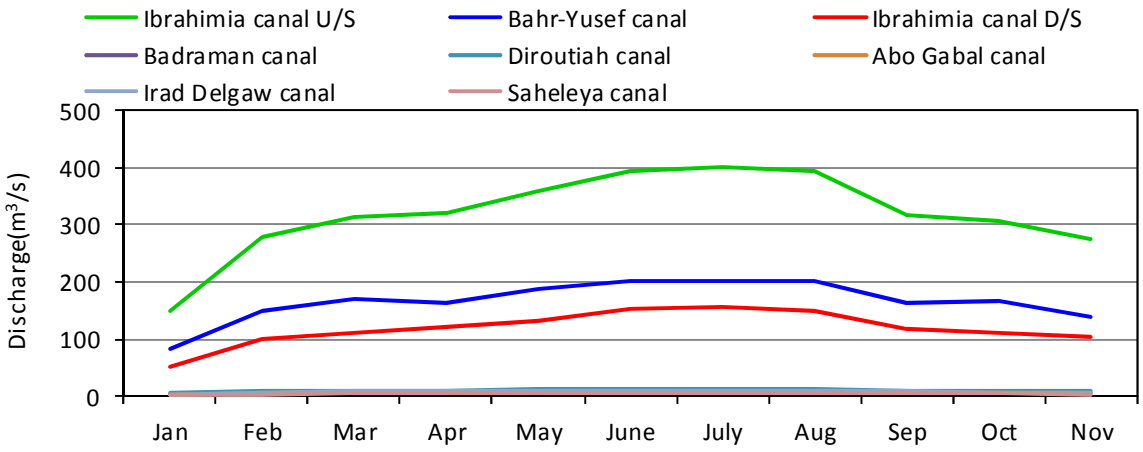

Figure 2-1.13 Discharge used for calibration (January-November 2015)

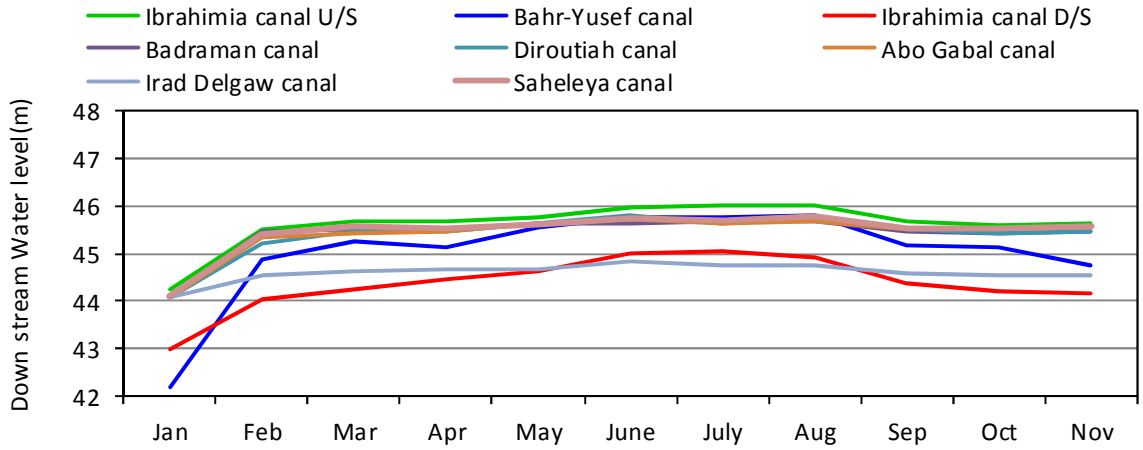

Figure 2-1.14 Water levels used for calibration (January-November 2015)

Table 2-1.9 Monthly discharge (predicted based on average monthly values from 1999 to 2014)

Discharge(m^3/s)	Jan	Feb	Mar	Apr	May	June	July	Aug	Sep	Oct	Nov	Dec
Ibrahimia canal U/S	111.0	286.9	323.9	339.6	345.2	411.3	418.1	414.7	340.7	316.1	285.8	226.4
Bahr-Yusef canal	51.0	141.0	164.0	167.0	171.0	203.0	206.0	206.0	166.0	150.0	139.0	103.0
Ibrahimia canal D/S	48.0	115.0	125.0	136.0	137.0	164.0	167.0	164.0	138.0	132.0	116.0	99.0
Badraman canal	2.5	6.5	7.4	7.7	7.9	9.4	9.5	9.4	7.7	7.2	6.5	5.1
Diroutiah canal	3.4	8.7	9.9	10.3	10.5	12.5	12.7	12.6	10.4	9.6	8.7	6.9
Abo Gabal canal	2.0	5.1	5.8	6.1	6.2	7.3	7.5	7.4	6.1	5.6	5.1	4.0
Irad Delgaw canal	2.6	6.7	7.6	8.0	8.1	9.6	9.8	9.7	8.0	7.4	6.7	5.3
Saheleya canal	1.5	3.8	4.3	4.5	4.6	5.5	5.6	5.5	4.5	4.2	3.8	3.0

Table 2-1.10 Monthly water level (calculated from Table 2-1.9)

D/S Water level(m)	Jan	Feb	Mar	Apr	May	June	July	Aug	Sep	Oct	Nov	Dec
Ibrahimia canal U/S	44.5	45.8	45.8	45.8	45.9	45.9	45.9	45.9	45.9	46.0	45.8	45.7
Bahr-Yusef canal	43.0	44.7	45.0	45.1	45.1	45.6	45.6	45.6	45.1	44.8	44.7	44.1
Ibrahimia canal D/S	42.7	44.2	44.4	44.5	44.6	44.9	45.0	44.9	44.6	44.6	44.2	44.0
Badraman canal	44.4	45.4	45.5	45.6	45.6	45.7	45.7	45.7	45.6	45.5	45.4	45.2
Diroutiah canal	44.3	45.4	45.6	45.6	45.6	45.7	45.7	45.7	45.6	45.5	45.4	45.1
Abo Gabal canal	43.9	44.8	44.9	45.0	45.0	45.2	45.2	45.2	45.0	44.9	44.8	44.5
Irad Delgaw canal	43.9	44.6	44.7	44.7	44.7	44.8	44.8	44.8	44.7	44.6	44.6	44.4
Saheleya canal	44.2	45.4	45.5	45.6	45.6	45.8	45.9	45.9	45.6	45.5	45.4	45.0

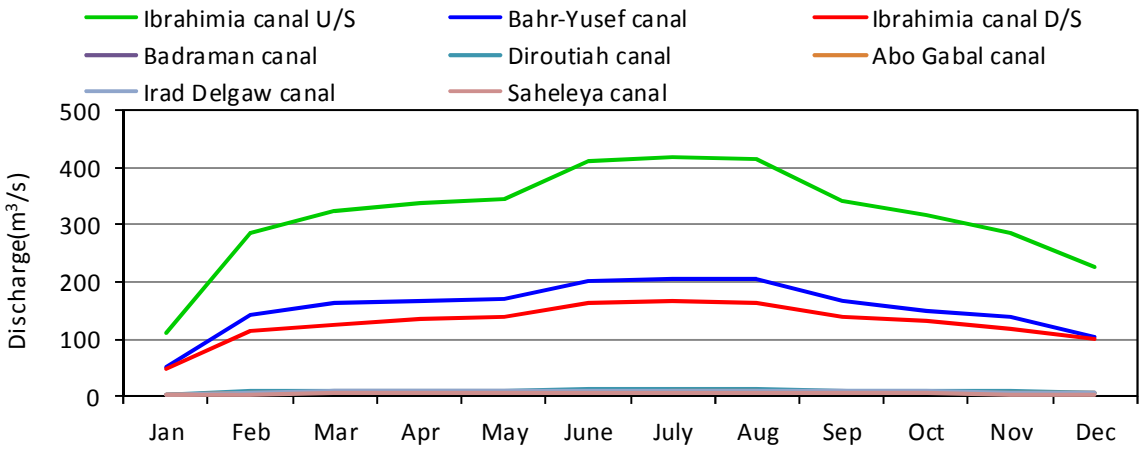

Figure 2-1.15 Calibrated monthly discharge (predicted based on average monthly values from 1999 to 2014)

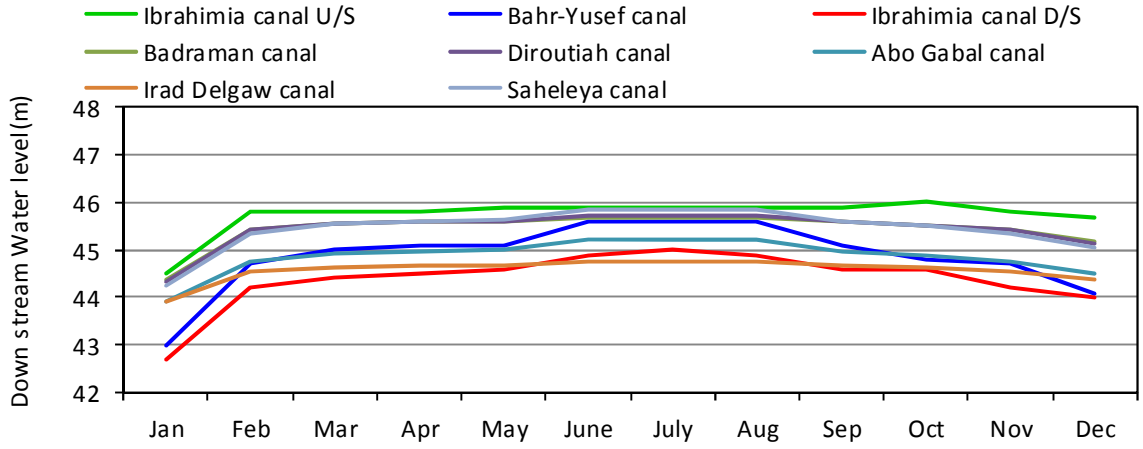

Figure 2-1.16 Calibrated monthly water level (calculated from Table 2-1.9)

iii) Grain size distribution of riverbed material

Out of all the riverbed material study results in the progress report on the physical hydraulic model test conducted by the HRI shown in Table 2-1.11 and Figure 2-1.17, the riverbed material data for the upper reaches of Ibrahimia canal was used. The results of HRI's riverbed material study were reflected in the calculations, and two representative particle diameters shown in Table 2-1.12 were set. The same materials were set for the whole calculated area in this analysis.

Table 2-1.11 Results of riverbed material study

Ibrahimia U/S		Ibrahimia D/S		Bahr-Yusef	
Diameter (mm)	Finer Weight(%)	Diameter (mm)	Finer Weight(%)	Diameter (mm)	Finer Weight(%)
1.4	97.6	1.4	41.1	1.4	97.9
1	97.3	1	41.0	1	97.5
0.85	97.0	0.85	40.9	0.85	97.0
0.5	92.1	0.5	40.6	0.5	89.6
0.355	64.8	0.355	39.3	0.355	70.9
0.212	0.4	0.212	5.4	0.212	1.7
0.15	0.2	0.15	1.8	0.15	0.3
0.075	0.1	0.075	0.2	0.075	0.1
0.063	0.1	0.063	0.1	0.063	0.1
0.01	0.0	0.001	0.0	0.001	0.0

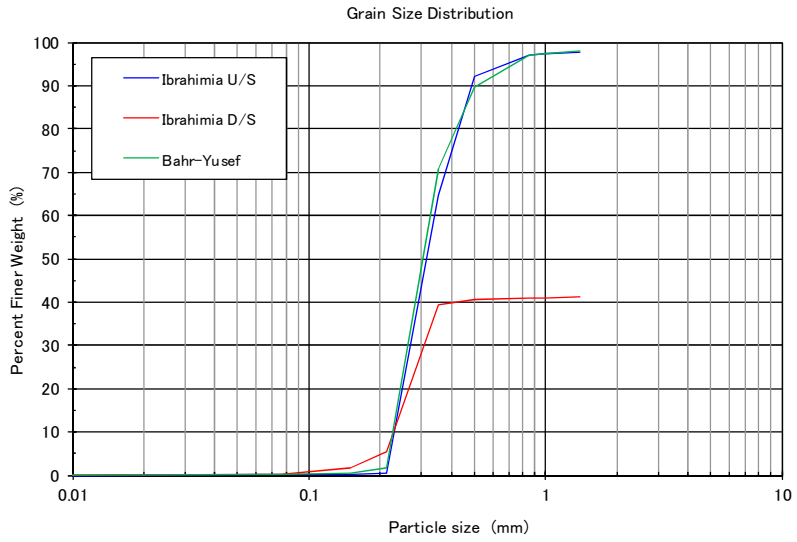

Figure 2-1.17 Grain size distribution of riverbed material

Table 2-1.12 Representative particle diameter and content rate in calculations

Representative particle diameter	Content rate
(mm)	(%)
0.6	34.1
0.25	65.6

iv) Bed load formula

The bed load discharges are computed using the following formula developed by Ashida and Michiue.

For the calculation of q_{bxk} sediment discharge per unit width in the x direction, and q_{byk} sediment discharge per unit width in the y direction, first q_{bk} bed load sediment per unit width is calculated using the Ashida-Michiue formula (2-4).

Next, sediment discharge is distributed in the x and y directions by flow velocity distribution on the bed surface, and q_{bxk} and q_{byk} are obtained.

Ashida-Michiue formula:

$$\frac{q_{bk}}{\sqrt{sgd_k^3}} = 17 p_{bk} \tau_{*ek}^{3/2} \left(1 - \frac{\tau_{*ck}}{\tau_{*k}}\right)\left(1 - \sqrt{\frac{\tau_{*ck}}{\tau_{*k}}}\right) \tag{2-4}$$

v) Suspended load formula

Suspended load is divided into rising flux and falling flux, and each is calculated as shown below using the suspended load formula.

◆Rising flux E_{sk}

Rising flux E_{sk} of D_k th grain is calculated as follows.

$$E_{sk} = W_{sk} C_{ek} \tag{2-5}$$

Where,

W_{sk}: Settling velocity of d_k th grain

C_{ek}: Concentration of D_k th grain at an equilibrium datum plane

C_{ek} Is obtained from the Ashida-Michiue equilibrium datum plane concentration formula as follows:

$$C_{ek} = 0.025 P_{bk} \left[\frac{g(\xi_0)}{\xi_0} - G(\xi_0)\right] \tag{2-6}$$

$$g(\xi_0) = \frac{1}{\sqrt{2\pi}} \exp\left(-\frac{1}{2}\xi_0^2\right) \tag{2-7}$$

$$G(\xi_0) = \frac{1}{\sqrt{2\pi}} \int_{\xi_0}^{\infty} \exp\left(-\frac{1}{2}\xi^2\right) d\xi \tag{2-8}$$

$$\xi_0 = \frac{W_{sk}}{0.75 u_*} \tag{2-9}$$

Where,

P_{bk}: Percentage of D_k th grain in the transition layer

u_*: Shear velocity

◆Falling flux D_{sk}

Falling flux D_{sk} of D_k th grain is calculated as follows.

$$D_{sk} = W_{sk} C_{ak} \tag{1-10}$$

Where,

C_{ak} : Sediment concentration of D_k th grain on the riverbed

Sediment concentration C_k of each grain size is obtained from the advection-diffusion equation.

vi) Boundary conditions

The bed load and suspended load are given together with the inflow from the upstream end of Ibrahimia canal.

The amount of sand from the upstream end is given the equilibrium sand feed based on bed slope.

The suspended load according to the flow is given by the C-Q formula shown below. Coefficient α and coefficient β are based on general values in *Hydraulics Formulae 1999* (edited by the Japan Society of Civil Engineers) and highly reproducible values for riverbed variation were set by the calibration calculations.

A= 1.5×10^{-7}, β= 2 were set in this analysis.

$$Q_{\sin} = \alpha Q^{\beta} \tag{1-11}$$

Where, Q_{sin}: Inflowing sediment (m^3/s)

Q: Discharge (m^3/s)

α: Coefficient ($4 \times 10^{-8} – 6 \times 10^{-6}$)

β: Coefficient

4) Analysis case

The analysis case is shown in Table 2-1.13. Riverbed variation calibration shows that it is possible to reproduce and evaluate trends in the riverbed variation of existing river channels. This is achieved by taking the riverbed surveyed in January 2016 after sediment removal as the initial riverbed, and reproducing the riverbed surveyed in November 2015 before sediment removal. Figure 2-1.18 shows the contour diagram of riverbed variations before and after sediment removal.

The typical flow for one year is applied to the constructed model and a prediction calculation of current (existing regulators) and planned (after construction of new regulators) riverbed variation is made. Places where there is significant deposition or corrosion around the regulators are identified from the results, and used as reference points for canal improvement projects,

including new regulators.

Table 2-1.13 Calculation case (riverbed variation analysis)

Case	Analysis Content	Riverbed	Facilities	Discharge
Riverbed variation calibration	Calibration	Initial: (2) Calibration object: (1)	Existing	11 months
Present state of riverbed variation	Present state	Initial: (2)	Existing	1 year
Riverbed variation planning	Plans	Initial: (2)	Planned overflow	1 year
Remarks	Riverbed conditions (1): Surveyed in Nov. 2015 (before sediment removal) (2): Surveyed in Jan. 2016 (after sediment removal)			

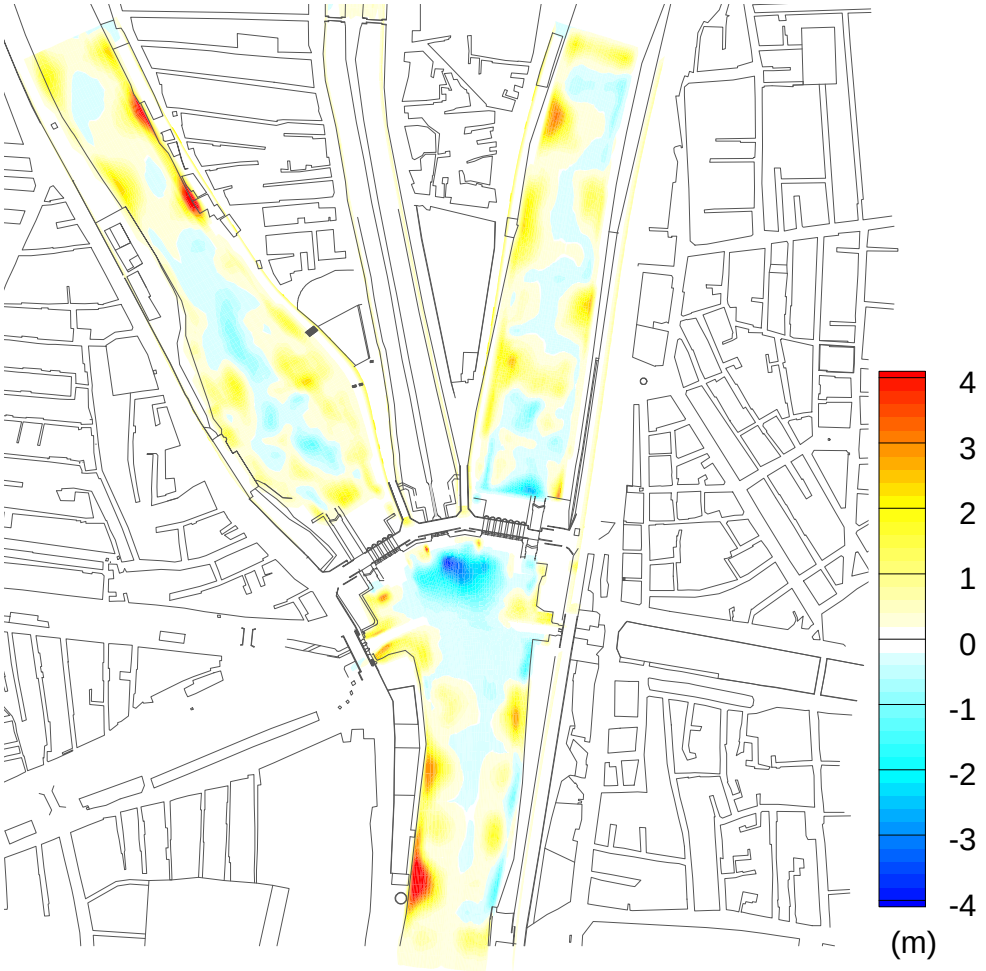

Figure 2-1.18 Change in bed elevation between Nov. 2015 and Jan. 2016

2-2 Evaluation of analysis results

(1) Flow analysis

a) Analysis results

1) Calibration

i) Discharge

Figure 2-2.1 shows the locations of the flow velocity observation points, and Table 2-2.1 and Figure 2-2.2 show flow discharge and cross-sectional average water levels at flow velocity observation points. The calculated flow discharge of the seven canals' regulators can reproduce the actual measured flow quite well.

ii) Average velocity

The average flow velocity at the flow velocity observation point is shown in Table 2-2.2 and Figure 2-2.3. The calculated average flow velocity indicates high reproducibility in all seven canals when compared with the measured average flow velocity.

iii) Cross-sectional velocity

The cross-sectional flow rate results are shown in Figures 2-2.4 to 2-2.10.
According to these, the calculated cross section flow velocity can reproduce the measured cross sectional flow velocity well.

iv) Velocity and vector map

Figure 2-2.11 to 2-2.12 are contour plots showing the flow velocity in color. Figure 2-2.13 is a diagram comparing the downstream of the Bahr Yusef regulator with the physical hydraulic model test, where the vortex on the left side of canal can be seen as the result of the flow analysis.

v) Evaluation

Judging from the calculated velocity and conformity degree of the discharge, the calculated value is found capable of reproducing an actual value.

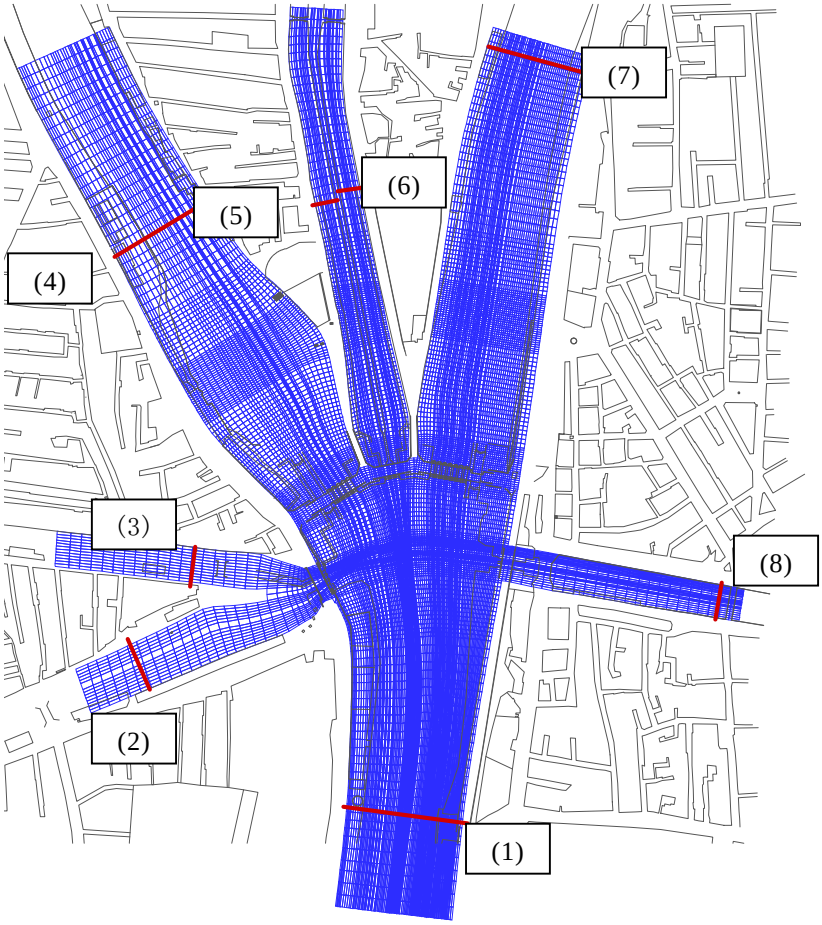

Figure 2-2.1 Locations of flow velocity observation points

Table 2-2.1 Discharge and cross-sectional average water level at the observation points (for verification)

Canal Name	Discharge (m3/s)			Water Level (m)		
	Calculated Value	Measured Value	Difference (Calc-Measure) (%)	Calculated Value	Measured Value	Difference (Calc-Measure) (%)
Ibrahimia canal U/S	355.0	355.0	0.0%	46.1	46.1	0.0%
Irad Delgaw canal	2.1	2.2	-0.4%	44.8	44.8	0.0%
Abo Gabal canal	6.2	6.1	0.6%	45.7	45.7	0.3%
Bahr-Yusef canal	171.5	170.6	0.5%	45.8	45.8	0.0%
Badraman canal	6.1	6.1	0.1%	45.7	45.7	0.0%
Dirutiah canal	9.2	9.2	-0.2%	45.9	45.9	0.0%
Ibrahimia canal D/S	156.8	157.3	-0.3%	45.0	45.0	0.0%
Saheliya canal	3.1	3.1	0.6%	45.7	45.7	0.0%

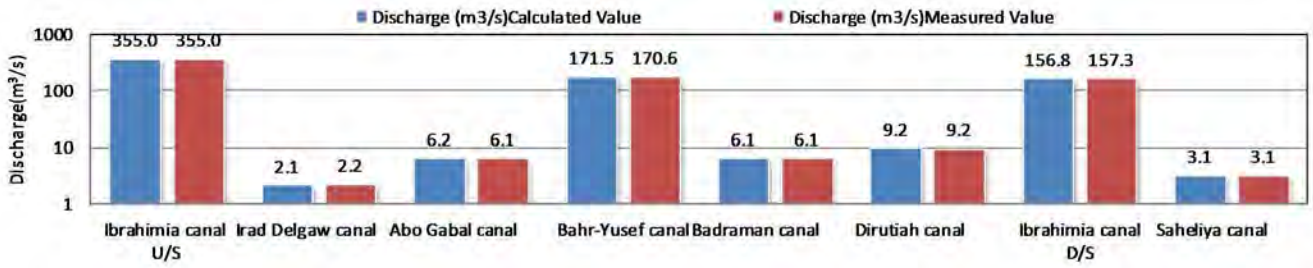

Figure 2-2.2 Discharge comparison graph

Table 2-2.2 Cross-sectional average velocity and correlation coefficient

Canal name	Average Velocity(m/s)	
	Calculated Value	Measured Value
Irad Delgaw canal	0.11	0.12
Abo Gabal canal	0.48	0.47
Badraman canal	0.32	0.32
)Dirutiah canal	0.33	0.33
Saheliya canal	0.25	0.25

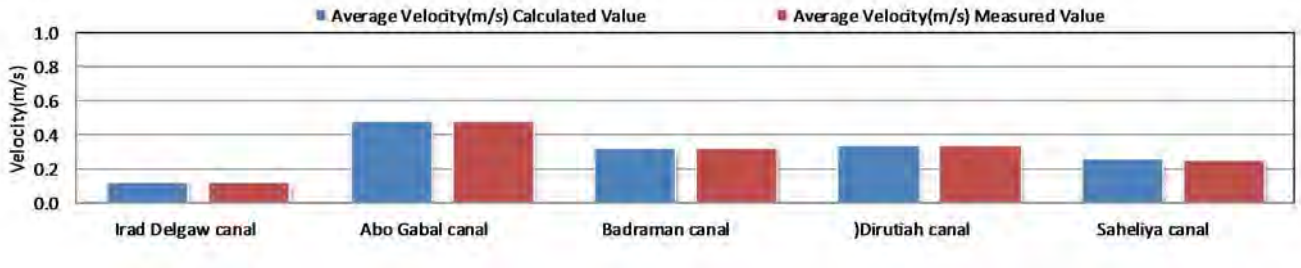

Figure 2-2.3 Average velocity comparison graph

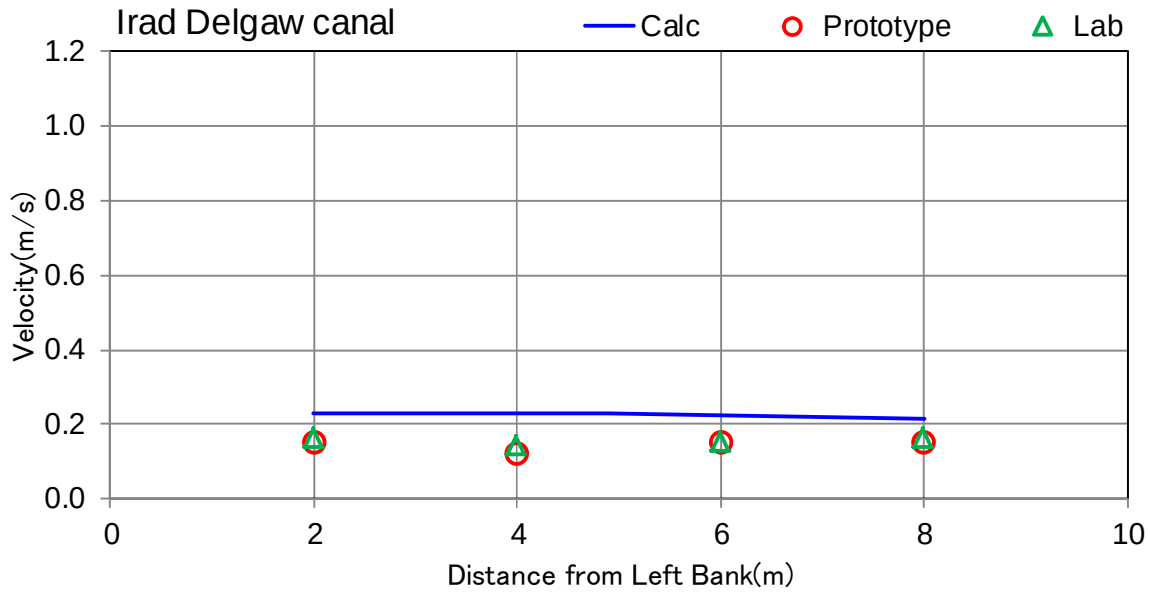

Figure 2-2.4 Comparison of the cross-section velocity in the Irad Delgaw canal

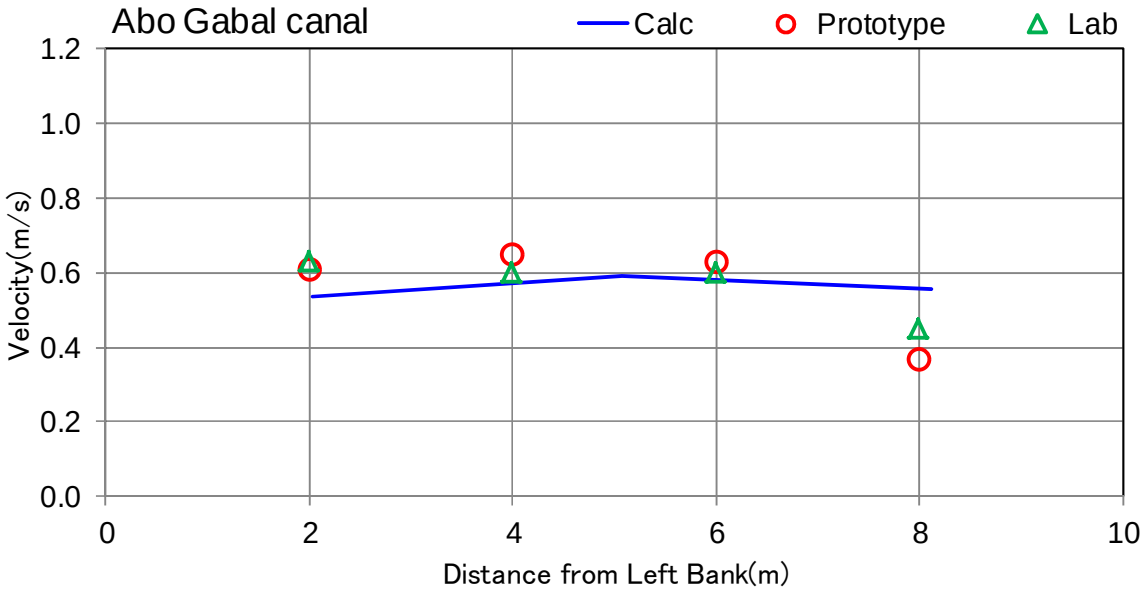

Figure 2-2.5 Comparison of the cross-section velocity in the Abo Gabal canal

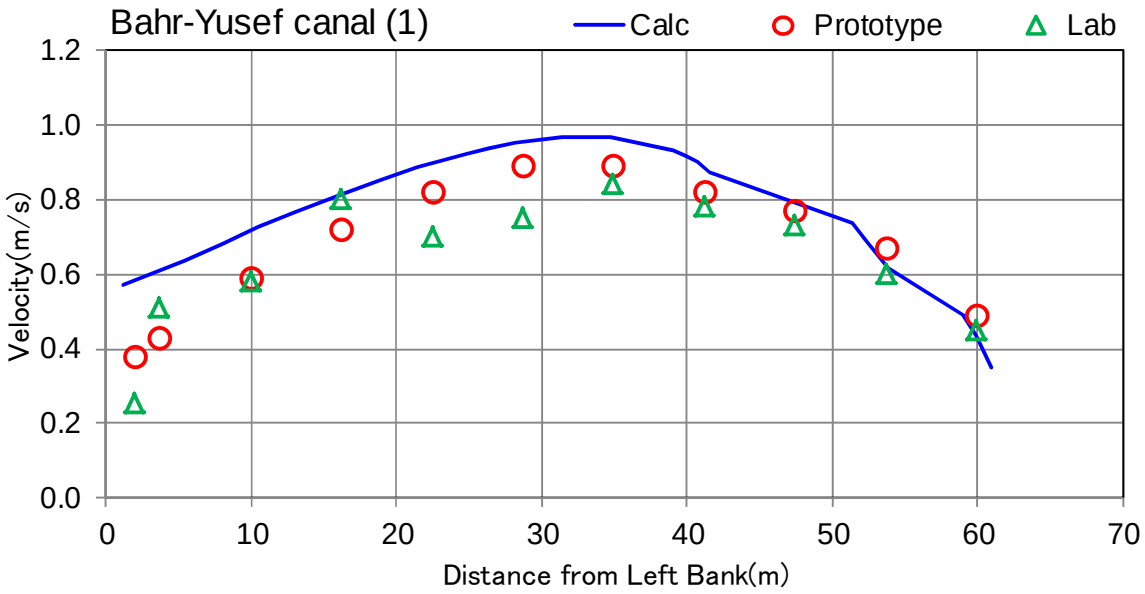

Figure 2-2.6 Comparison of the cross-section velocity in the Bahr Yusef canal

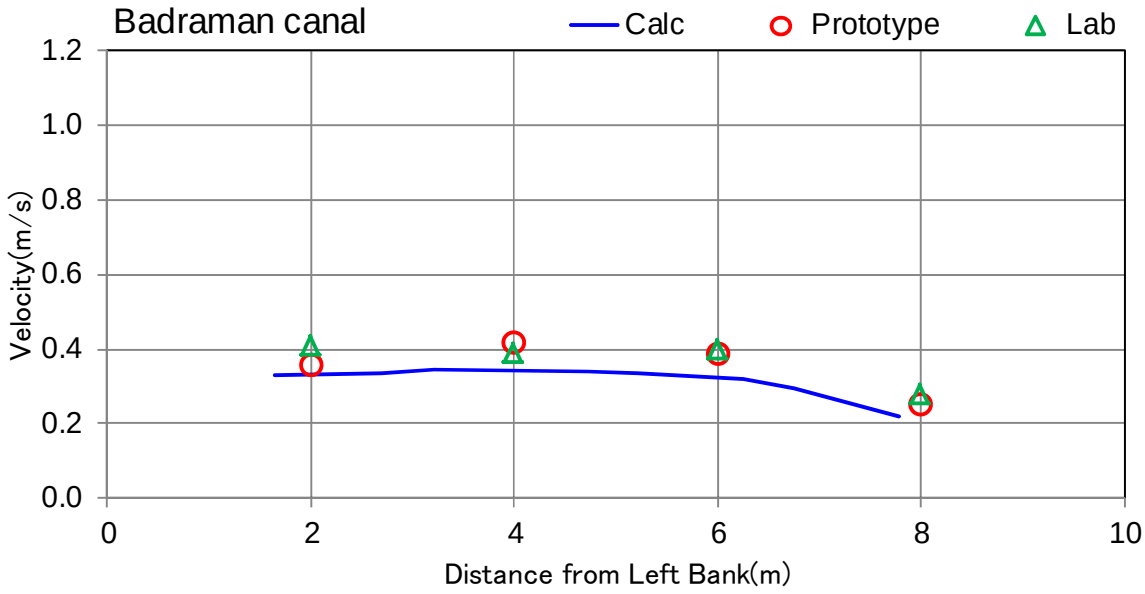

Figure 2-2.7 Comparison of the cross-section velocity in the Badraman canal

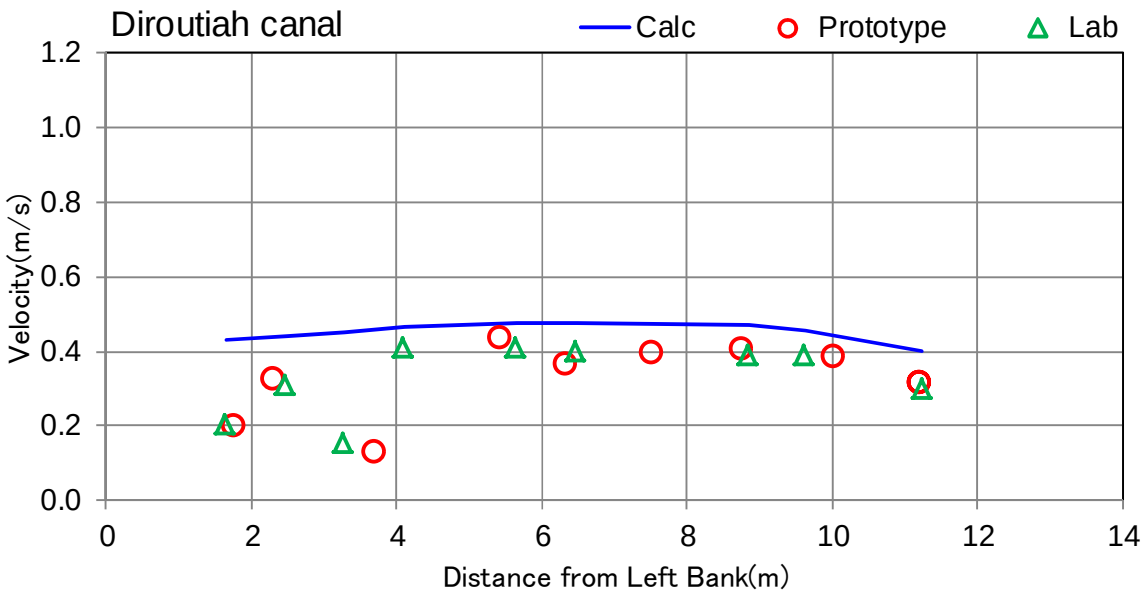

Note: Because actual survey velocity of around 3.8m from the left bank did not factor in the shape of the canal, the correlative analysis does not account for this.

Figure 2-2.8 Comparison of the cross-section velocity in the Diroutiah canal

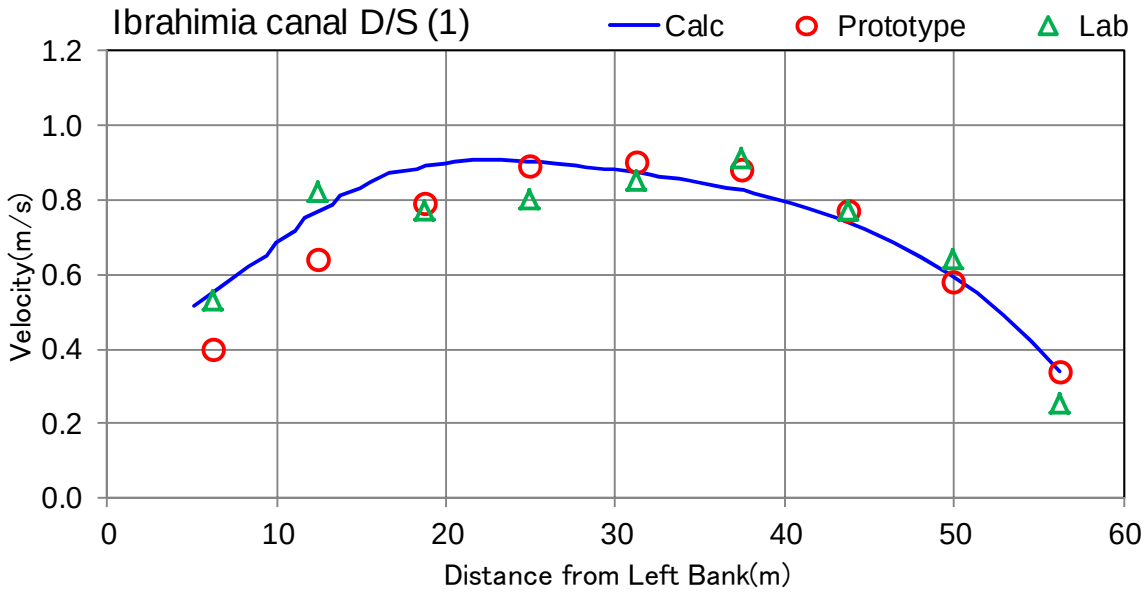

Figure 2-2.9 Comparison of the cross-section velocity in the Ibrahimia canal

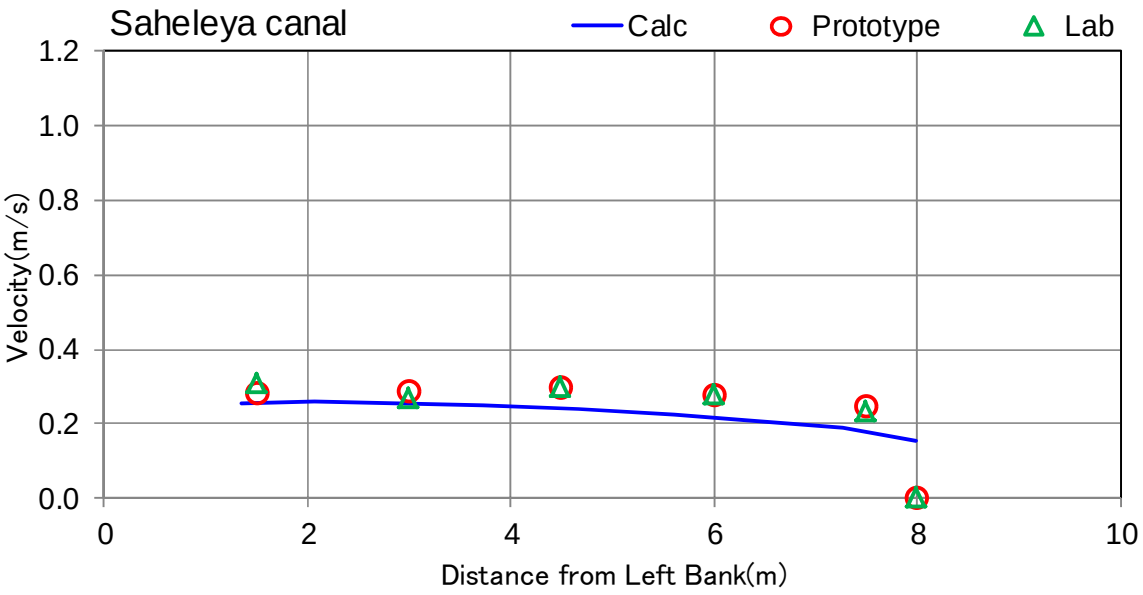

Figure 2-2.10 Comparison of the cross-section velocity in the Sahelyia canal

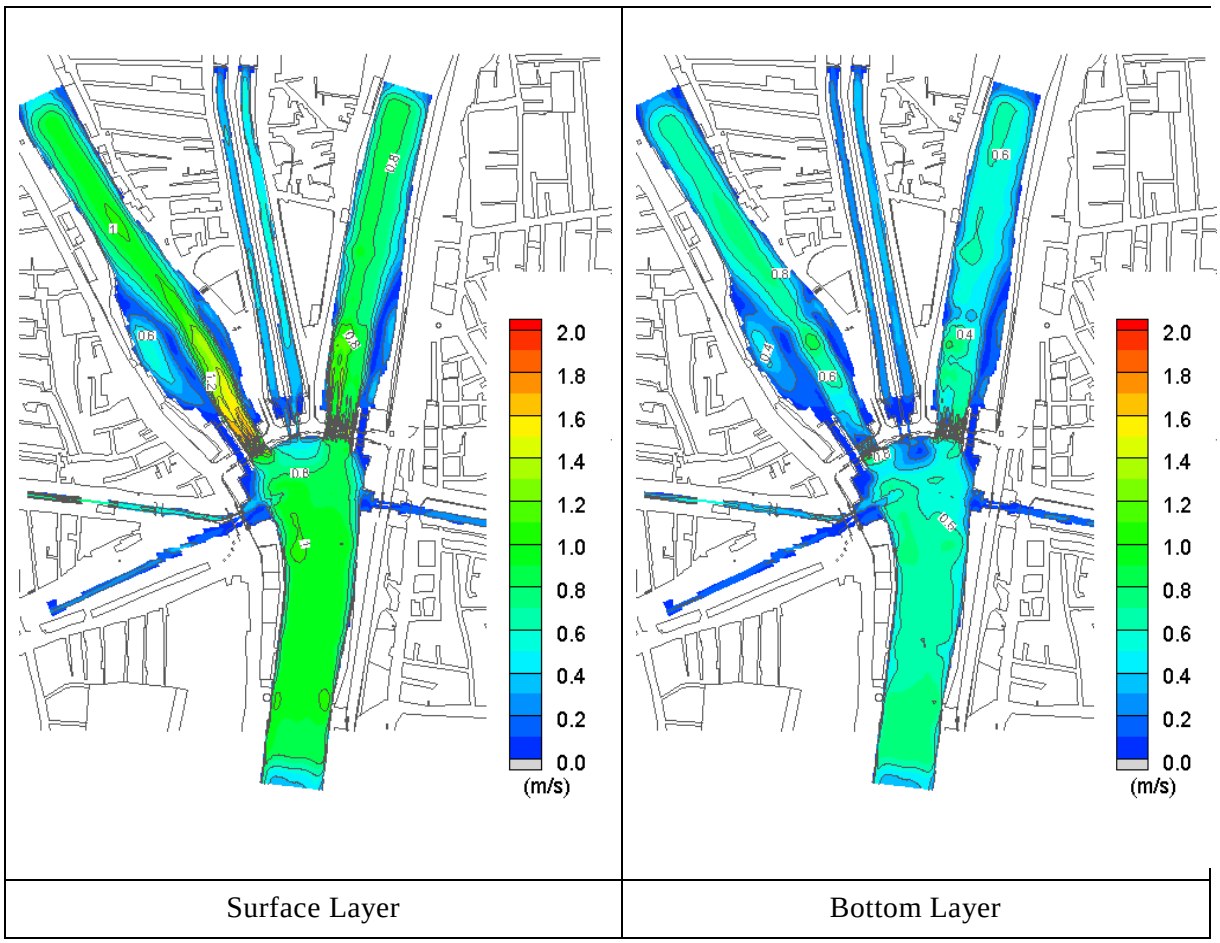

Surface Layer	Bottom Layer

Figure 2-2.11 Flow velocity contour map (calibration stage)

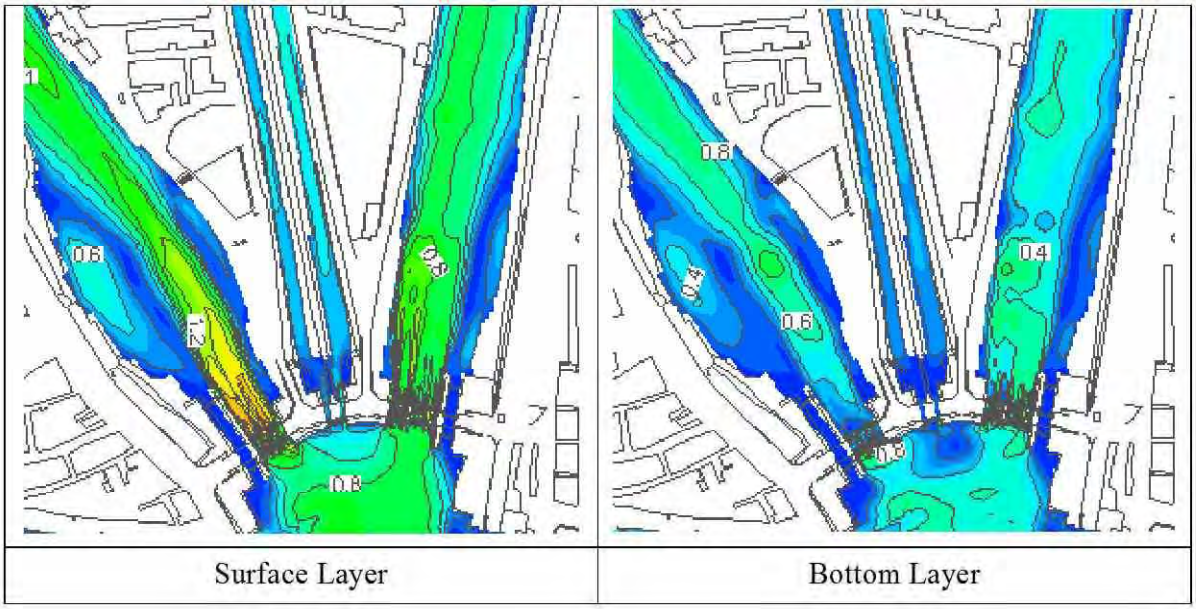

Figure 2-2.12 Flow velocity contour map
(calibration stage, enlarged view of area around DGRs)

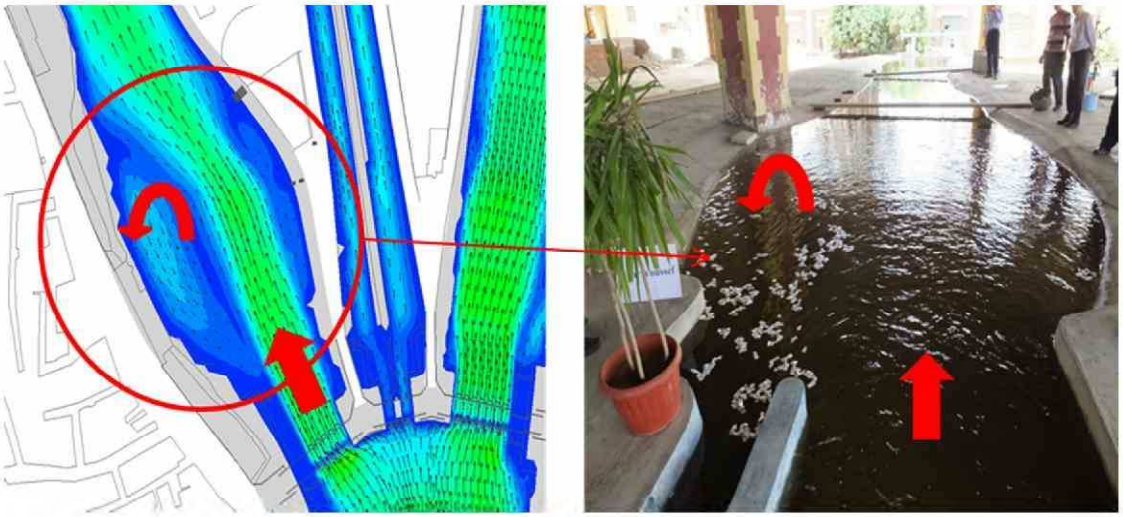

Figure 2-2.13 Comparison between the result of MMA and physical hydraulic model test
(Bahr Yusef canal)

2) Present state

The flow conditions during planned flow distribution were analyzed in the present state.

A comparison of discharge and cross-sectional average water levels at the flow velocity observation points is shown in Table 2-2.3. The discharge comparison is shown in Figure 2-2.14, and the flow velocity contour is shown in Figure 2-2.15 and Figure 2-1.16.

The results showed that an area of slow velocity formed on both banks downstream of the Bahr Yusef regulator, and on the right bank downstream of the Ibrahimia regulator, and that eddies were observed, particularly on the left bank downstream of the Bahr Yusef regulator. It was confirmed that there were no areas surpassing the permission flow velocity (large regulator 2m/s, small regulator 1.5m/s) of the regulator at a regulator spot.

Table 2-2.3 Discharge and cross-sectional average water levels at the observation points (present state)

Canal Name	Discharge(m^3/s)		Water Level(m)	
	Calculated Value	Target Value	Calculated Value	Target Value
Ibrahimia canal U/S	455.0	455.0	46.2	46.3
Irad Delgaw canal	8.2	9.0	45.9	45.9
Abo Gabal canal	6.7	7.0	46.0	45.9
Bahr-Yusef canal	232.9	227.0	45.8	45.8
Badraman canal	11.0	9.0	45.9	45.9
Diroutiah canal	12.2	12.0	45.9	45.9
Ibrahimia canal D/S	186.3	186.0	45.1	45.1
Saheleya canal	5.0	5.0	45.9	45.9

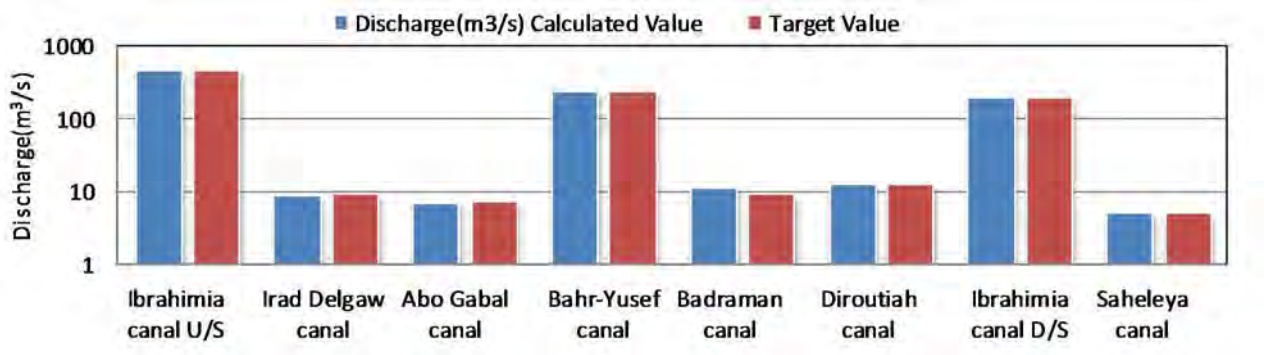

Figure 2-2.14 Discharge comparison graph (present state)

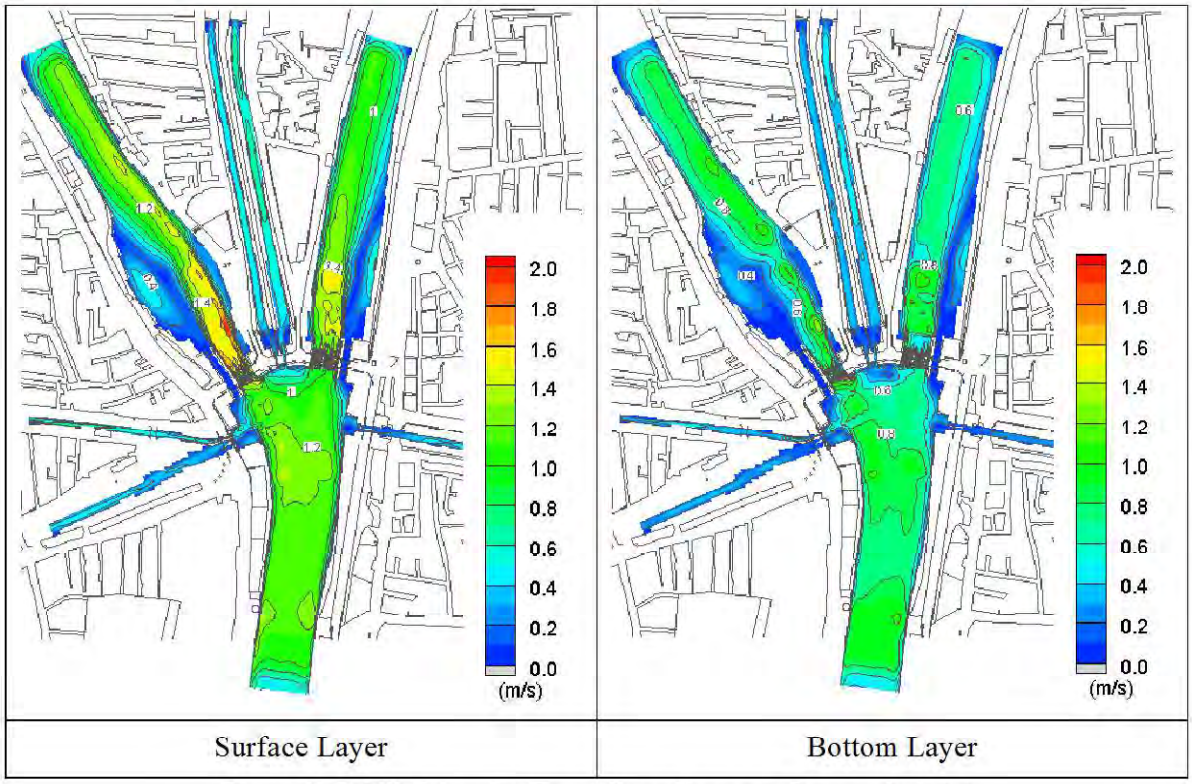

Surface Layer | Bottom Layer

Figure 2-2.15 Flow velocity contour diagrams (present state)

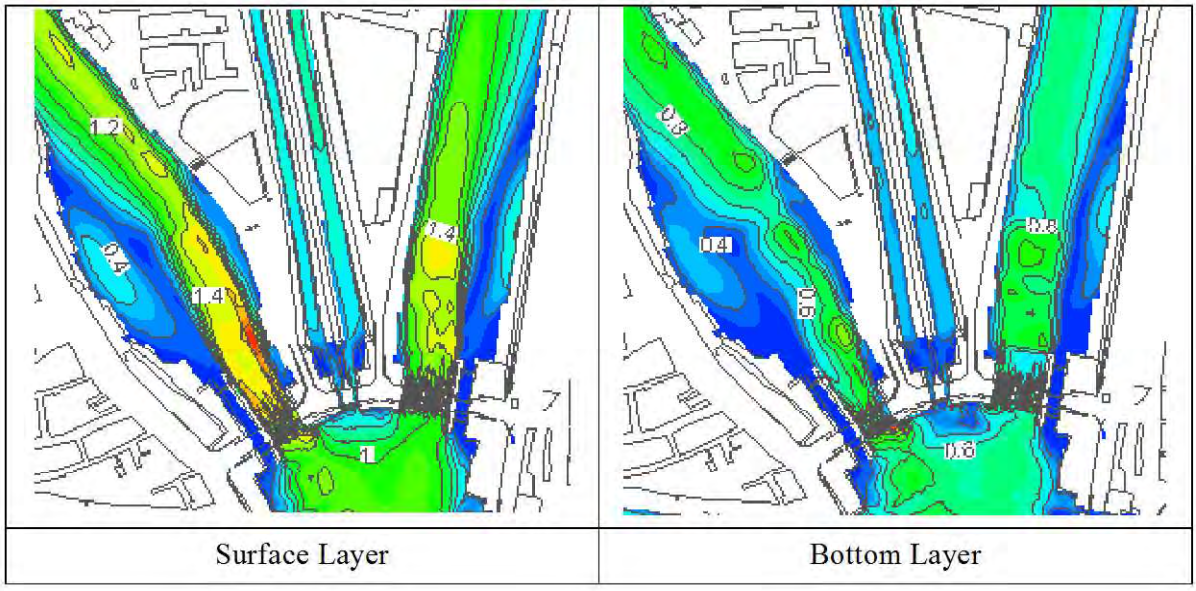

Surface Layer | Bottom Layer

Figure 2-2.16 Flow velocity contour diagrams (present state, enlarged view of vicinity of DGRs)

3) Planning

The flow conditions in design discharge with the underflow and overflow regulator discharge systems were analyzed in the plan.

Table 2-2.4 shows a comparison of the discharge and cross-sectional average water level at the flow velocity observation points. Figure 2-2.17 shows a comparison of the discharge. Figures 2-2.18 to 2-2.21 show the flow velocity contour.

From the results, it was found that areas of slow velocity formed on the left bank downstream of Bahr Yusef regulator and on the right bank both upstream and downstream of Ibrahimia regulator.

There is almost no difference in the flow velocity of the regulator in both overflow and underflow. This may be due to the fact that the depth of the regulator flow is 5m or more. In addition, it was found that the value of the gate on the right side of the flow velocity of the bottom layer of the Ibrahimia regulator had become quite large. This means that the number of gates that regulate the flow ahead of the upstream existing regulator are concentrated on the right bank, and that there is a margin towards the right bank due to the expansion of the downstream of the right bank after it passes through the new bank.

It is understood that no region of the regulator has a flow velocity of 2m/s or more.

Table 2-2.4 Discharge and cross-sectional average water levels at the observation points (planning stage)

Canal Name	Discharge(m^3/s)			Water Level(m)		
	Calculated Value		Target Value	Calculated Value		Target Value
	Underflow	Overflow		Underflow	Overflow	
Ibrahimia canal U/S	455.0	455.0	455.0	46.3	46.3	46.3
Irad Delgaw canal	6.6	5.0	9.0	45.9	45.9	45.9
Abo Gabal canal	8.7	8.2	7.0	46.1	46.0	45.9
Bahr-Yusef canal	230.3	231.5	227.0	45.8	45.8	45.8
Badraman canal	8.9	9.0	9.0	45.9	45.9	45.9
Diroutiah canal	11.8	11.9	12.0	45.9	45.9	45.9
Ibrahimia canal D/S	183.7	184.6	186.0	45.1	45.1	45.1
Saheliya canal	5.0	5.0	5.0	45.9	45.9	45.9

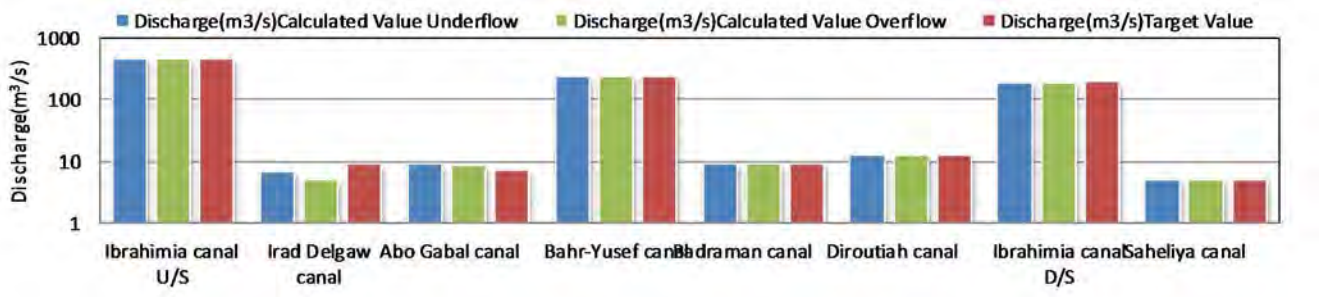

Figure 2-2.17 Discharge comparison graph (planning stage)

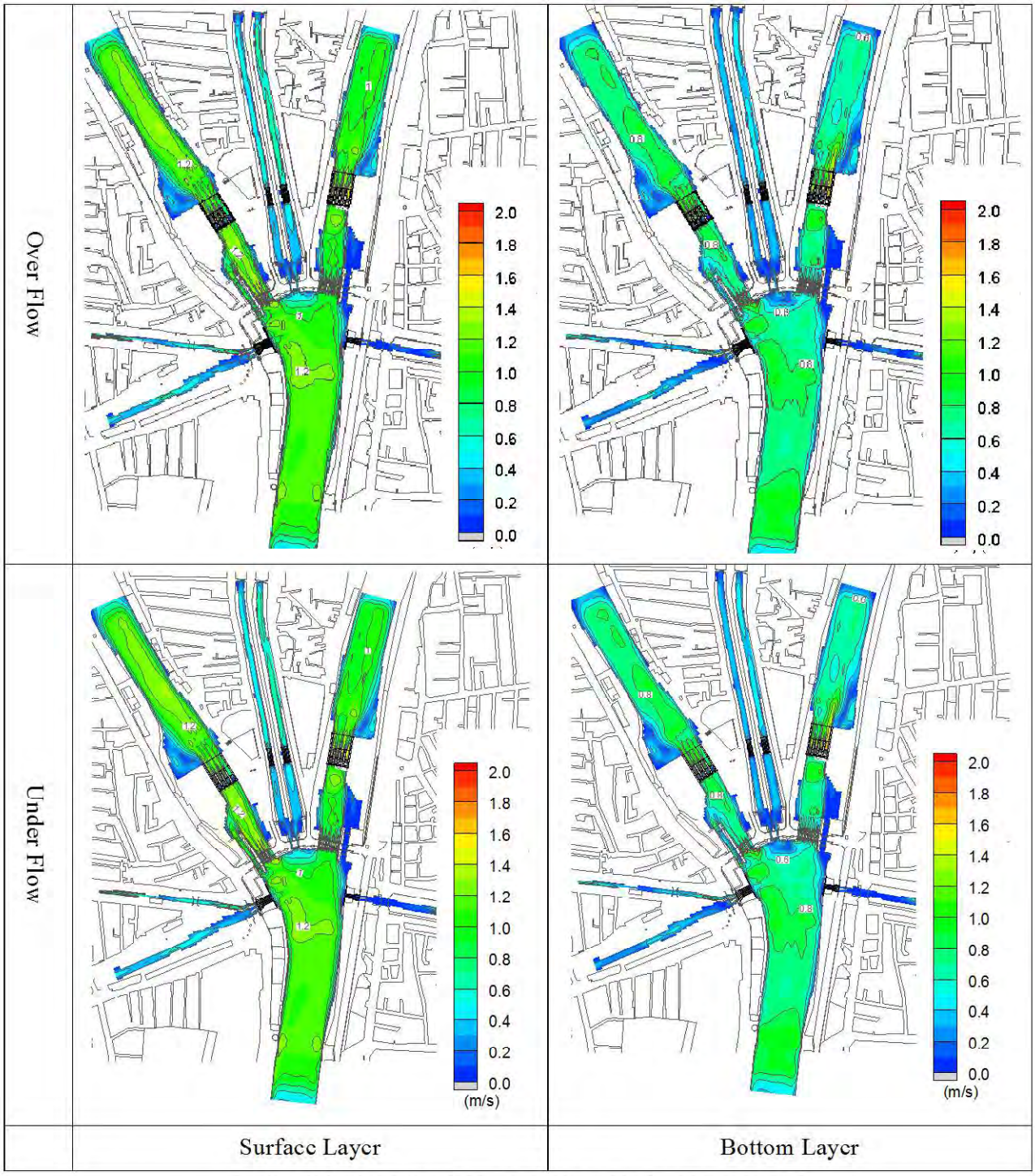

Figure 2-2.18 Flow velocity contour map (planning stage)

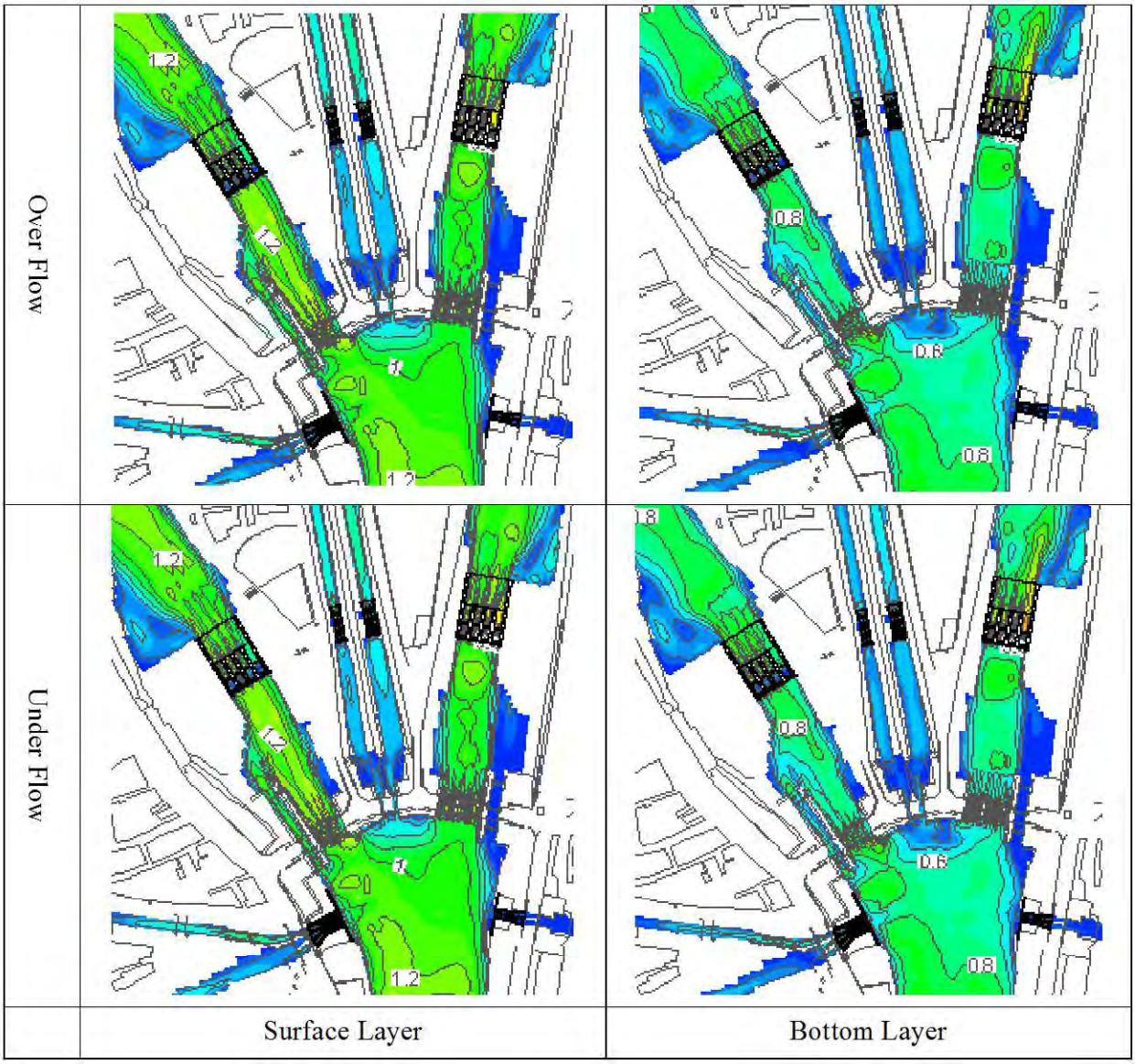

Figure 2-2.19 Flow velocity contour map
(planning stage, enlarged view of vicinity of DGRs)

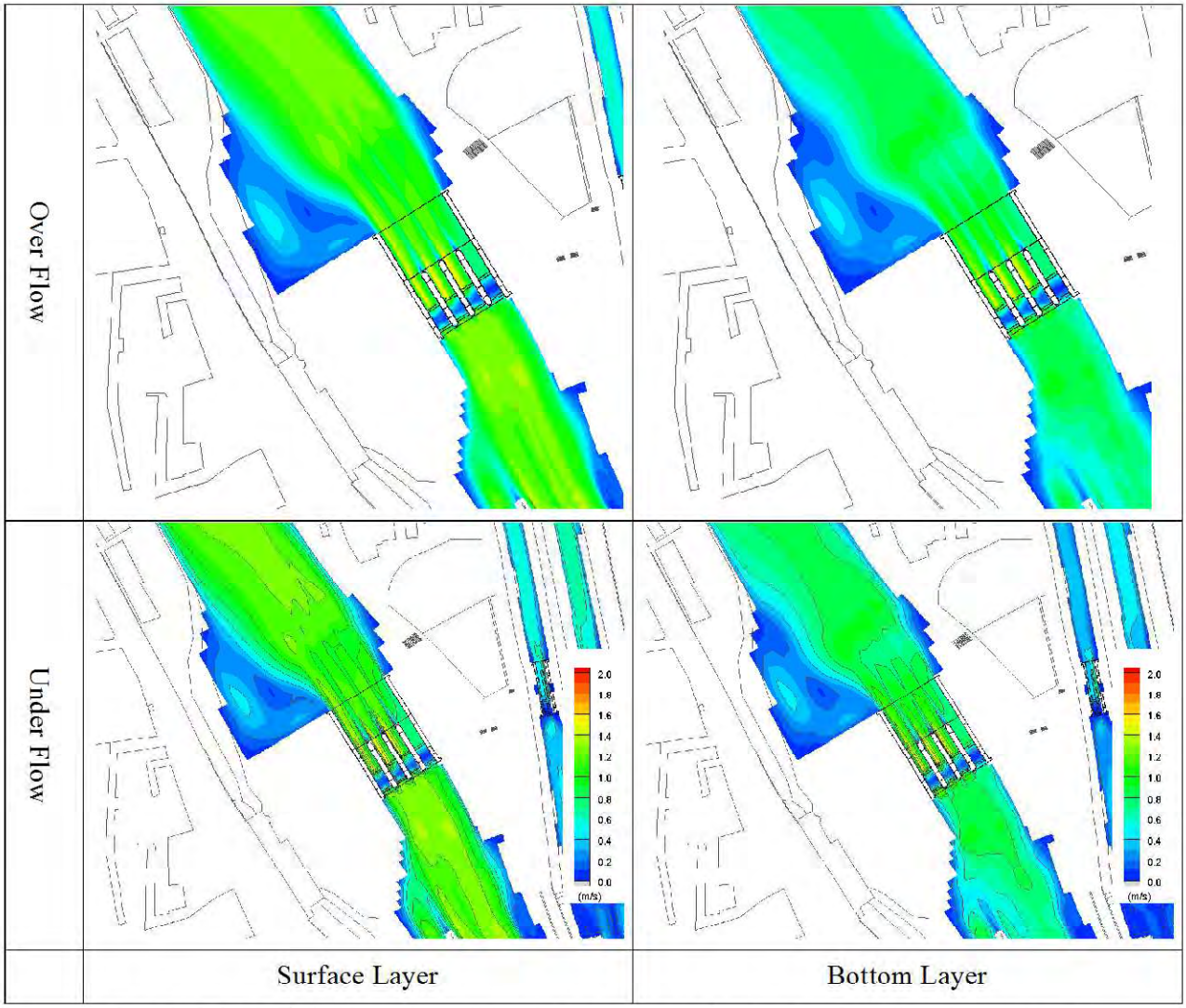

Figure 2-2.20 Flow velocity contour map (planning stage, new Bahr Yusef regulator)

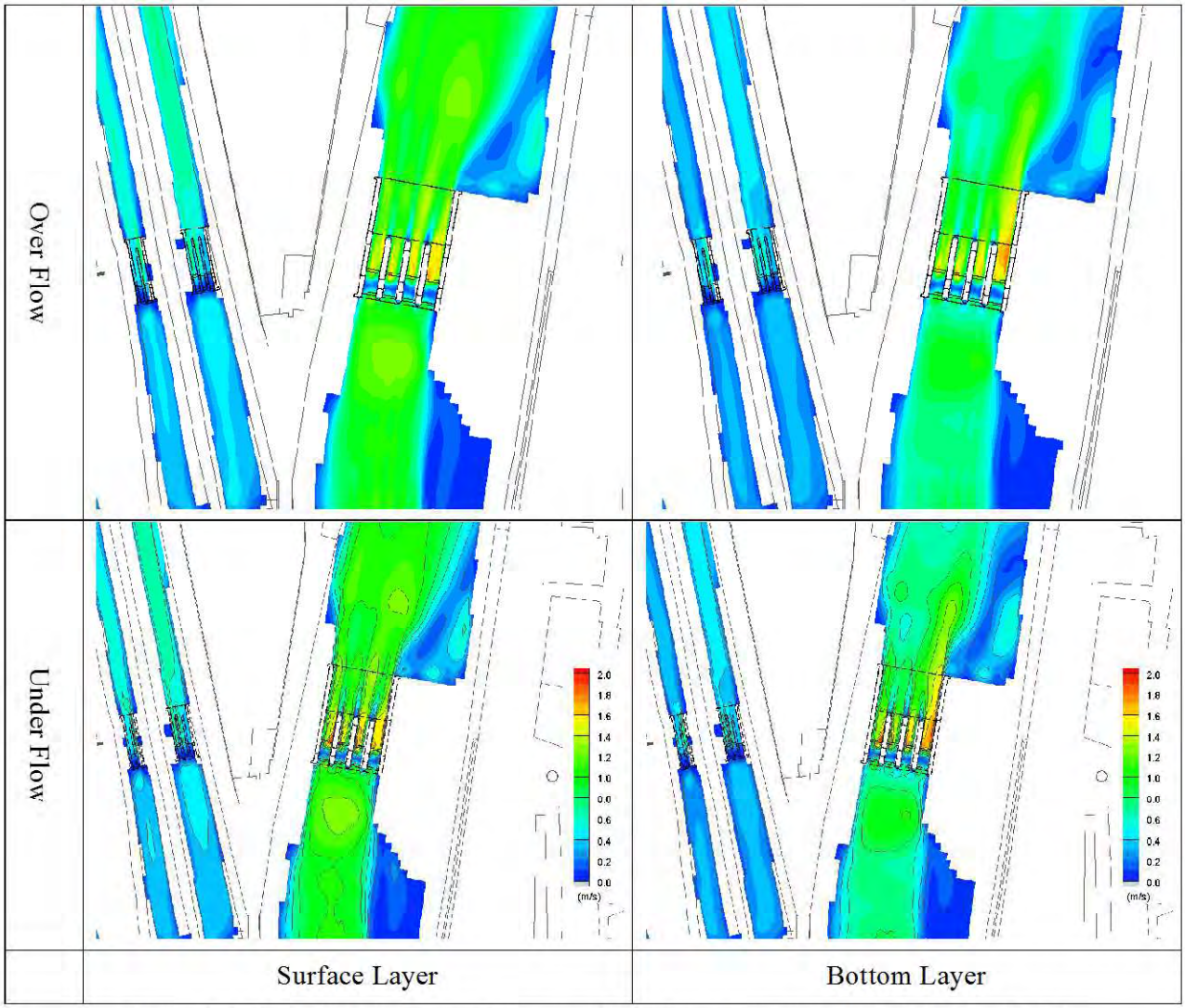

Figure 2-2.21 Flow velocity contour map (planning stage, new Ibrahimia regulator)

b) Evaluation

It was confirmed that the five new regulators could effectively distribute the planned discharge to the seven canals.

In addition, from the analysis result at the design flow, the possibility of scouring was found to be concentrated in the dangerous part where the flow is high velocity, and where the flow velocity of the plan is higher than the present flow.

Figures 2-2.22 to 2-2.25 show the flow velocity difference diagrams obtained by subtracting the present flow velocity from the planned flow velocity. According to these, the clearly marked yellow and red areas show where the flow velocity of the plan is higher than that in the present state. The figures also show that flow velocity in the planning state decreases compared to the present state because the area between DGRs and NDGRs becomes a pool area.

These show that the flow velocity decreases due to the influence of the new regulator.

As the flow velocity decreases in this section, there is a possibility that sediment will increase, so careful attention is required to maintain and manage this section.

Regarding the possibility of scouring and danger spots due to high flow velocity; places susceptible to scouring are identified and then evaluated from the results of analysis at design discharge. The evaluation covers places and areas where the planned flow velocity exceeds the present velocity. The construction zones of the new regulators, aprons, etc. are excluded from evaluation.

Over Flow	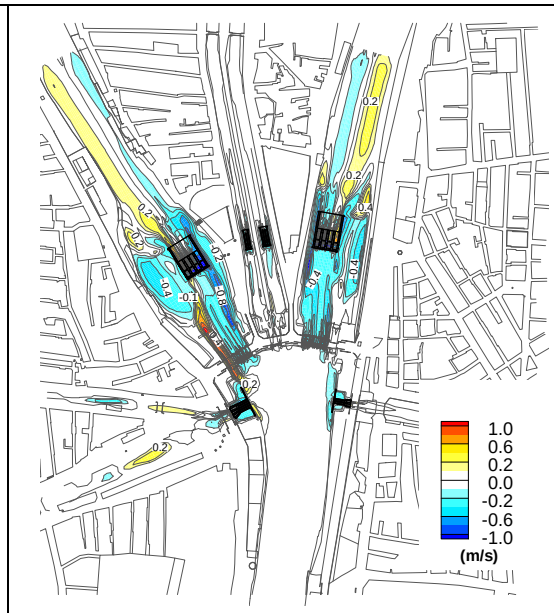	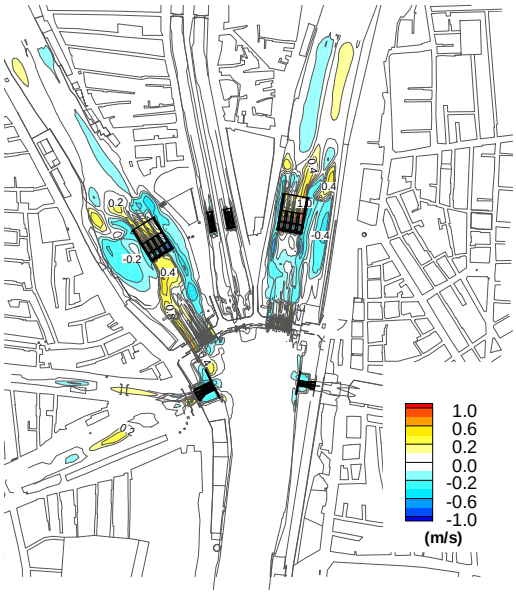
Under Flow	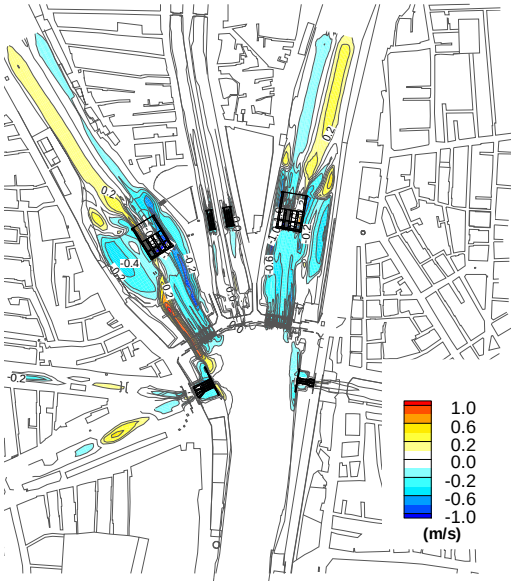	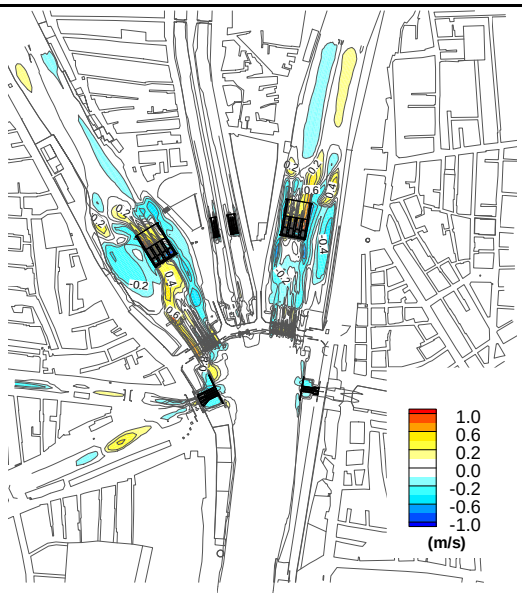
	Surface Layer	Bottom Layer

Figure 2-2.22 Difference in flow velocity (planning-present state)

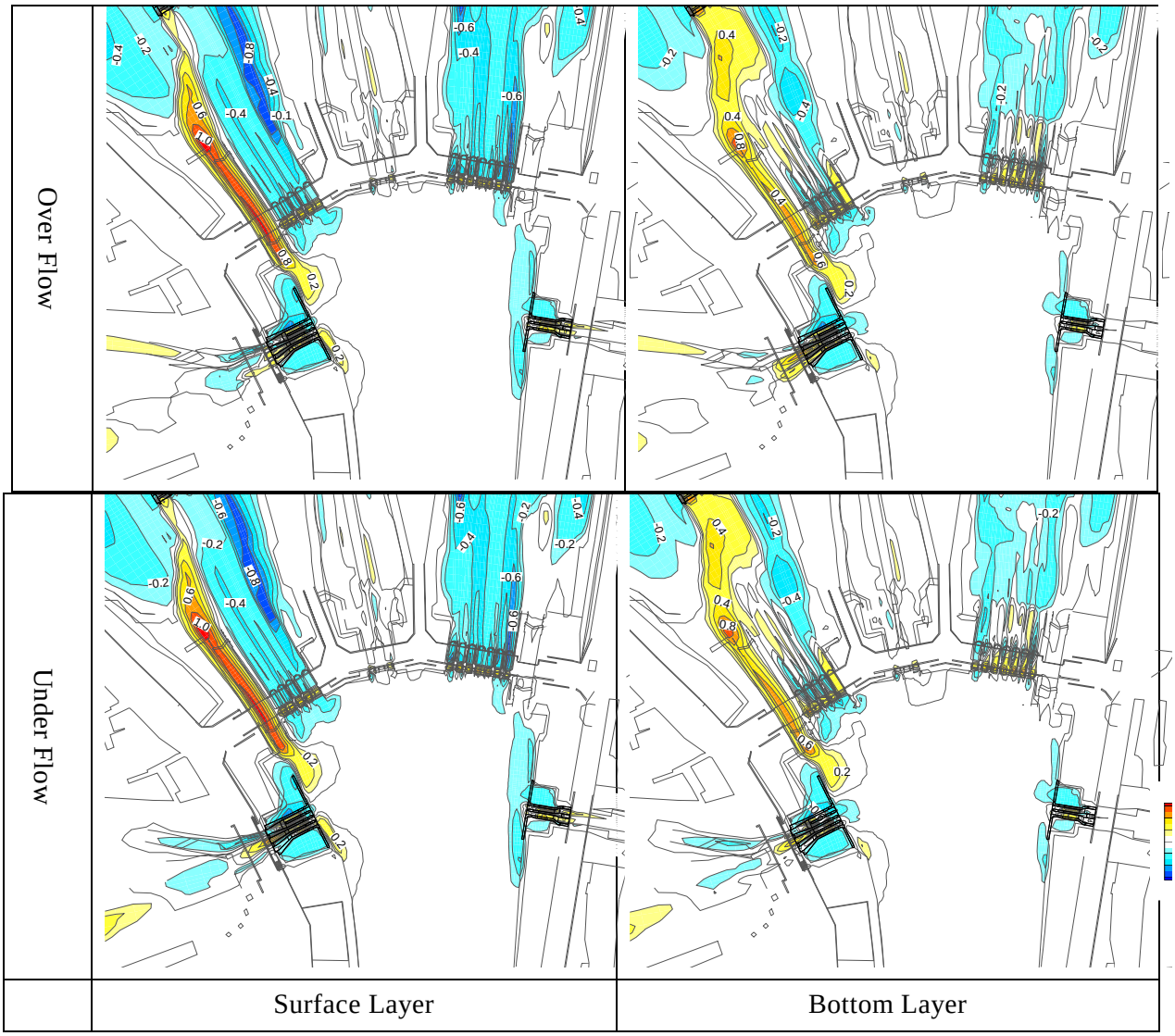

Figure 2-2.23 Difference in flow velocity (planning-present state, around DGRs)

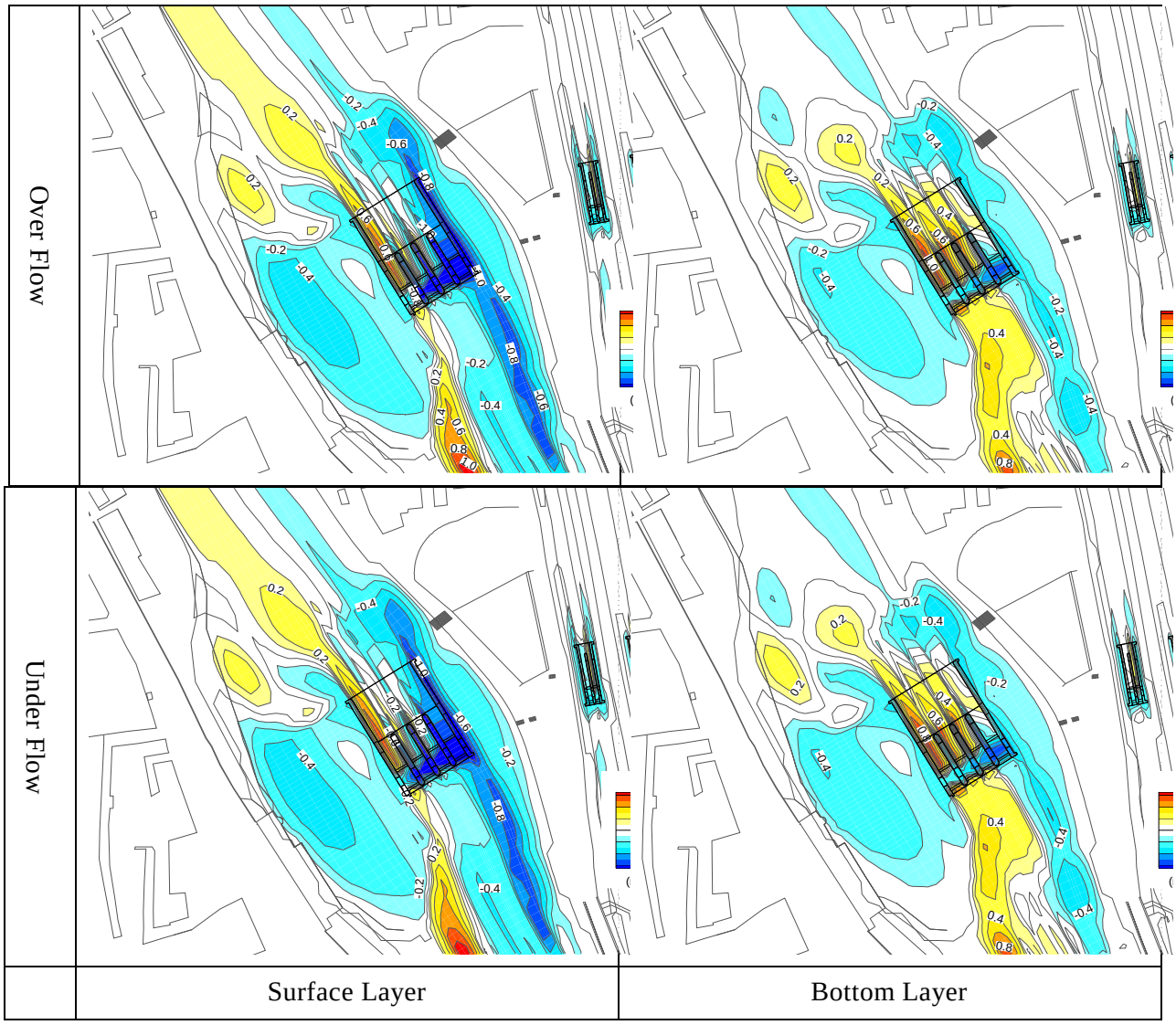

Figure 2-2.24 Difference in flow velocity
(planning-present state, around the new Bahr Yusef regulator)

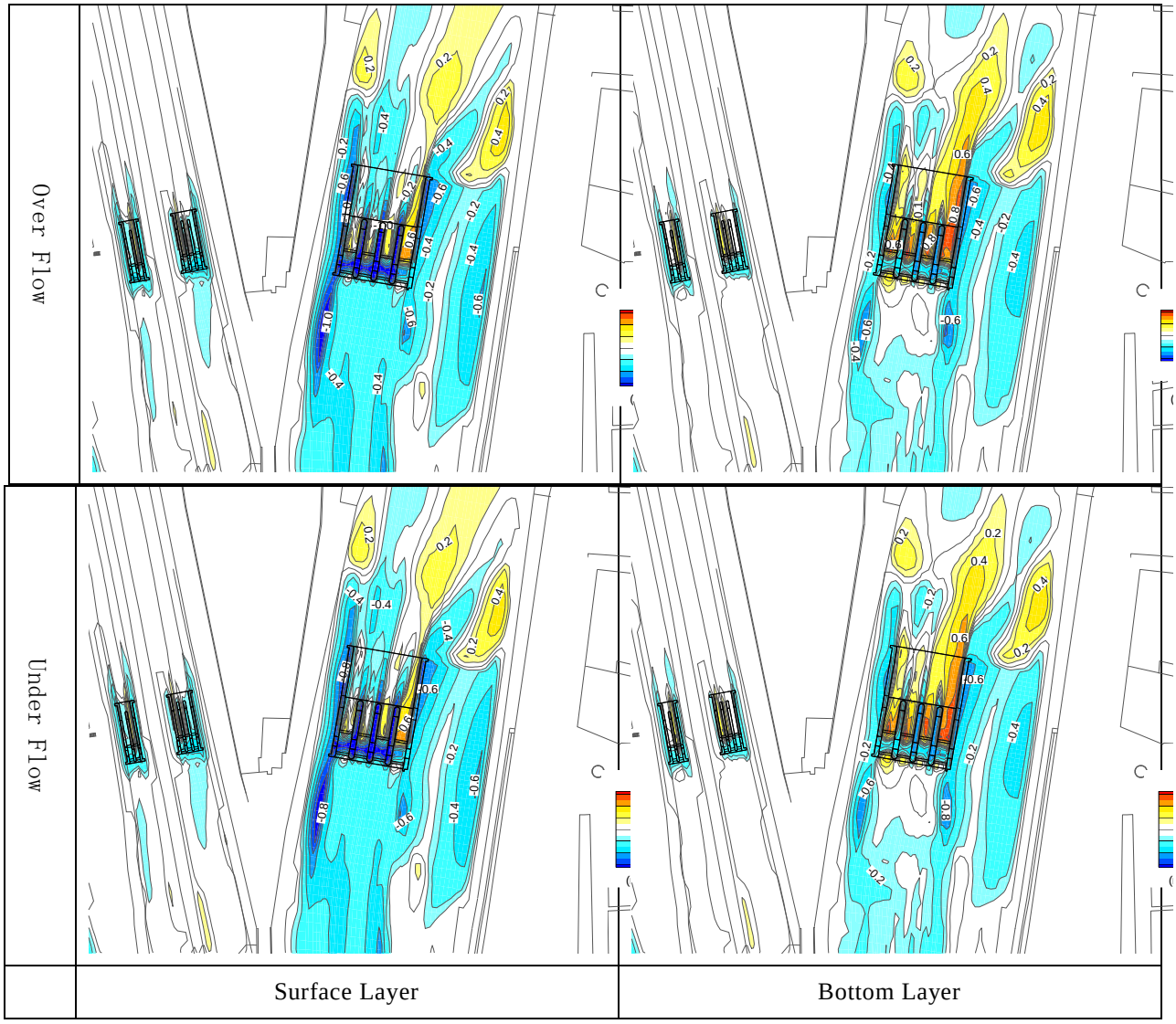

Figure 2-2.25 Difference in flow velocity
(planning – present stage, around the new Ibrahimia regulator)

The results of the present state and planned flow velocity distributions are shown below.
In order to determine the required bed protection, the flow velocity distribution of the riverbed is evaluated.
At the present state, the maximum riverbed flow velocity near the downstream side of the newly built regulator is 0.8m/s to 1.0m/s at the Bahr Yusef canal, and 0.8m/s at the Ibrahimia canal. At the planning stage, it is 1.0m/s at the Bahr Yusef canal, and 0.8m/s to 1.4m/s at the Ibrahimia canal.
At the Ibrahimia regulator in particular, flow velocity is concentrated at the rightmost bank around the four gates. The region with the fast flow velocity extends to the downstream of the apron. The flow velocities of the remaining three canals are within the range of the apron.
Except for the concentration of local flow velocities in Ibrahimia canal, both Bahr Yusef and Ibrahimia canals show stable flow conditions in the apron after passing through the regulator.

Table2-2.5 Difference in flow velocity at the downstream of new regulators

Item		Bahr Yusef	Ibrahimia
Maximum Velocity (m/s)	Present state	0.8～1.0	0.8
	Plan	1.0	0.8～1.4
	Difference (Present – Plan)	0～0.2	0～0.6
Status of flow		Flow velocity distribution stabilizes around 30m downstream from edge of apron	With the exception of one right bank, low velocity distribution stabilizes around 30m downstream from edge of apron
Range of bed protection		around 30m downstream from edge of apron	around 30m downstream from edge of apron

The countermeasures against the protective bed downstream of the apron due to the concentration of the flow velocity at the right bank side of the new Ibrahimia regulator include:

1. In the long term, it is desirable to operate all four vents with equal distribution.
2. A short-term countermeasure would be the installation of stone pitching. However, since this falls outside the realm of temporary works, the installation of stone pitching may be carried out during the winter closure period.

With regard to these, attention must be paid to the relation between the arrangement of the bed protection, the construction plan and the operation plan of the gate.

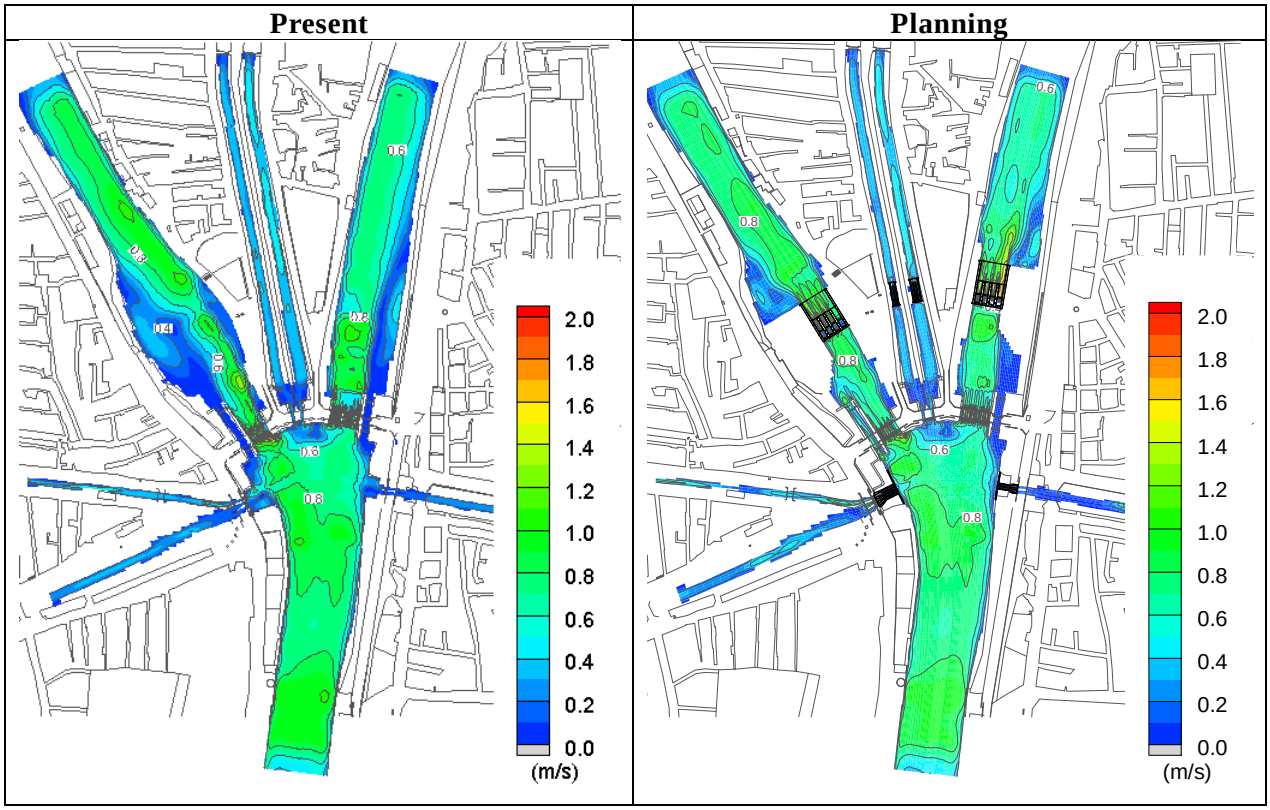

Figure 2-2.26 Flow velocity on the riverbed (present and planning stage)

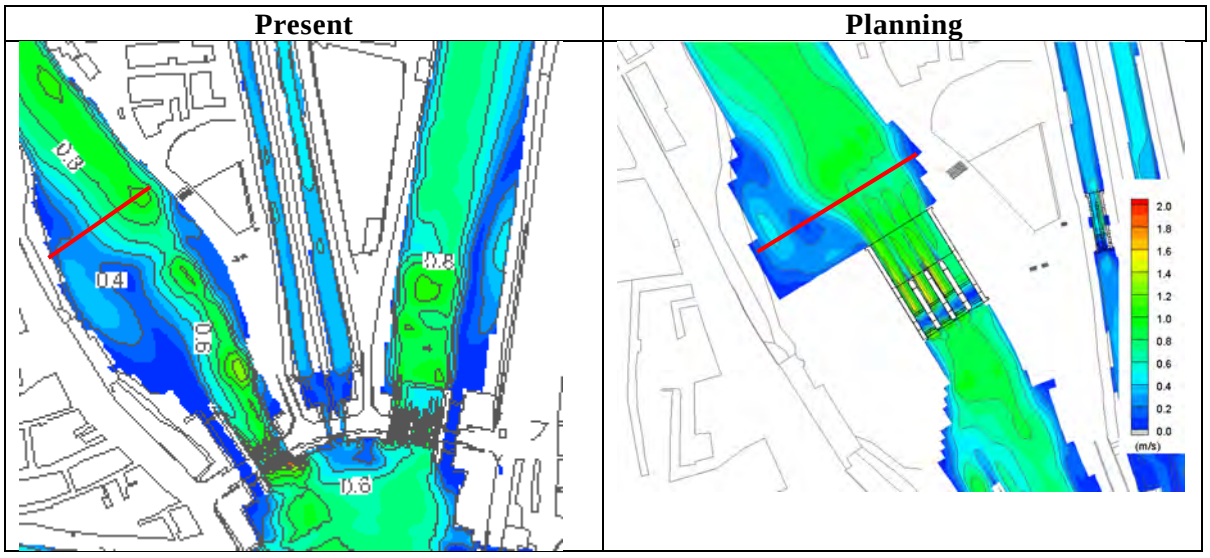

Note: The red line indicates the point 30m from the downstream end of the apron.

Figure 2-2.27 Flow velocity on the riverbed
(present and planning stage, around the new Bahr Yusef regulator)

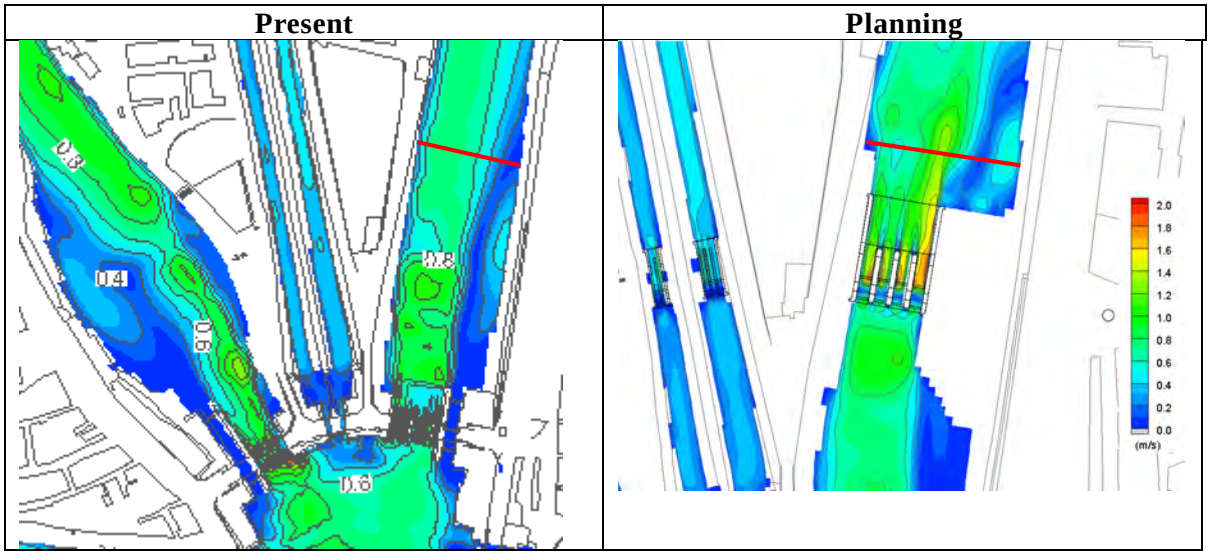

Note: The red line indicates the point 30m from the downstream end of the apron.

Figure 2-2.28 Flow velocity contour map of riverbed (Ibrahimia regulator)

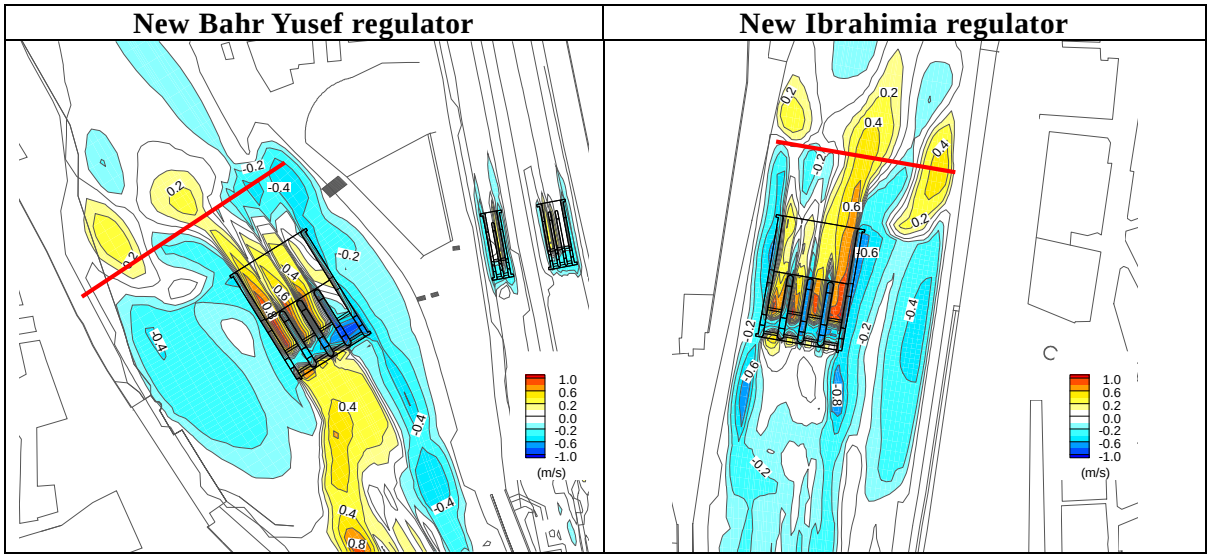

Note: The red line indicates the point 30m from the downstream end of the apron.

Figure 2-2.29 Difference in flow velocity of riverbed
(Bahr Yusef and Ibrahimia regulators, present-planning stage)

5) Implementation of plan flow analysis for comparison with physical hydraulic model

The topographic data of January 2016 was utilized in the analysis of the present and planning stage to confirm the influence on the regulator design. On the other hand, the topographic data of August 2015 was utilized in the physical hydraulic model test conducted by HRI.

In the beginning, it was enough to grasp only the tentative results of the mathematical model analysis and the physical hydraulic model test. However, applying the same topographic data was required after the TAC decision in order to make a more detailed comparison. To this end, another case study was conducted with topographic data from Aug. 2016 instead of Jan. 2016. The results are shown below.

i) Conditions of analysis

In order to compare the results of both models, the following conditions were applied to the mathematical model analysis.

The object of analysis for the comparison is the planned new DGR.

Table 2-2.6 Analysis condition for the comparison with PHMT

Analysis Condition	As of Basic Design Report (BDR)	Analysis for comparison
1.Topography survey data	January 2016	August 2015
2.Computation mesh	The total number of meshes: 198,380	Same as BDR
3.Boundary condition	Upstream canal of the existing NGRs : Discharge End of each canal : Water level	Same as BDR
4.Water level and discharge	Planning stage (NDGRs)	Same as BDR

1. Topographic conditions: topographic data from August 2015 is applied to match the conditions of the physical hydraulic model test (Figures 2-2.31 and 2-2.32).
2. Computation mesh: The computation mesh is the same as the one in the Basic Design Report (Figure 2-2.30).

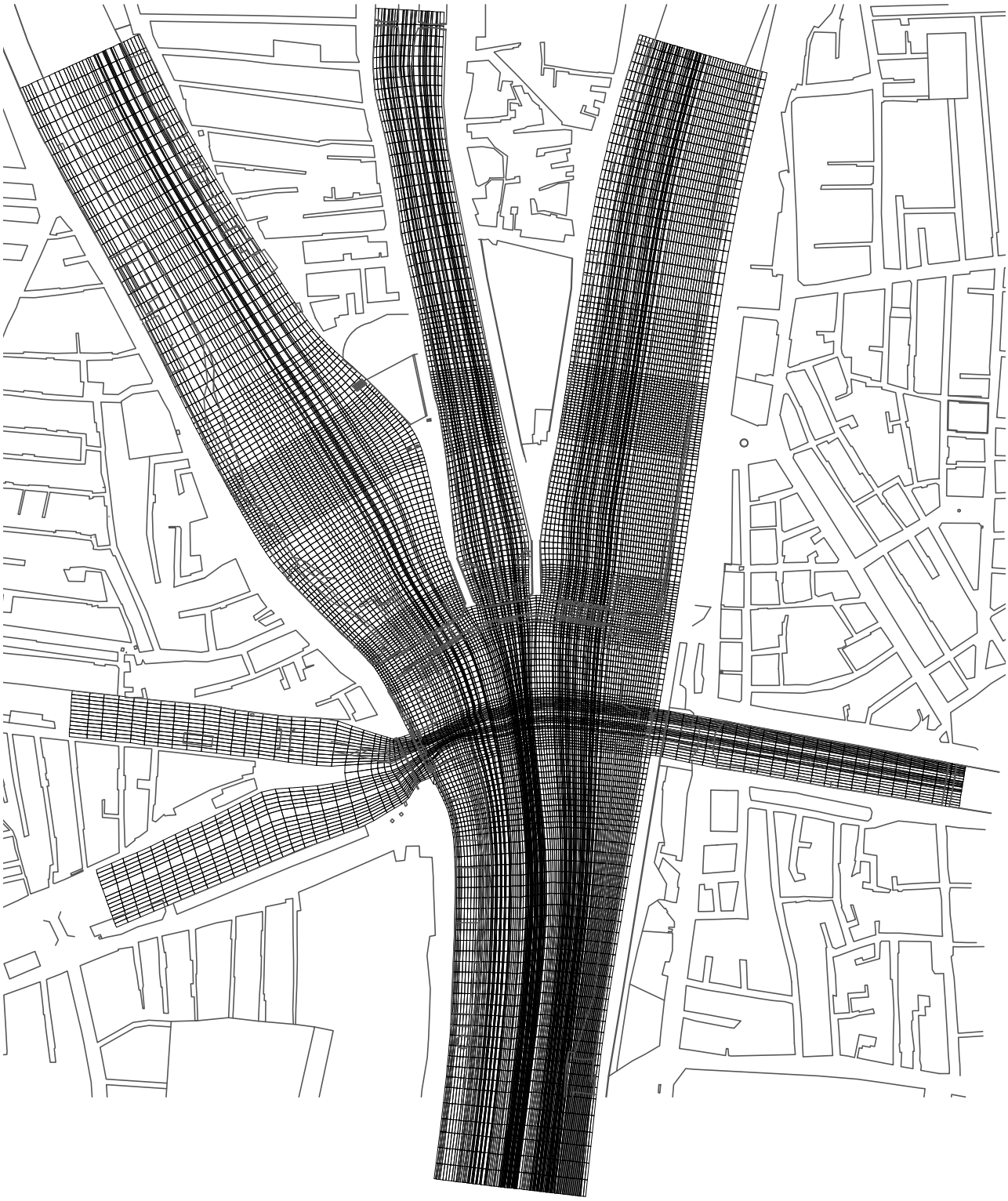

Figure 2-2.30 Computation mesh for canal (comparison with PHMT)

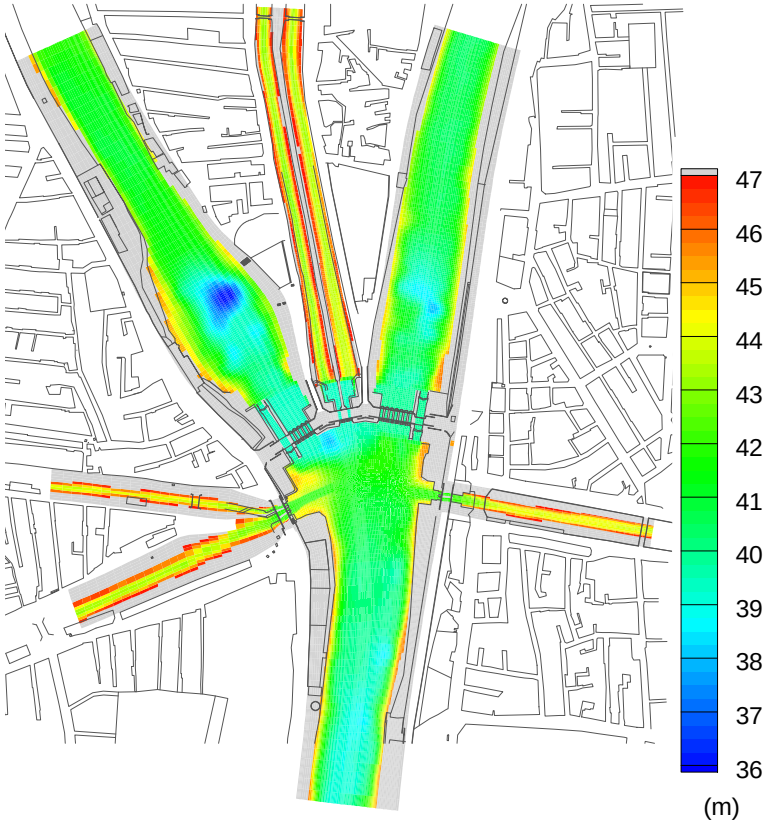

Figure 2-2.31 Topographic contour map based on the surveyed data in August 2015 (calibration and present state)

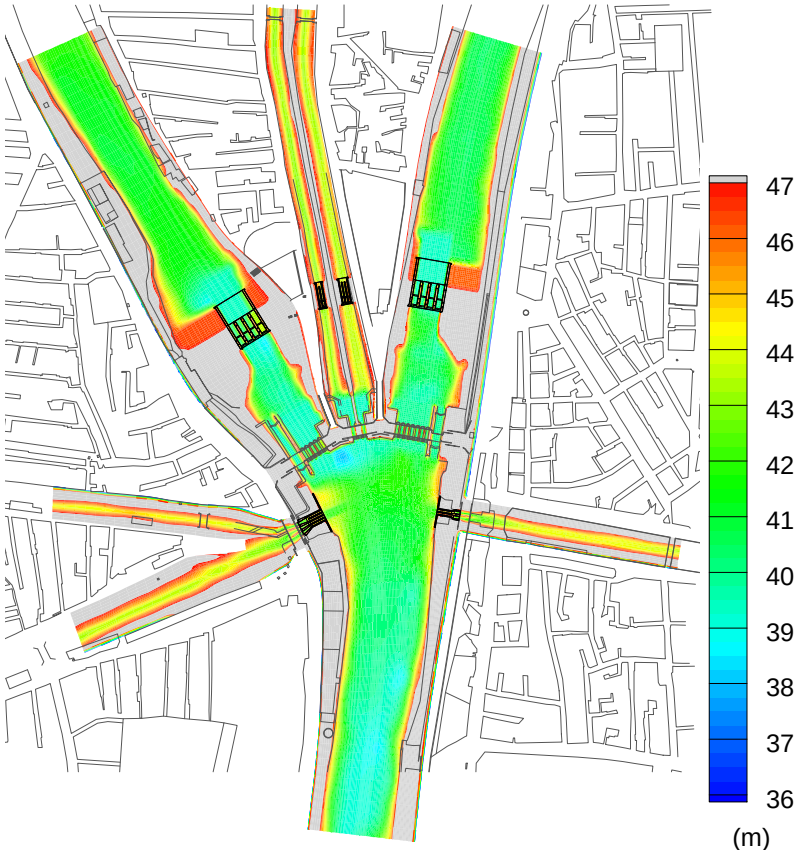

Figure 2-2.32 Topographic contour map based on the surveyed data in August 2015 (planning stage)

・Boundary conditions

The boundary conditions are as followings:

- ✓ Discharge boundary: at the upstream of the existing DGRs
- ✓ Water level boundary: at the end of each canal

・Water level, inflow to NDGRs, and outflow from each NDGR

The water level boundary is adjusted according to the data provided by the Water Distribution Sector shown in Table 2-2.7 (the same boundary is applied in the design of the NDGRs). The discharge boundary is given as 455m^3/s at the upstream end.

Table 2-2.7 Analysis condition of water level, inflow and outflow

Item	US. of Regulators	DS. of regulators							Remarks
	existing DGRs	Bahr Yusef	Ibrahimia	Badraman	Diroutiah	Abo Gabal	Irad Delgaw	Sahelyia	
Water Level(m)	46.30	45.82	45.13	45.90	45.90	45.90	45.90	45.90	Target Value
Inflow (m^3/s)	455	—	—	—	—	—	—	—	Up stream
Outflow of regulator (m^3/s)	—	27	186	9	12	7	9	5	Target Value

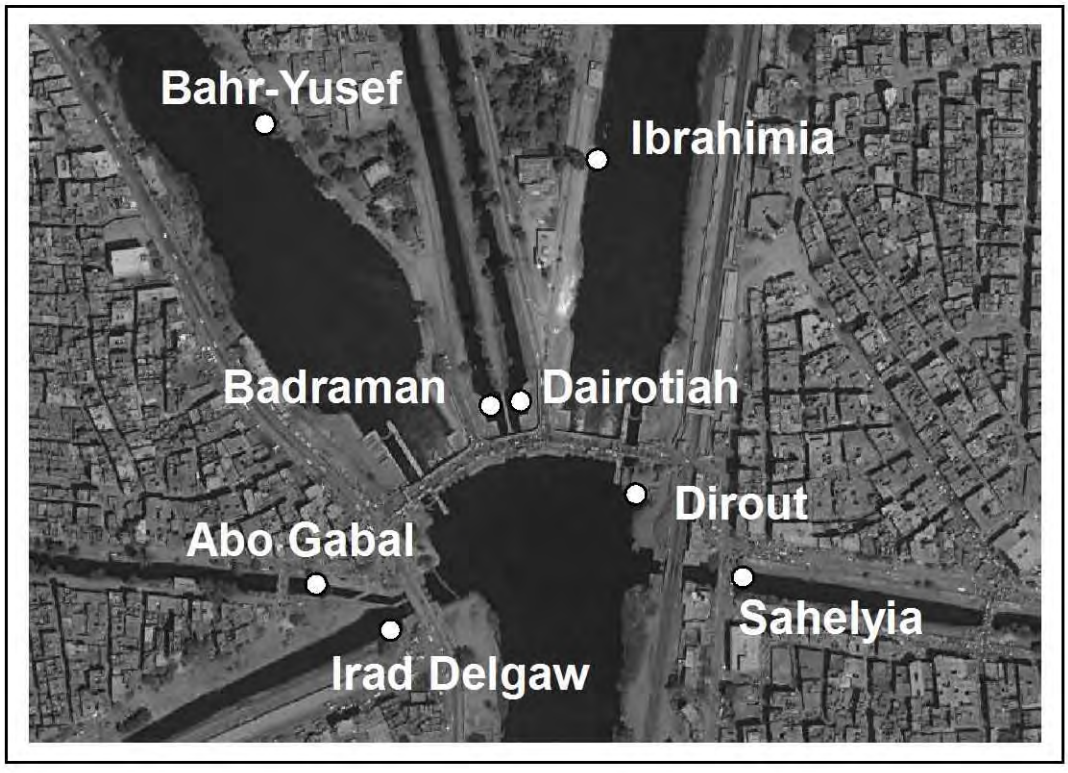

Figure 2-2.33 Measuring point of water level

ii) Results and evaluation of analysis

Figure 2-2.34 shows the location of the observation sections, and Table 2-2.8 and Figure 2-2.35 both show the comparison between the observed water level and discharge volume, and the calculated water level and discharge volume at each section.

Firstly, the results in the figures and the table show similar average discharge and water levels, which indicate that the calculations under the conditions above are good enough to show the flow state at the planning stage.

Figure 2-2.36 and Figure 2-2.37 show the velocity distribution map of the surface layer and the bottom layer in the planning stage. Figure 2-2.38 and Figure 2-2.39 show the enlarged map of Figure 2-2.36 around the two new large regulators.

Secondly, the results above, show the stagnation area in the downstream of the new regulators as recorded in the physical hydraulic model: on the left bank of the Bahr Yusef canal, and the right bank of the Ibrahimia canal. According to Figure 2-2.39, the bottom flow velocity at the first vent from the right side is faster than that at the other new Ibrahimia vents, which also corresponds to the physical hydraulic model test results.

Figure 2-2.40 shows the water level distribution map at the planning stage. Figure 2-2.42 and Figure 2-2.43 show the cross-sectional velocity distribution at each cross-section: 30m, 50m, and 100m downstream from the new regulators as located and marked in Figure 2-2.41.

Results from those figures indicate the followings;

- The flow velocity distribution at 30m and 50m downstream of each regulator effectively reproduce the effect of piers, showing the lower velocities with regular distance (Figure 2-2.42, and 2-2.43).
- The velocity at the 30m downstream from the new regulators is at most 1.2m/s on average, showing lower velocity further downstream.

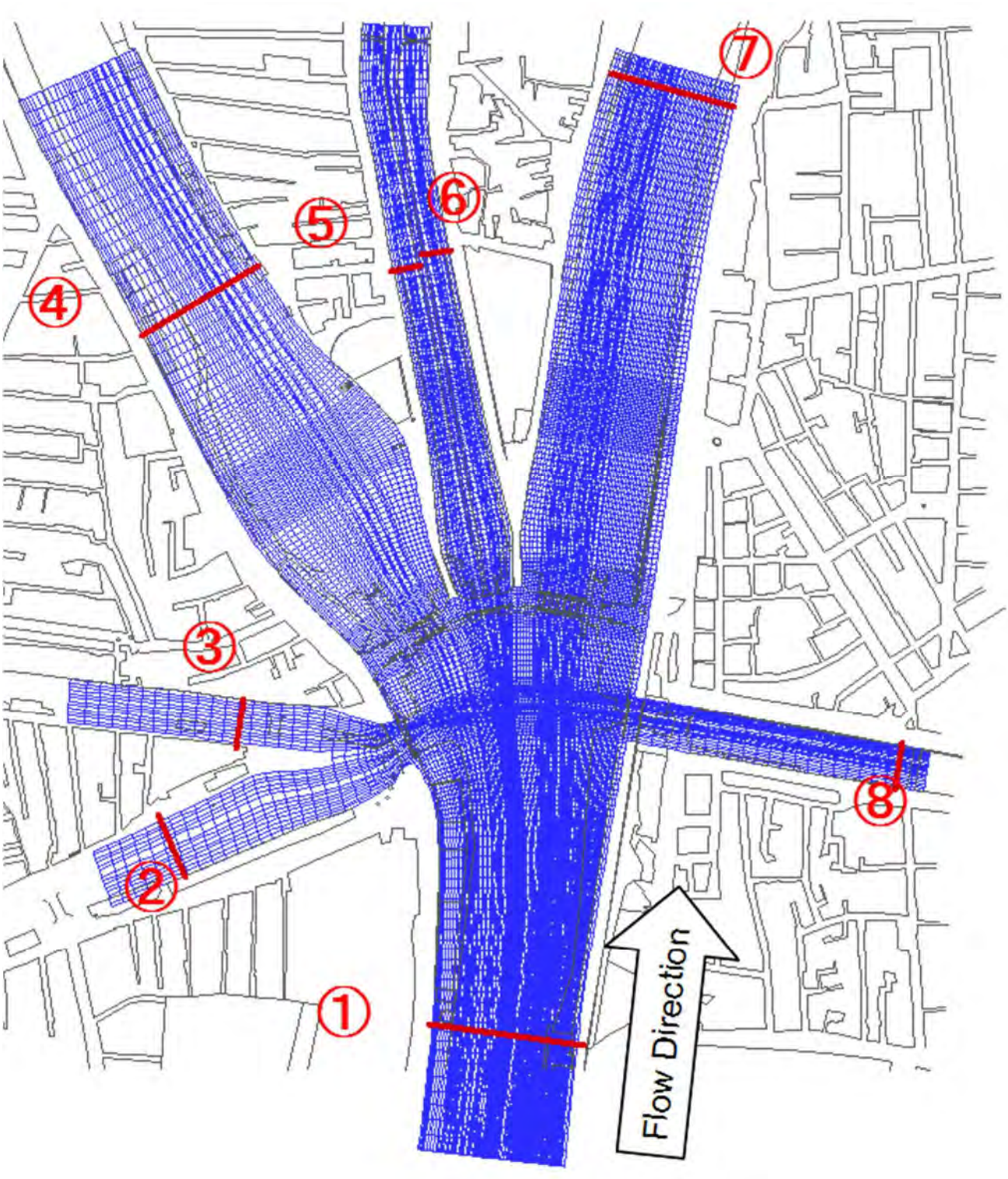

Figure 2-2.34 Observation sections

Table 2-2.8 Comparison between the calculation results (calc) and observed results (target) of the discharge volume and the average water level at the observation sections

Canal name	Discharge			Water level		
	Calc	Target	Difference	Calc	Target	Difference
Ibrahimia canal U/S	455.0	455.0	0.0%	46.3	46.3	-0.1%
Irad Delgaw canal	9.0	9.0	-0.3%	45.8	45.9	-0.2%
Abo Gabal canal	7.1	7.0	1.5%	46.0	45.9	0.2%
Bahr Yusef canal (1)	228.7	227.0	0.7%	45.8	45.8	0.0%
Badraman canal	8.9	9.0	-0.7%	45.9	45.9	0.0%
Dairutiah canal	11.9	12.0	-0.7%	45.9	45.9	0.0%
Ibrahimia canal D/S (	184.4	186.0	-0.8%	45.1	45.1	0.0%
Sahelyia canal	5.0	5.0	-0.7%	45.9	45.9	0.0%
		(m^3/s)	(%)		(m)	(%)

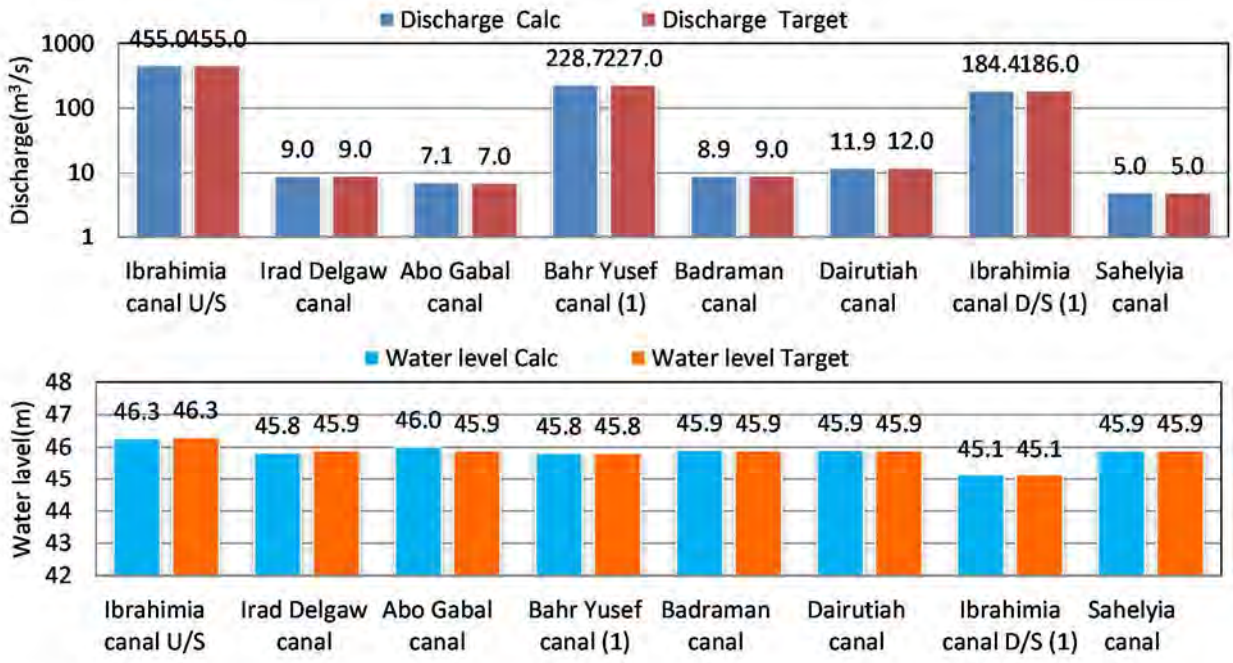

Figure 2-2.35 Comparison between the calculation results (calc) and observed results (target) of the discharge volume and the average water level at the observation sections

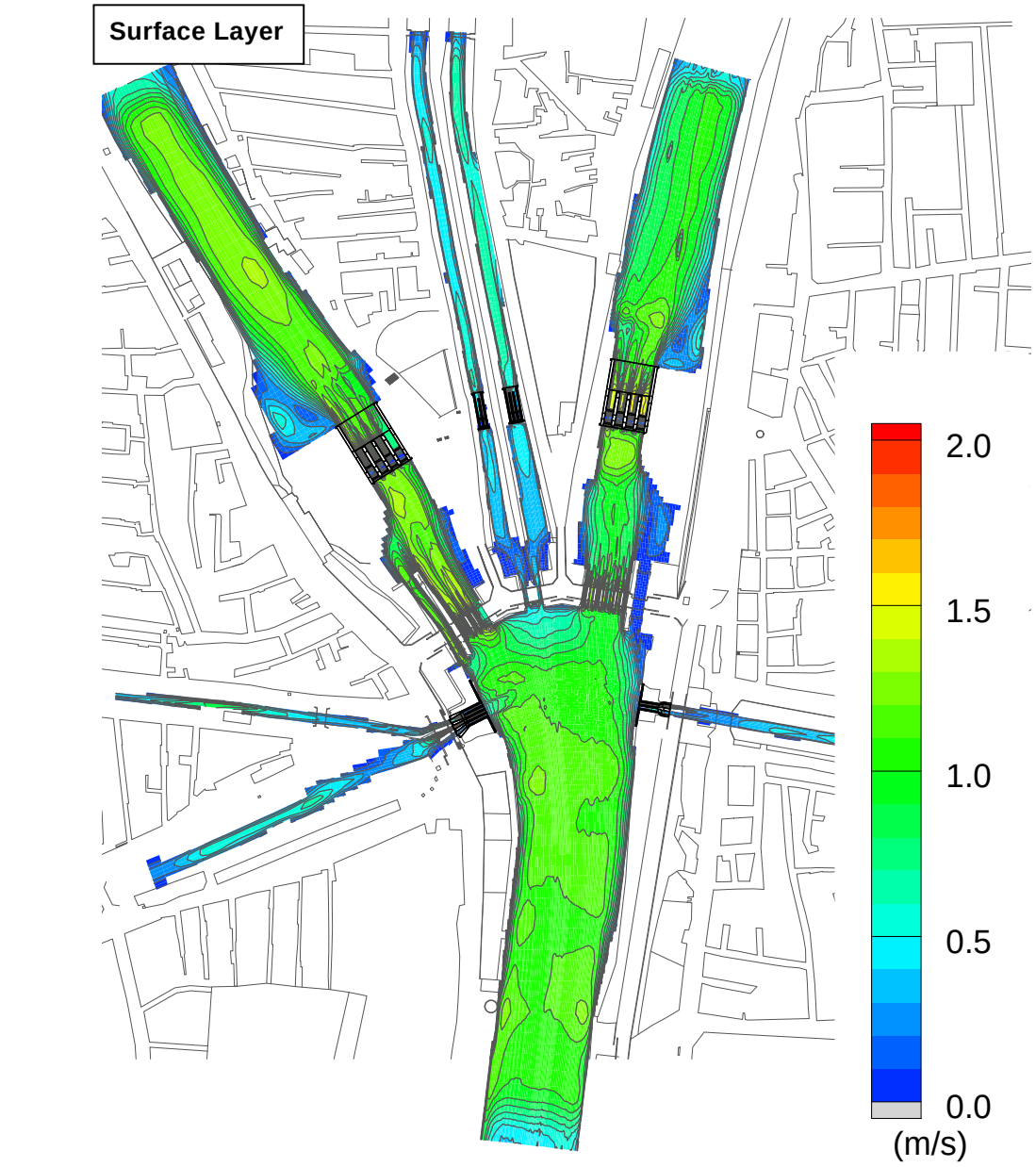

(a) All area

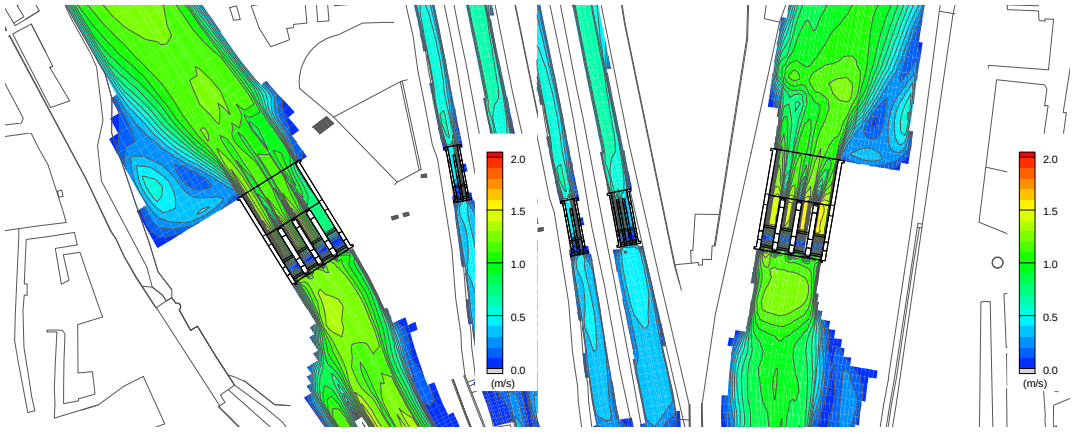

(b) Bahr Yusef new regulator (c) Ibrahimia new regulator

Figure 2-2.36 Velocity contour map of the surface layer at the planning stage

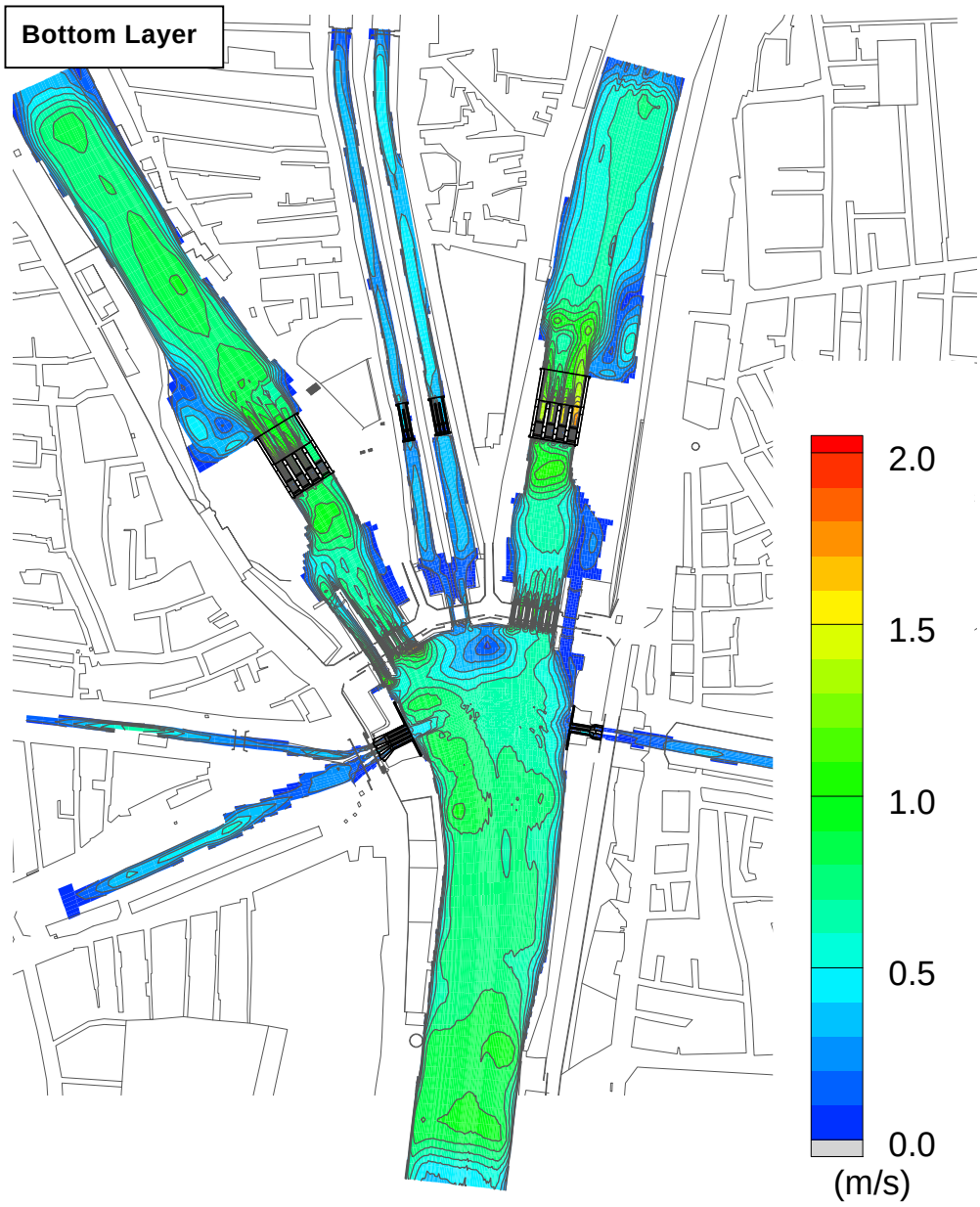

(b) All area

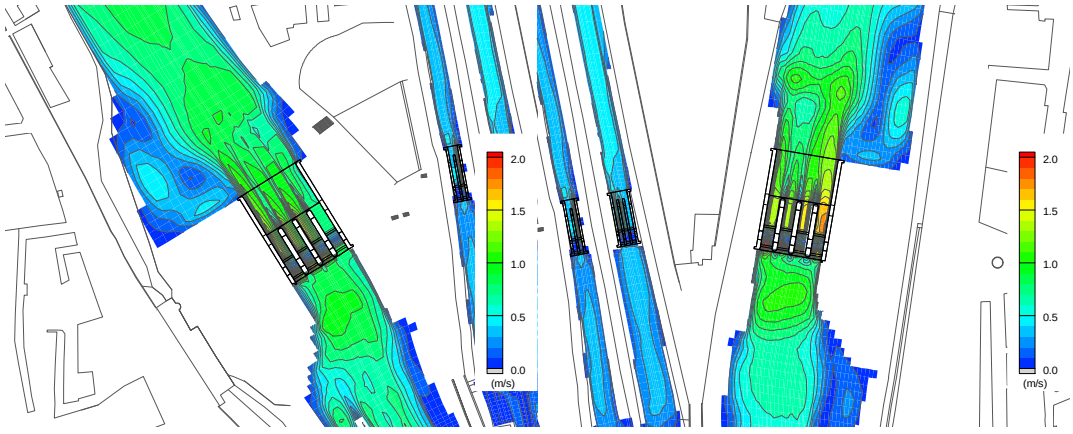

(b) Bahr Yusef new regulator (c) Ibrahimia new regulator

Figure 2-2.37 Velocity contour map of the bottom layer at the planning stage

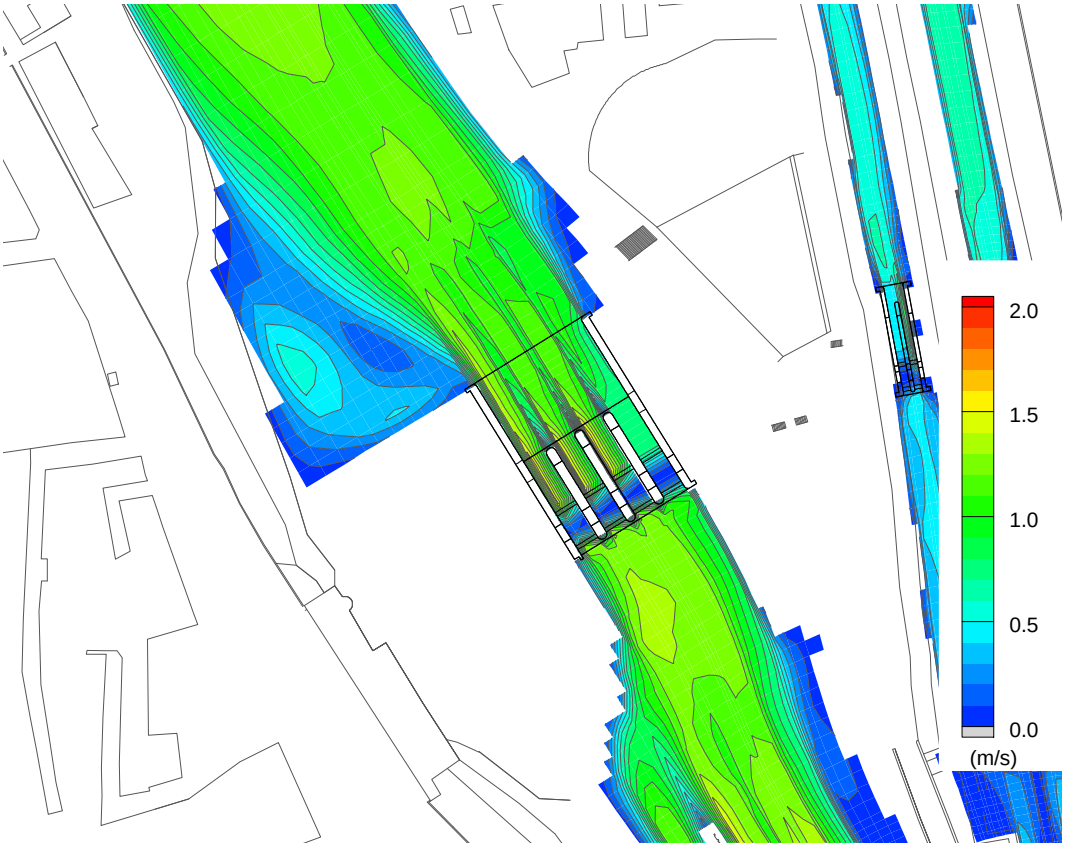

Figure 2-2.38 Velocity contour map of the surface layer at the planning stage (around the new Bahr Yusef regulator)

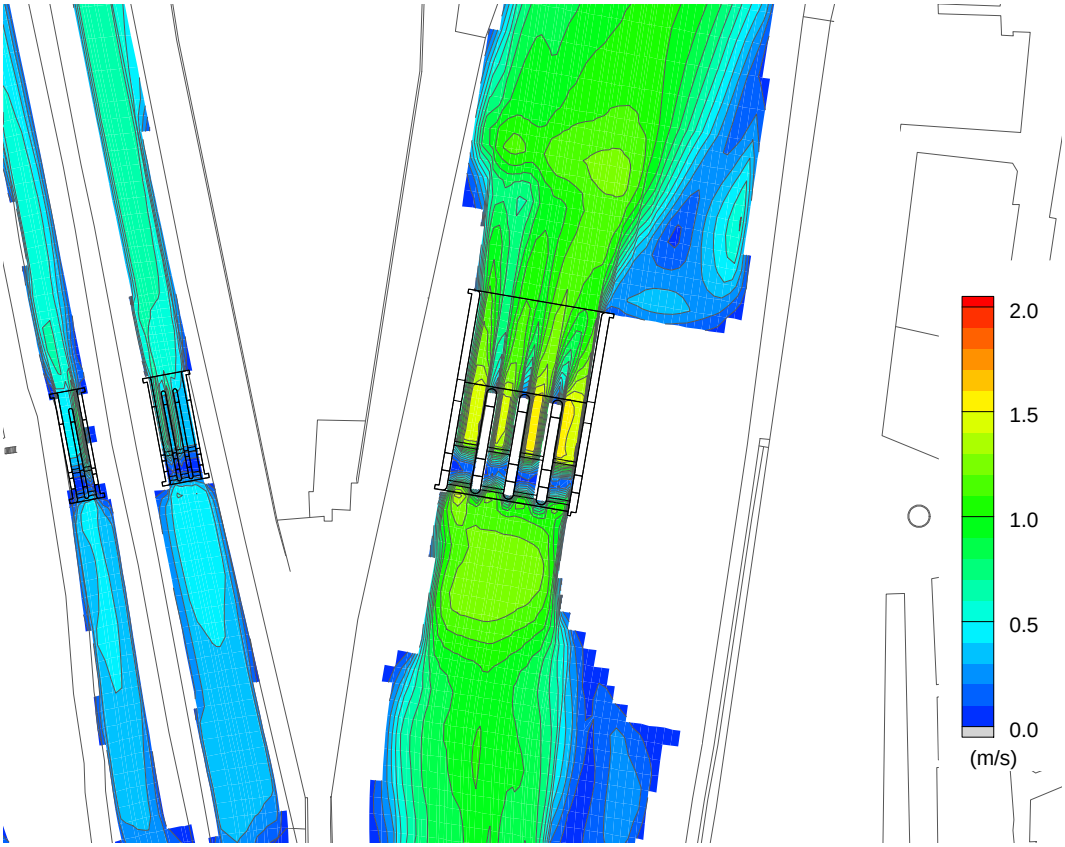

Figure 2-2.39 Velocity contour map of the surface layer at the planning stage (around the new Ibrahimia regulator)

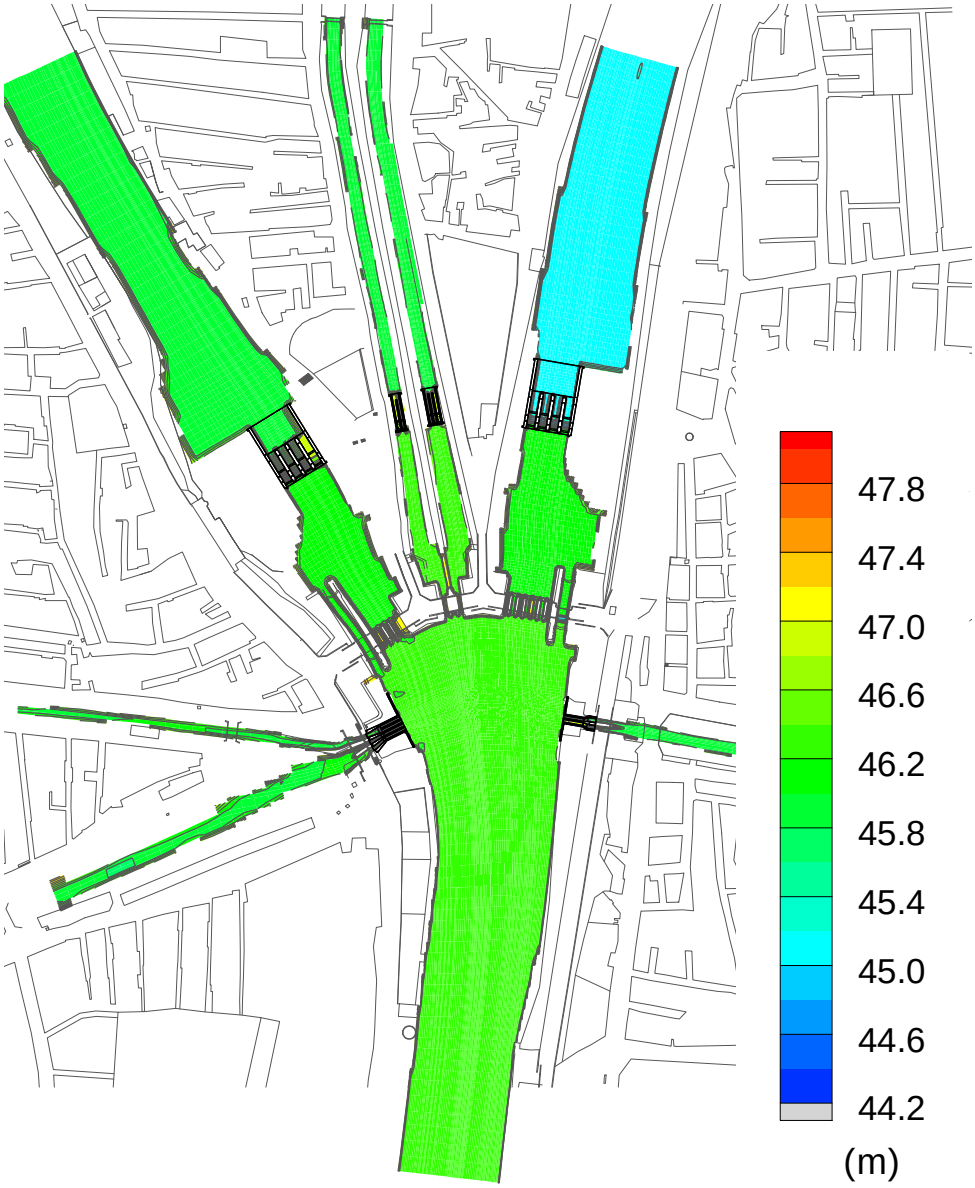

Figure 2-2.40 Water level contour map at the planning stage

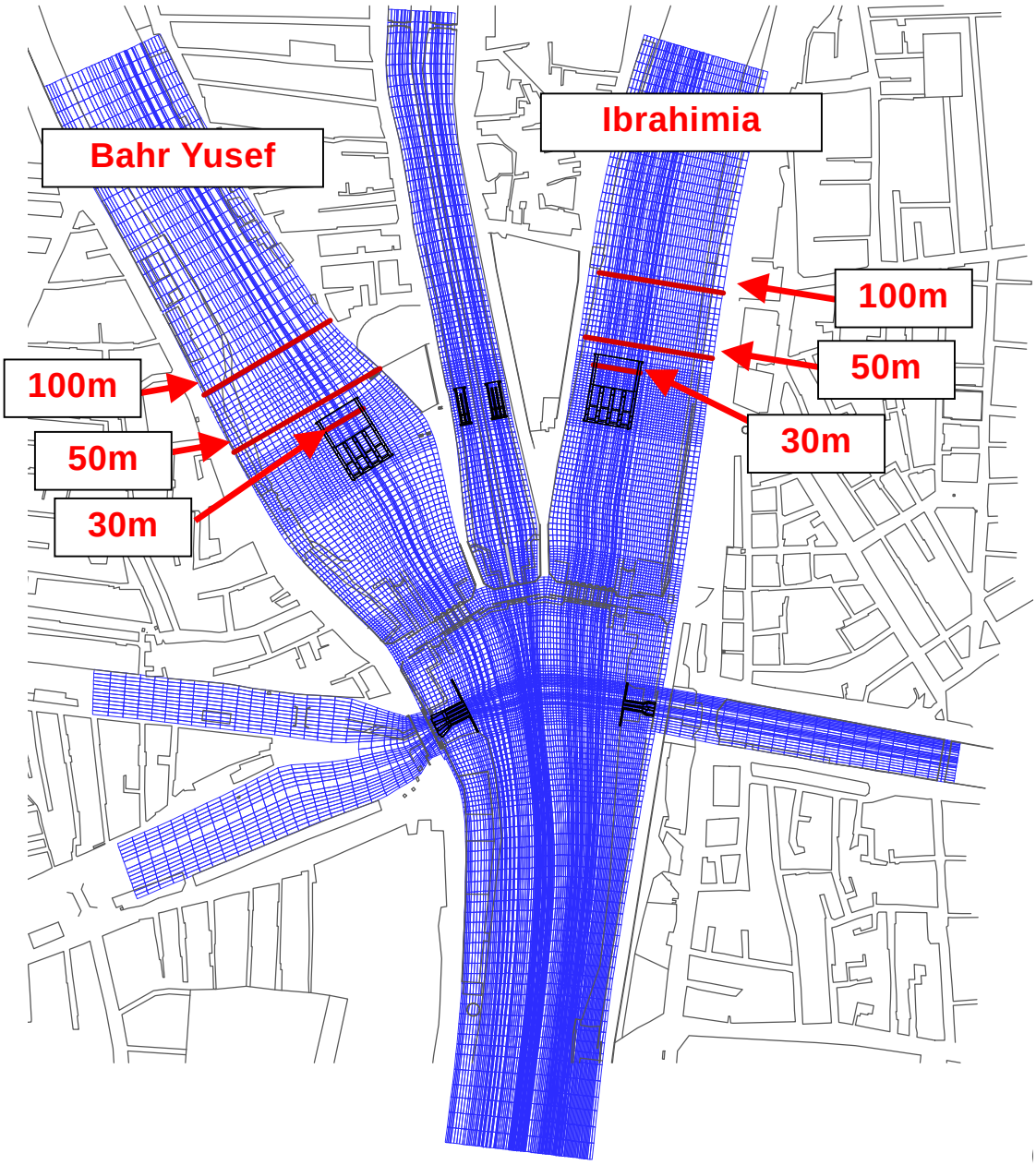

Figure 2-2.41 Location of the cross-sectional lines

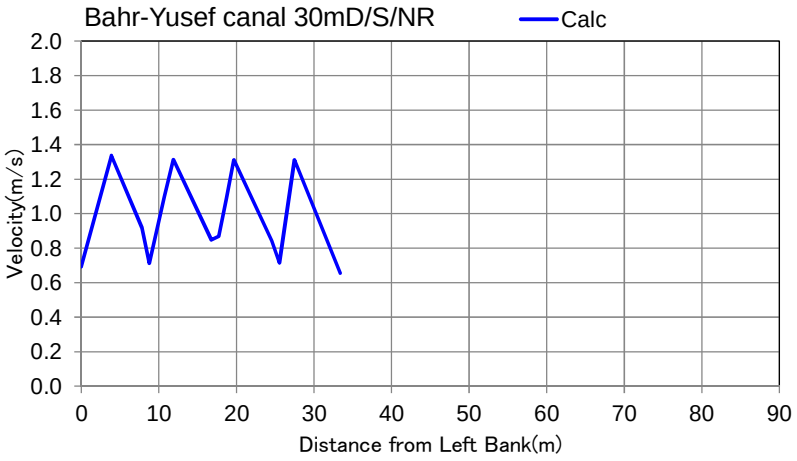

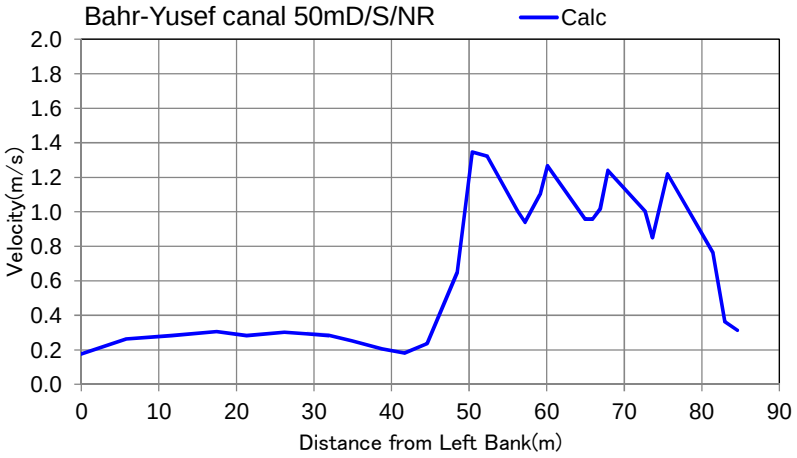

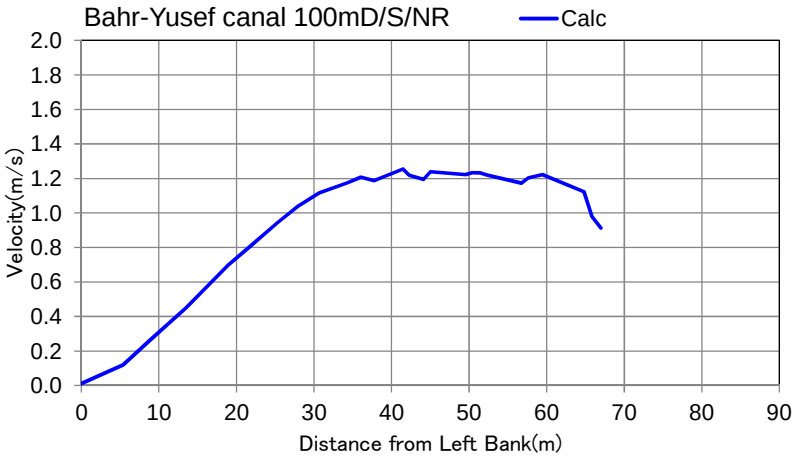

Figure 2-2.42 Cross-sectional velocity
(Bahr Yusef canal 30, 50, 100m downstream of the new regulator)

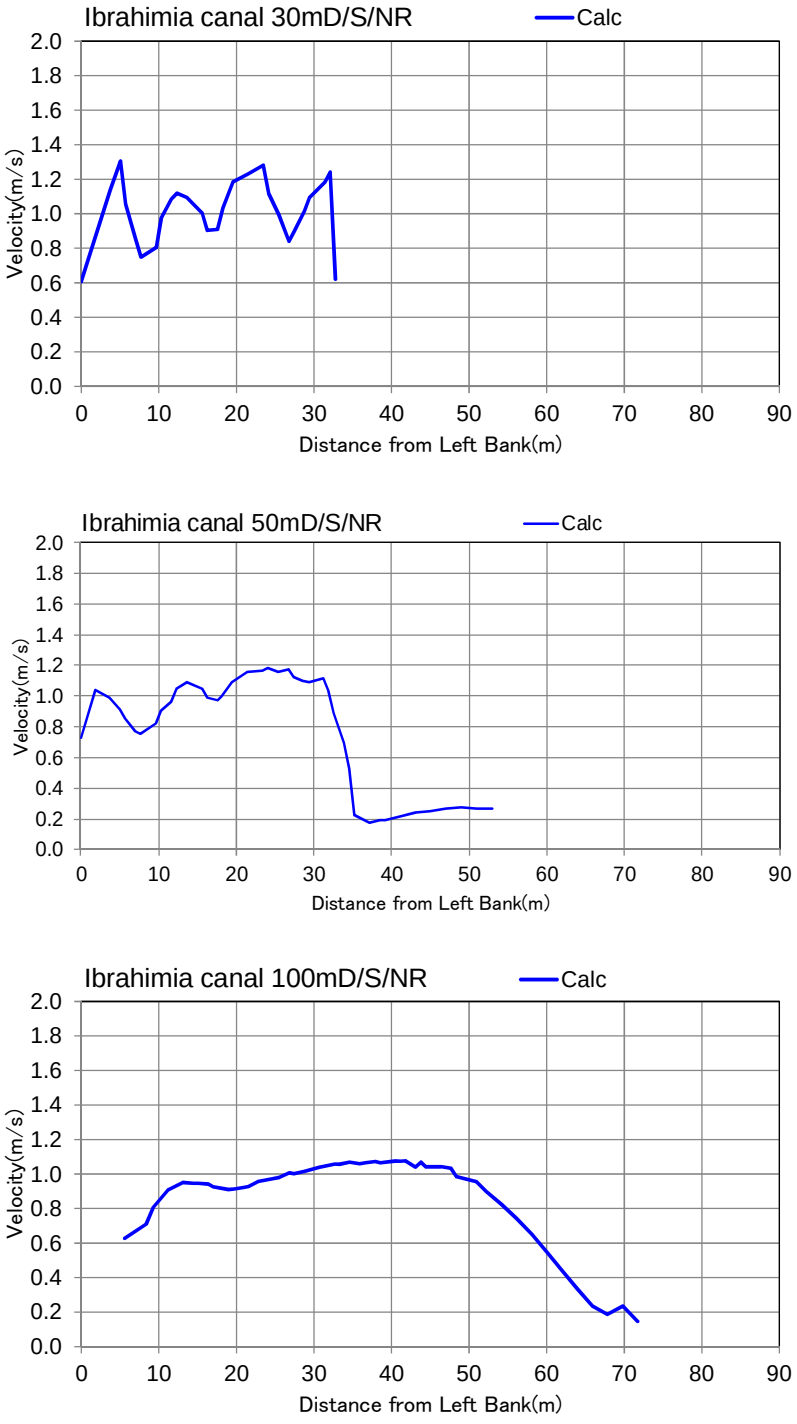

Figure 2-2.43 Cross sectional velocity
(Ibrahimia canal 30, 50, 100m downstream of the new regulator)

6) Analysis of flow situation after changing sill elevation of upstream small-scale regulators

After the basic design was settled, RGBS requested to change sill elevation values of two upstream small-scale regulators to a lower height. After examining the possibility, it was decided to change the elevation values as described below. This flow situation analysis was conducted at the design stage in order to confirm the impacts of changing sill elevations of the two upstream small-scale regulators.

Survey values acquired in January 2016 in the same topographic map as in that to which the regulator design was applied were used for survey data such as canal conditions.

a) Analysis conditions

For comparison of the results of tests using the both models, the following conditions are applied in the flow situation analyses. The analyses for the comparison were made for the new Dirout Group of Regulators (in the design stage).

Table 2-2.9 Analytical conditions

Analysis Conditions	Basic Design Report (BDR)	Analysis for Comparison
1. Topographic data	January 2016	Same as BDR
2. Number of meshes	198,380 meshes in total	Same as BDR
3. Boundary conditions	Upstream side of existing regulators: Discharge End of each canal: Water level	Same as BDR
4. Water level discharge	Design stage (new regulators)	Same as BDR
5. Sill elevation value of 2 upstream small-scale regulators	New Abo Gabal Regulators: EL. 44.15m New Saheliya Regulators: EL. 44.65m	New Abo Gabal Regulators: EL. 43.6m New Saheliya Regulators: EL. 43.0m

i) Topographic conditions

The topographic data from the survey conducted in January 2016 was applied. (Fig. 2-2.44)

ii) Number of meshes

The total number of meshes was the same as described in the Basic Design Report. (Fig. 2-2.45)

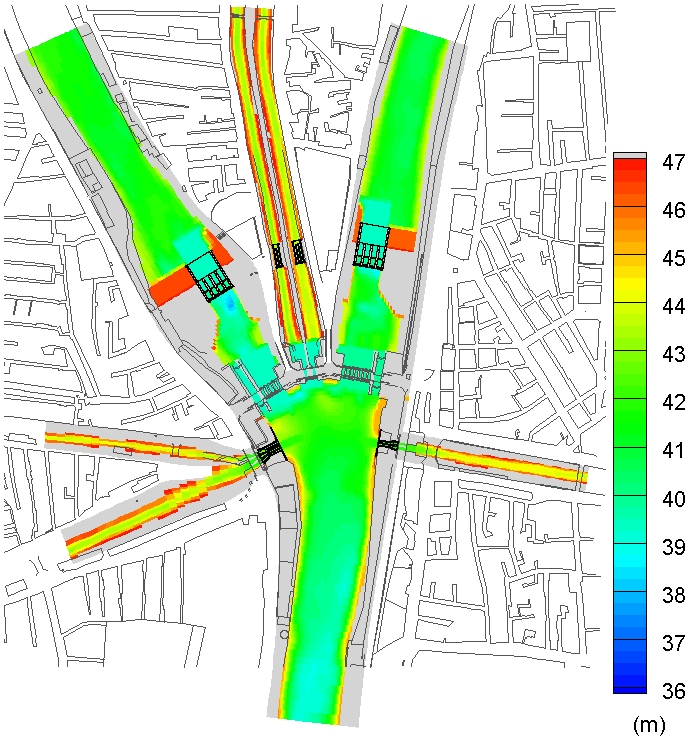

Figure 2-2.44 Topographic map (design in January 2016 – new regulators)

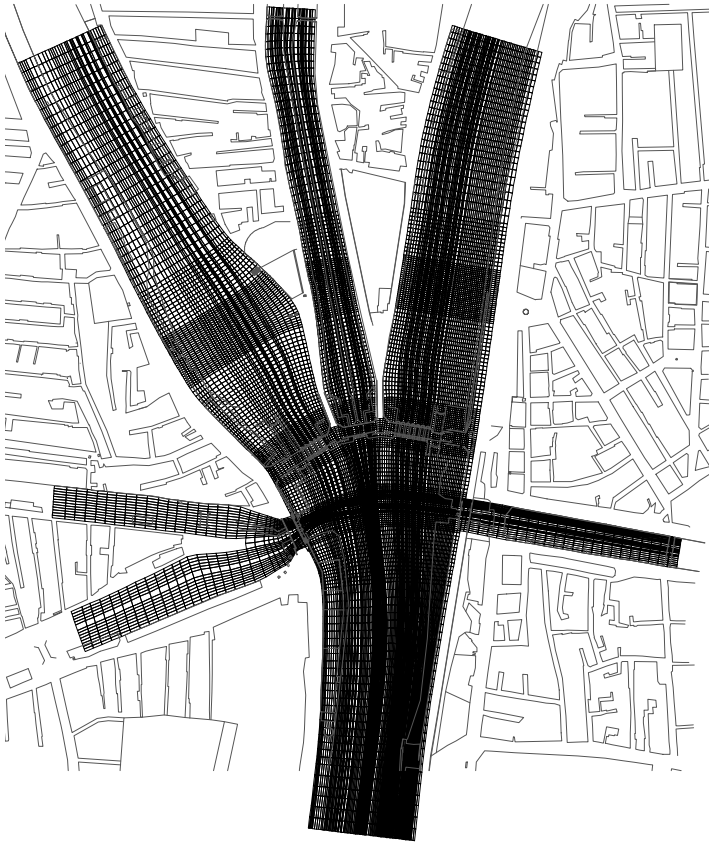

Figure 2-2.45 Canal meshes map

iii) Boundary conditions

The boundary conditions are as follows:

- Discharge boundary: Upstream side of the existing regulators
- Water level boundary: At each canal end

iv) Water level, inflow in each regulator and discharge from each new regulator

The water level applied as the water level boundary is based on the data of the Water Allocation Bureau as shown in Table 2-2.10 (this is also applied to the design of the new regulators). The discharge boundary is 455 m^3/s at the upstream end.

Table 2-2.10 Water level, inflow in regulators and discharge from new regulators

Item	US. of Regulators	DS. of regulators							Remarks
	existing DGRs	Bahr Yusef	Ibrahimia	Badraman	Diroutiah	Abo Gabal	Irad Delgaw	Sahelyia	
Water Level (m)	46.30	45.82	45.13	45.90	45.90	45.90	45.90	45.90	Target Value
Inflow (m^3/s)	455	—	—	—	—	—	—	—	Up stream
Outflow of regulator (m^3/s)	—	27	186	9	12	7	9	5	Target Value

b) Analysis results and evaluation

It was discovered that, even if the sill elevation of the upstream small-scale regulators was changed, the discharge conditions in the vicinity of the regulators had no change because the inflow quantity into each small-scale canal was controlled to the same quantity as before the change of the sill elevation value. Therefore, it can be said that the change of the sill elevation of the two upstream small-scale regulators has no impact on the design discharge.

The discharge comparison maps of the DGRs are shown in Figure 2-2.46, the discharge comparison maps of the vicinity of the new Abo Gabal regulators in Figure 2-2.47, and the discharge comparison maps of the vicinity of the new Saheliya regulators in Figure 2-2.48. Each figure shows that the discharge has no change before and after the change of the sill elevation.

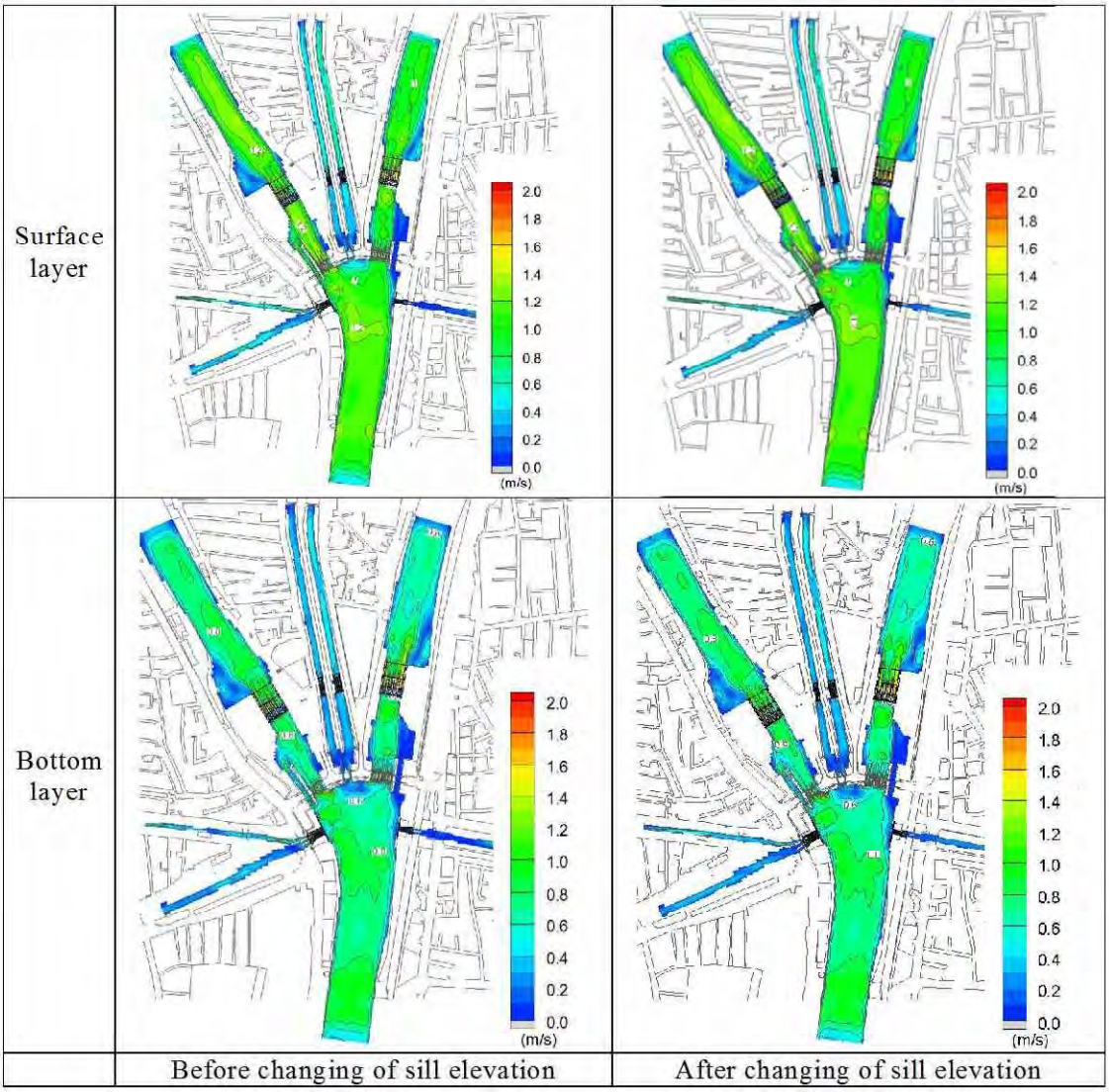

Figure 2-2.46 Discharge comparison maps of DGRs

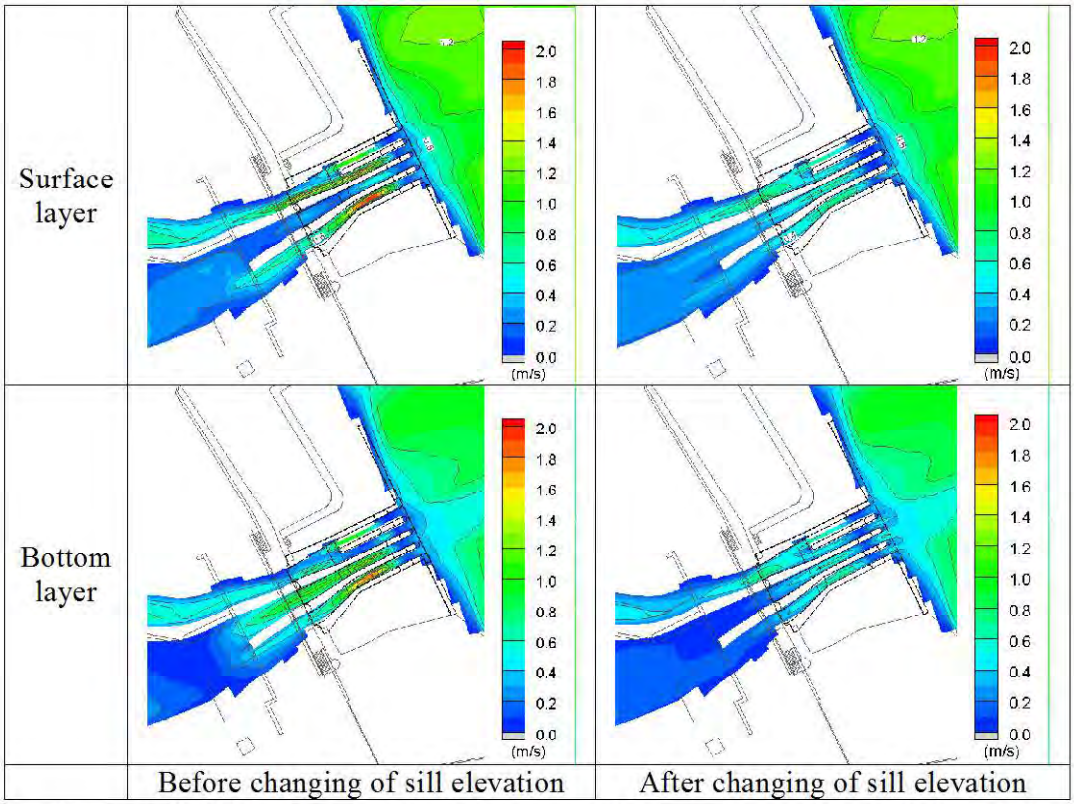

Figure 2-2.47 Discharge comparison maps of vicinity of new Abo Gabal regulator

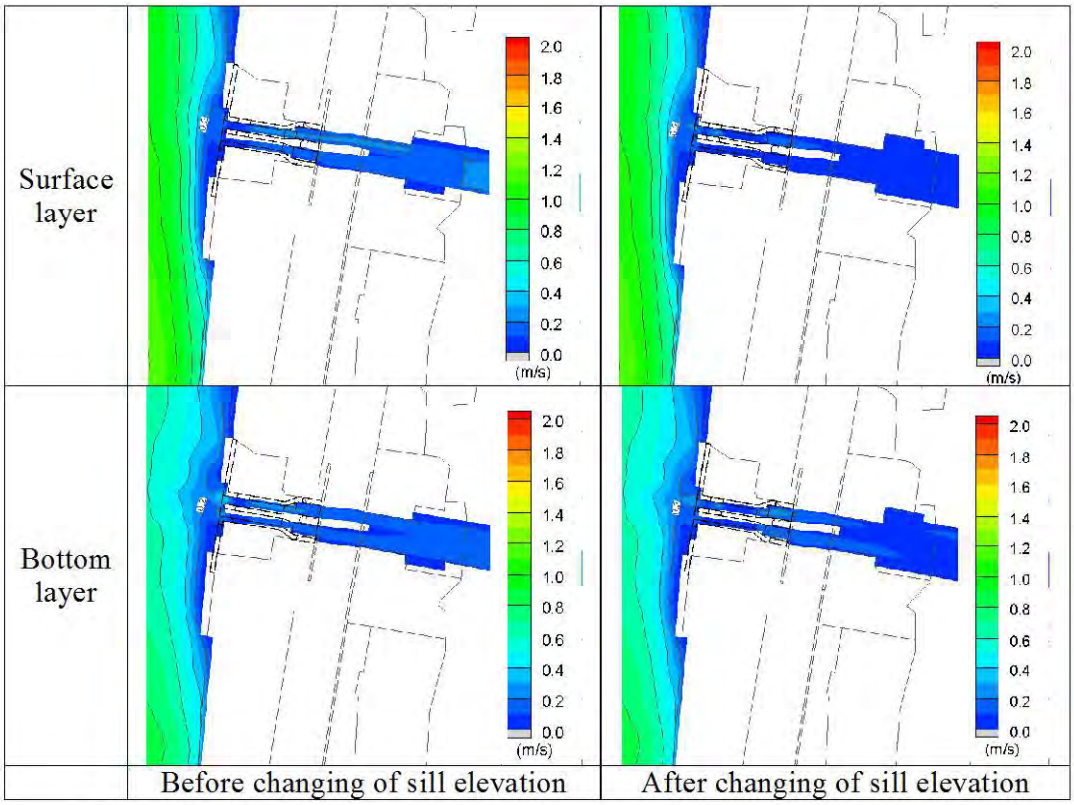

Figure 2-2.48 Discharge comparison maps of vicinity of new Saheliya regulator

7) Installation of guiding wall at the two upstream small-scale regulators

In the two upstream small-scale regulators of the DGRs, sedimentation occurs on the front of the regulators, and there is concern that the water intake function will decline.

The planned facility is to be installed on the front of the existing regulator to reduce the influence of sediment and ensure effective water intake.

The hydrological analysis confirmed that planned intake and sedimentation on the front of the new regulator would decrease.

On the other hand, to further stabilize the water intake function, a proposal was made to install a flow-guiding wall at the front of the intake regulator. The pros and cons of this proposal are discussed below.

For the Sahelyia regulator with a maximum discharge of 5 m^3/s, a flow condition analysis was conducted under the conditions of the designed discharge when a flow-guiding wall of about 6m was installed in front of the new regulator. The flow velocity contour map is shown below.

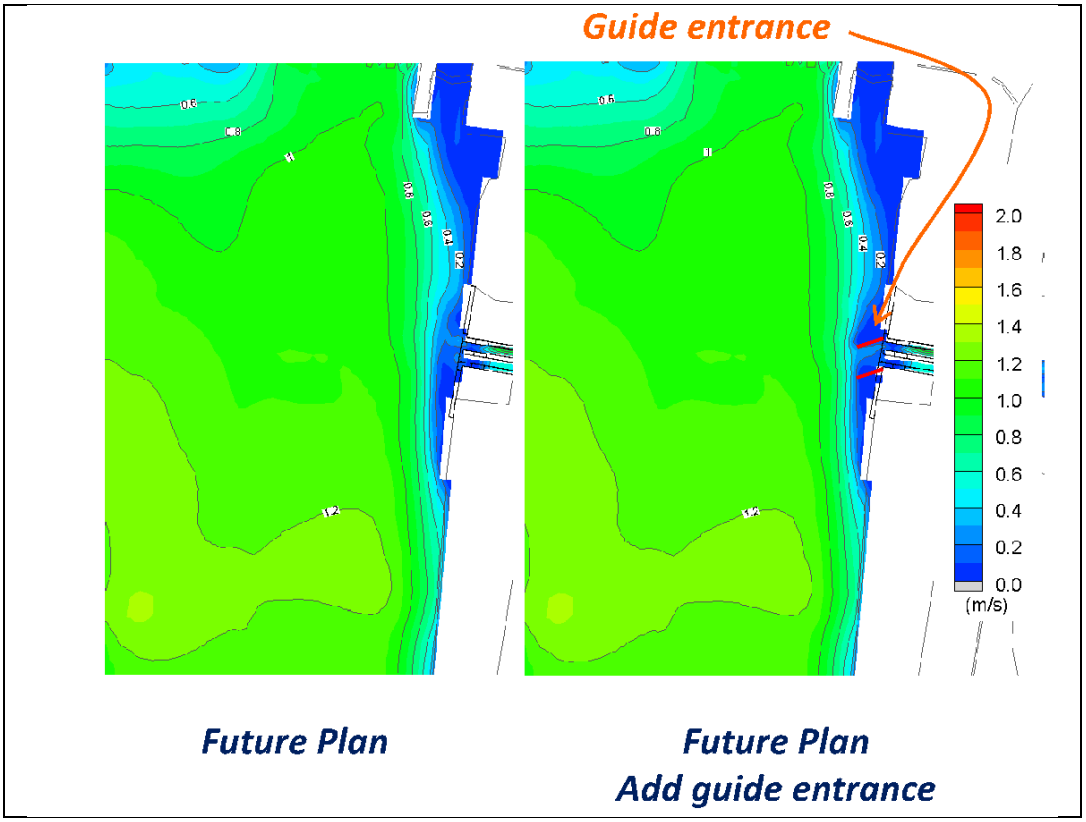

Figure 2-2.49 Flow velocity contour map
(when 10 m flow-guiding wall is installed on the front of the new Sahelyia regulator)

i) Intake

Before installing the flow-guiding wall, the front side of the regulator had a slow flow region with a flow velocity of 0.2m/s or less and in the absence of approaching flow velocity, intake discharge was present.

The analysis conducted with the guiding wall showed that the 10m wall only caught the slow flowing water that moved at a flow velocity of 0.2m/s or less, and that the desired effect of

increasing the water intake discharge due to the installation of the guiding wall was only minimally achieved. Therefore, the installation of the guiding wall to the two upstream small scale regulators was judged to be inutile.

ii) Sedimentation

The installation of the guiding wall has potential negative impacts, such as: the expansion of the sediment-catching range due to the aggressive introduction of sediment into the canal, and the reduction of sediment removal efficiency at the front of the regulator.

iii) Other

The installation of a flow-guiding wall will increase construction costs.

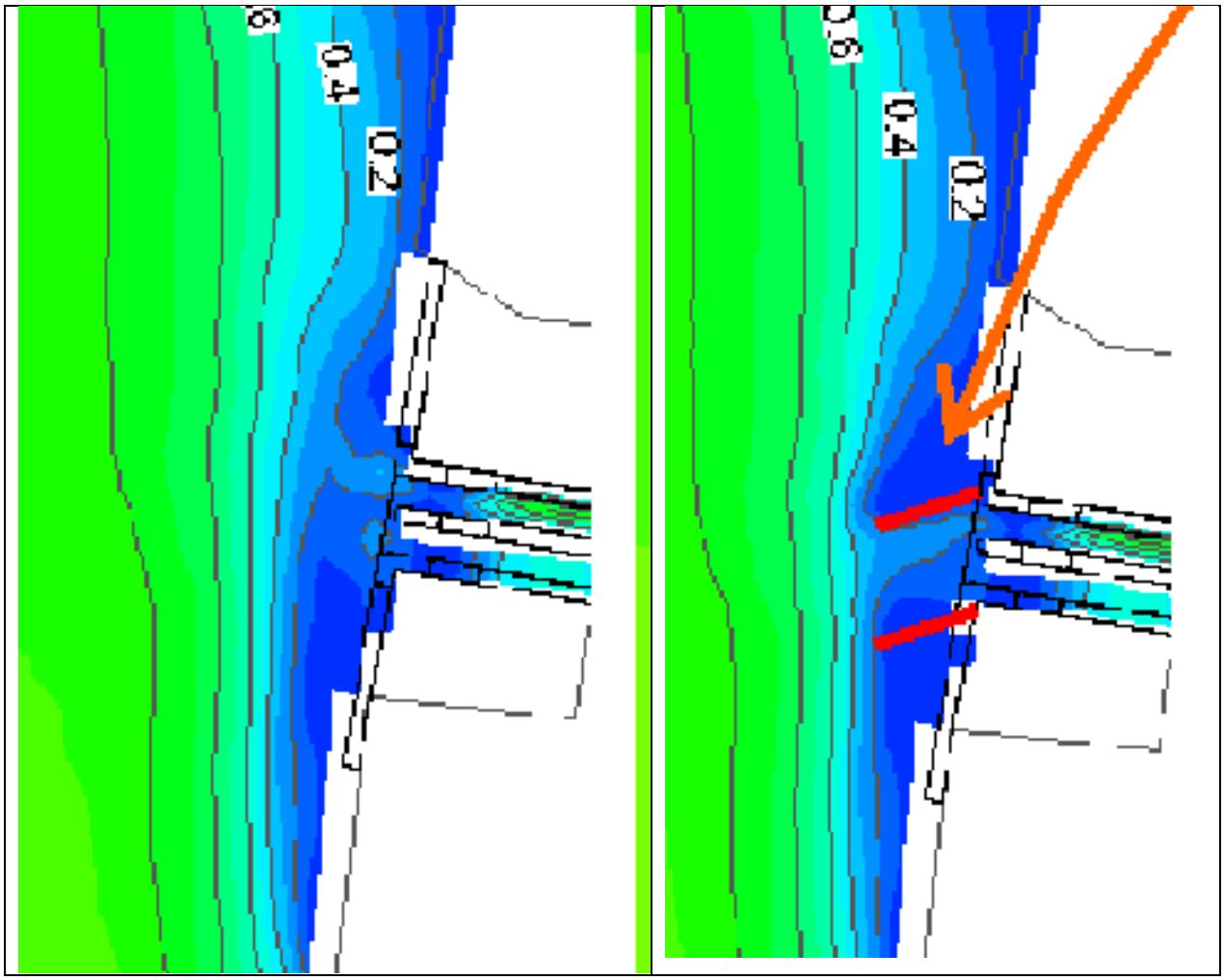

Figure 2-2.50 Flow velocity contour map (around the new Sahelyia regulator)

8) Impacts of navigation lock opening of existing Ibrahimia regulator on the new Sahelyia regulator and new Ibrahimia regulator

Navigation lock is installed in the existing Bahr Yusef regulator and the existing Ibrahimia regulator and are closed at present. After construction of the NDGRs, the navigation lock of the existing Bahr Yusef regulator will be opened; nevertheless, it was presumed that the navigation lock of the existing Ibrahimia regulator would remain closed because the neighboring area of these navigation locks would be used for another purpose after the surrounding area of the new DGRs is redeveloped. The hydraulic analysis was also made on the condition that there was no discharge from this navigation lock.

As a result, it was discovered that the flow velocity tended to be a little gentle in the front of the new Sahelyia regulator located on the upstream side of the existing Ibrahimia regulator and that the bottom flow velocity might be concentrated at the right-bank gates of the new Ibrahimia regulator.

This analysis was conducted to confirm the flow situation in the front of the new Sahelyia regulator and in the vicinity of the new Ibrahimia regulator by performing hydraulic analysis on the condition that the navigation lock of the existing Ibrahimia regulator were open.

a) Analysis conditions

The analysis conditions were the same as in the basic design, using the survey data in January 2016, the maximum discharge in the design stage and the sill elevation of the two (2) upstream small-scale regulators in the basic design.

b) Analysis results and evaluation

If the navigation lock of the existing Ibrahimya regulator is open, it was found that the flow in the front of the new Sahelyia regulator directed toward its sides and that the concentration of the bottom flow velocity on to the right-bank gates of the new Ibrahimia regulator was alleviated.

The discharge comparison maps of the upstream and downstream sides of the existing Ibrahimia regulator are shown in Figure 2-2.51, the discharge comparison maps of the new Sahelyia regulator in in Figure 2-2.52 and the discharge comparison maps of the new Ibrahimia regulator in Figure 2-2.53.

From these results, it can be said that it is better to open the navigation lock of the existing Ibrahimia regulator.

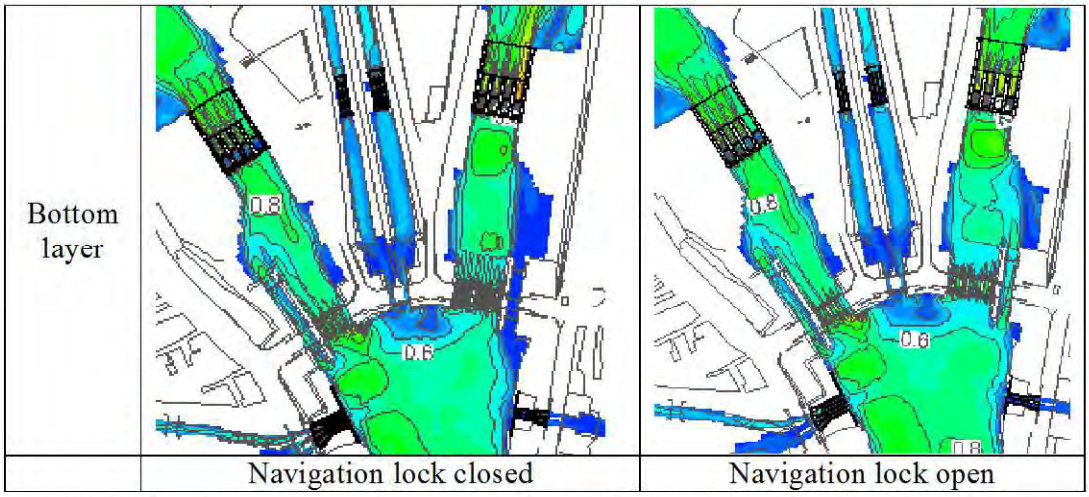

Figure. 2-2.51 Discharge comparison maps of upstream and downstream sides of existing Ibrahimia regulator

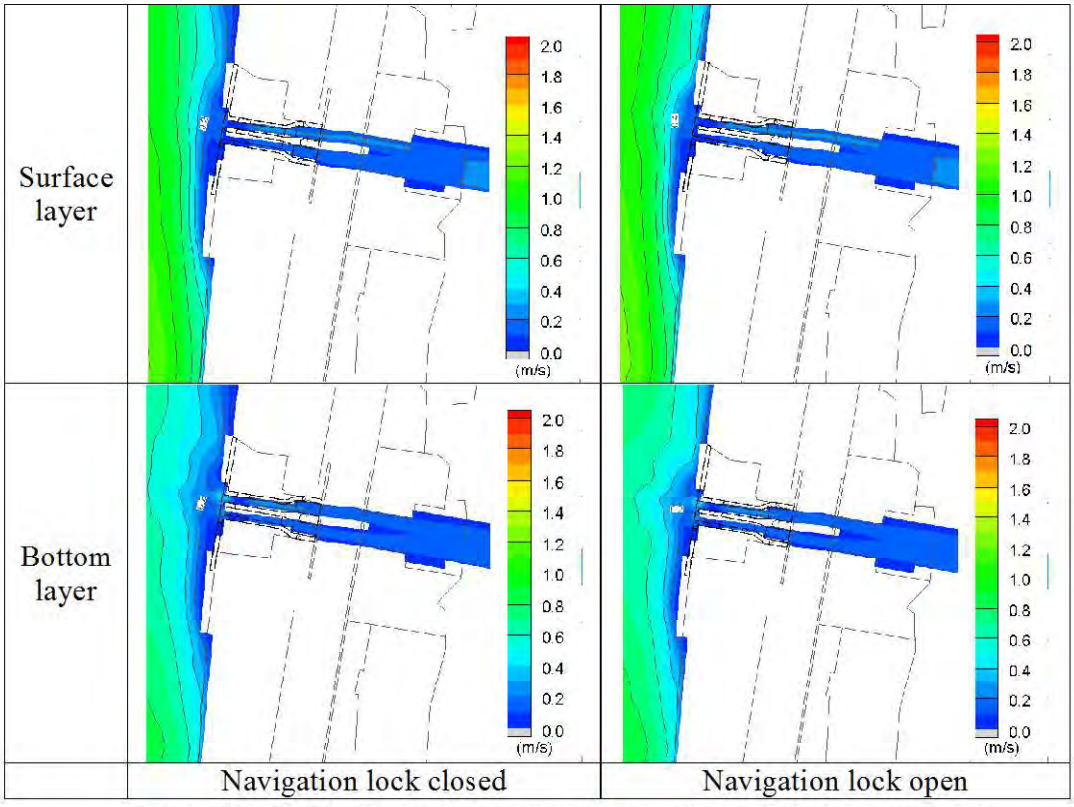

Figure 2-2.52 Discharge comparison maps of new Sahelyia regulator

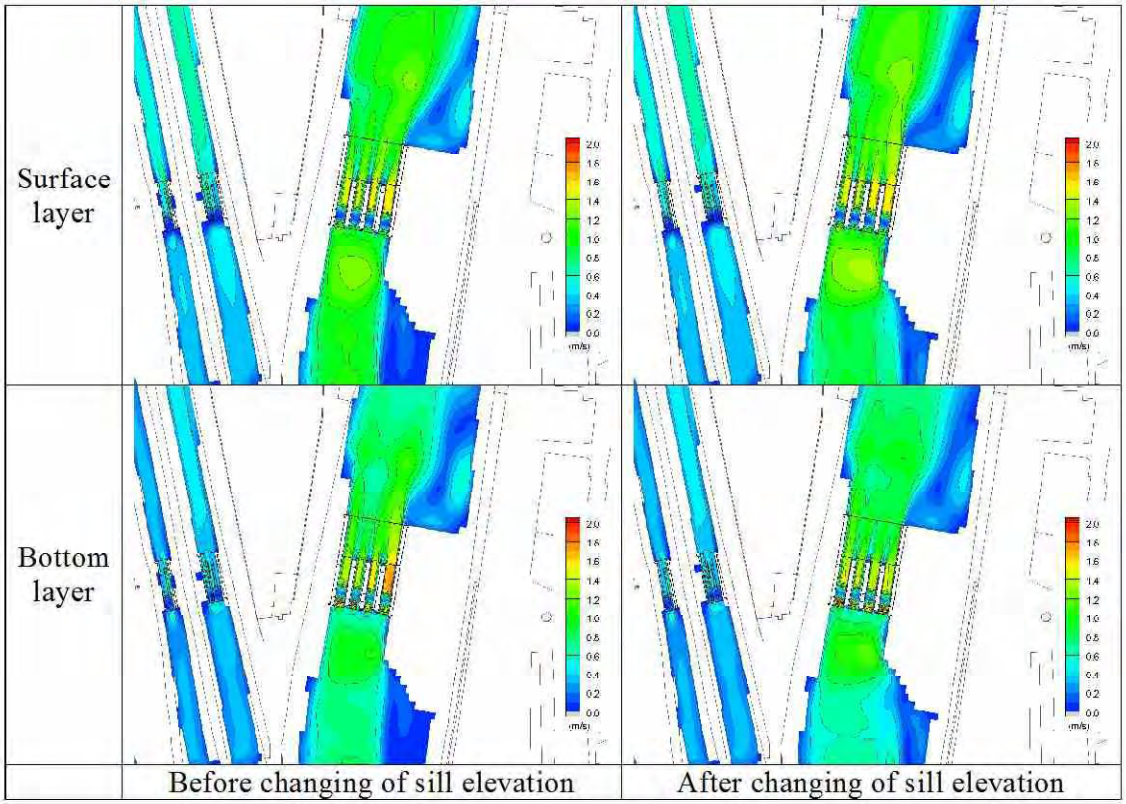

Figure 2-2.53 Discharge comparison maps of new Ibrahimia regulator

(2) Riverbed Variation Analysis

a) Analysis Results

1) Calibration

Taking the riverbed in January 2016 to be the initial riverbed for calibration, calculations were made for 11 months. Figure 2-2.54 shows a comparison between the observed riverbed variations and the riverbed variations at the end of the computation. The results of the erosion in the middle of the diversion channel showed that there was discharge from the Badraman regulator and the Diroutiah regulator when the water level was low.

However, in the analysis, there was no record of the regulators' operations, and there was too little erosion recorded in the calculations. In contrast, deposition trends at the front and the side of the Abo Gabal regulator and in front of the Sahelyia regulator have been reproduced. The presence of erosion trends downstream of the Ibrahimia regulator was therefore confirmed, as exhibited in actual performance. From the above, this analysis is judged to have reproduced trends in riverbed variation around the DGRs.

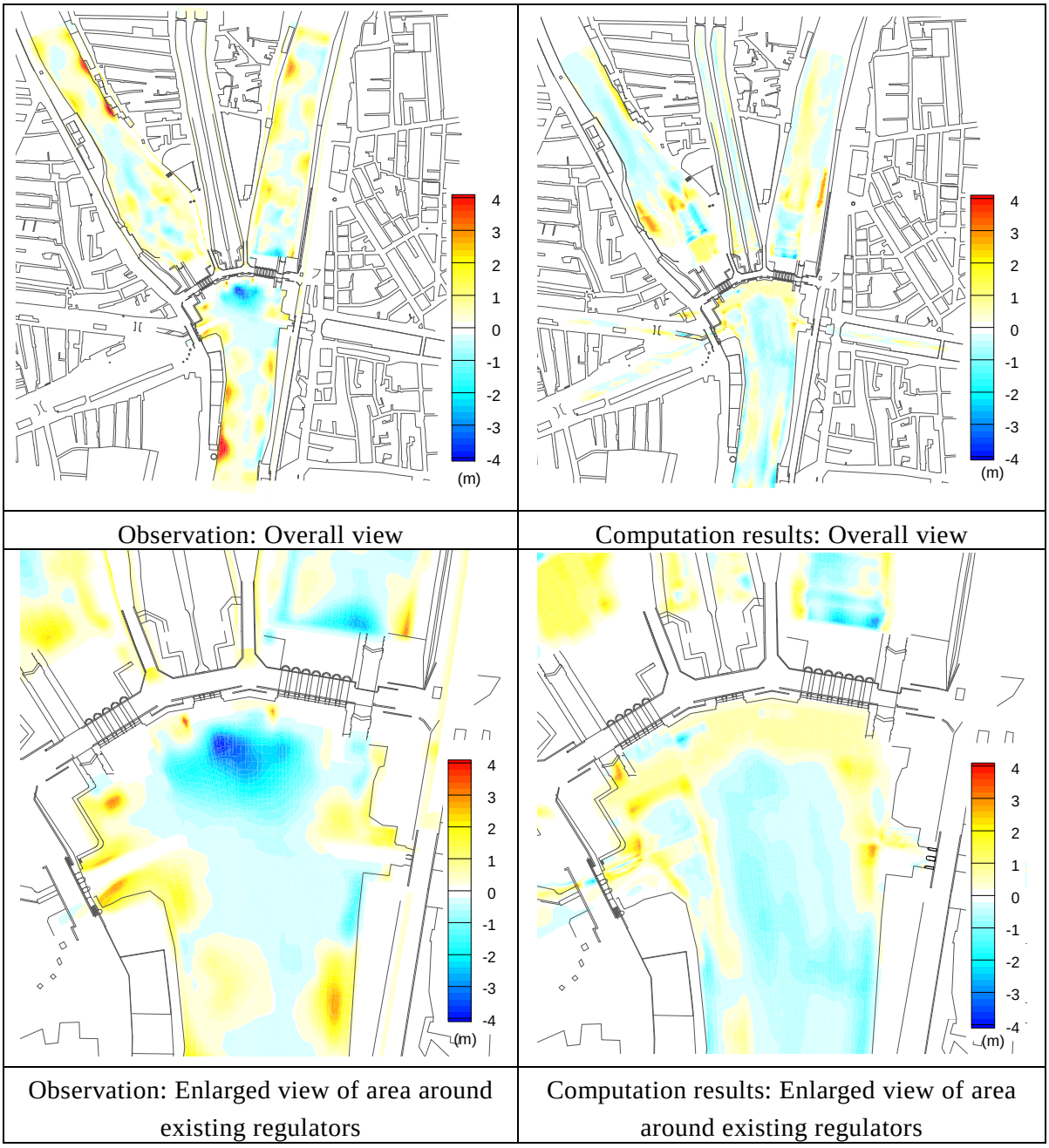

Observation: Overall view	Computation results: Overall view
Observation: Enlarged view of area around existing regulators	Computation results: Enlarged view of area around existing regulators

Figure 2-2.54 Result of the riverbed variation analysis (calibration stage)

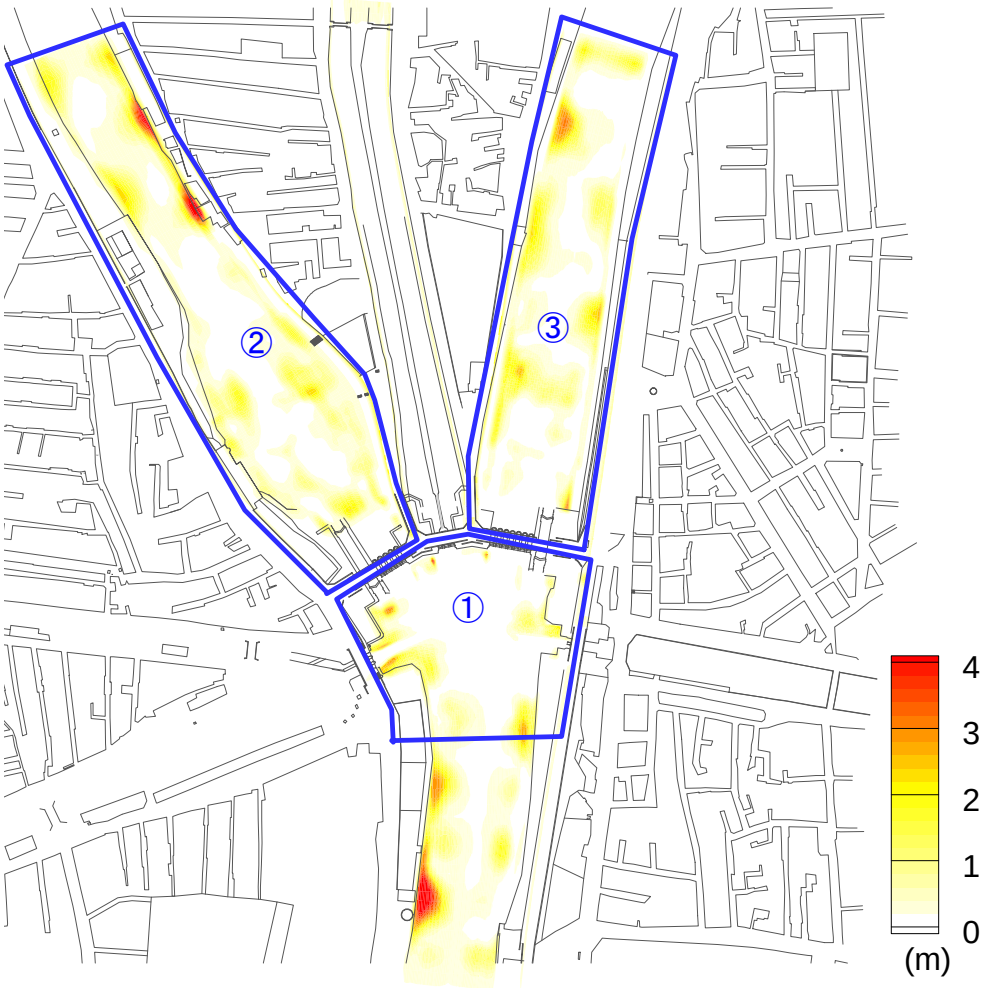

Figure 2-2.55 Distribution of sedimentation area

Table 2-2.11 Comparison of sediment volume

	Area	Sedimentation	
		Calc	Obs
①	Existing Regulator-Upstream150m	5,500	5,400
②	Bahr Yusef canal D/S	14,600	17,300
③	Ibrahimia canal D/S	10,100	12,400

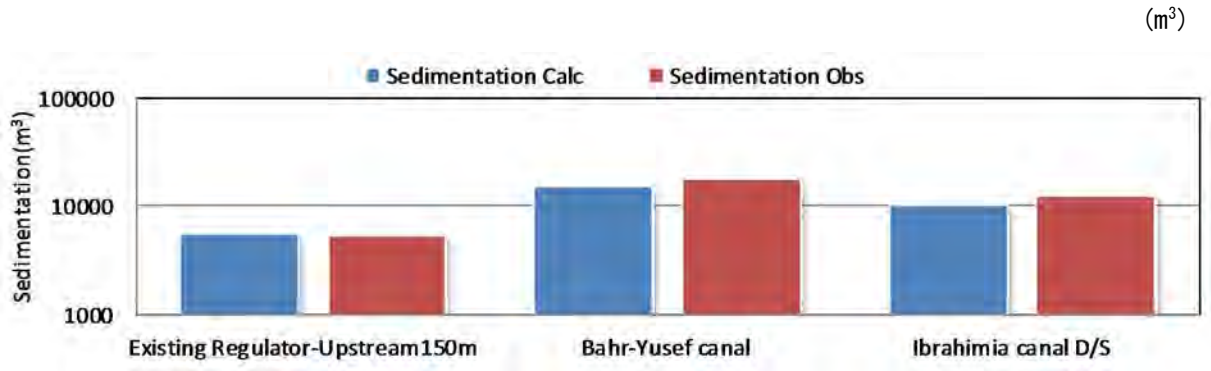

Figure 2-2.56 Comparison of sediment volume

2) Present Conditions

Riverbed variation was calculated based on average discharges for one year under present conditions. Figure 2-2.57 shows the riverbed variations at the end of the computation. Deposition is relatively substantial at the Ibrahimia regulator, because suspended sediment flows down the regulator and accumulates around 120m downstream, where the water is deep and the current is slow.

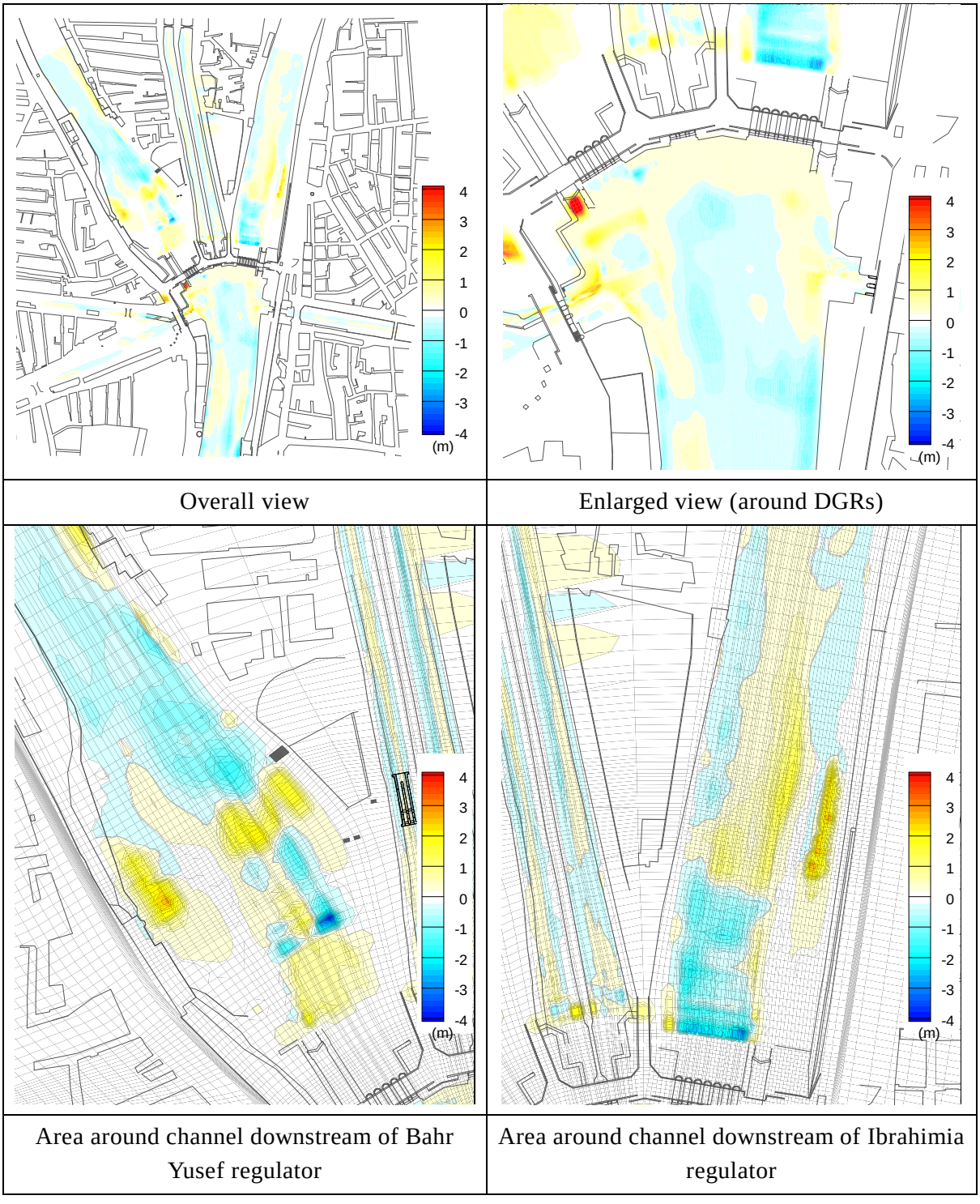

Overall view	Enlarged view (around DGRs)
Area around channel downstream of Bahr Yusef regulator	Area around channel downstream of Ibrahimia regulator

Figure 2-2.57 Result of the riverbed variation analysis (present state)

3) Planning

Similar to the previous calculations under present conditions, planned riverbed variation was calculated using the given average discharges for one year. Figure 2-2.58 shows the riverbed variations at the end of the computation. In the area around the diversion channels of the existing regulators, there is significant deposition in front of and at the side of the Abo Gabal regulator and on the side of the Ibrahimia canal. There is slight deposition in front of the new Ibrahimia regulator and relatively extensive erosion on the downstream of the new regulator. Relatively extensive erosion can be confirmed downstream of the new Bahr Yusef regulator. The Abo Gabal and Sahelyia regulators jut out along the canal banks where there are less slow-flowing areas. As a result, there is less deposition in front of and at the side of these regulators compared with the prediction results for the existing canals.

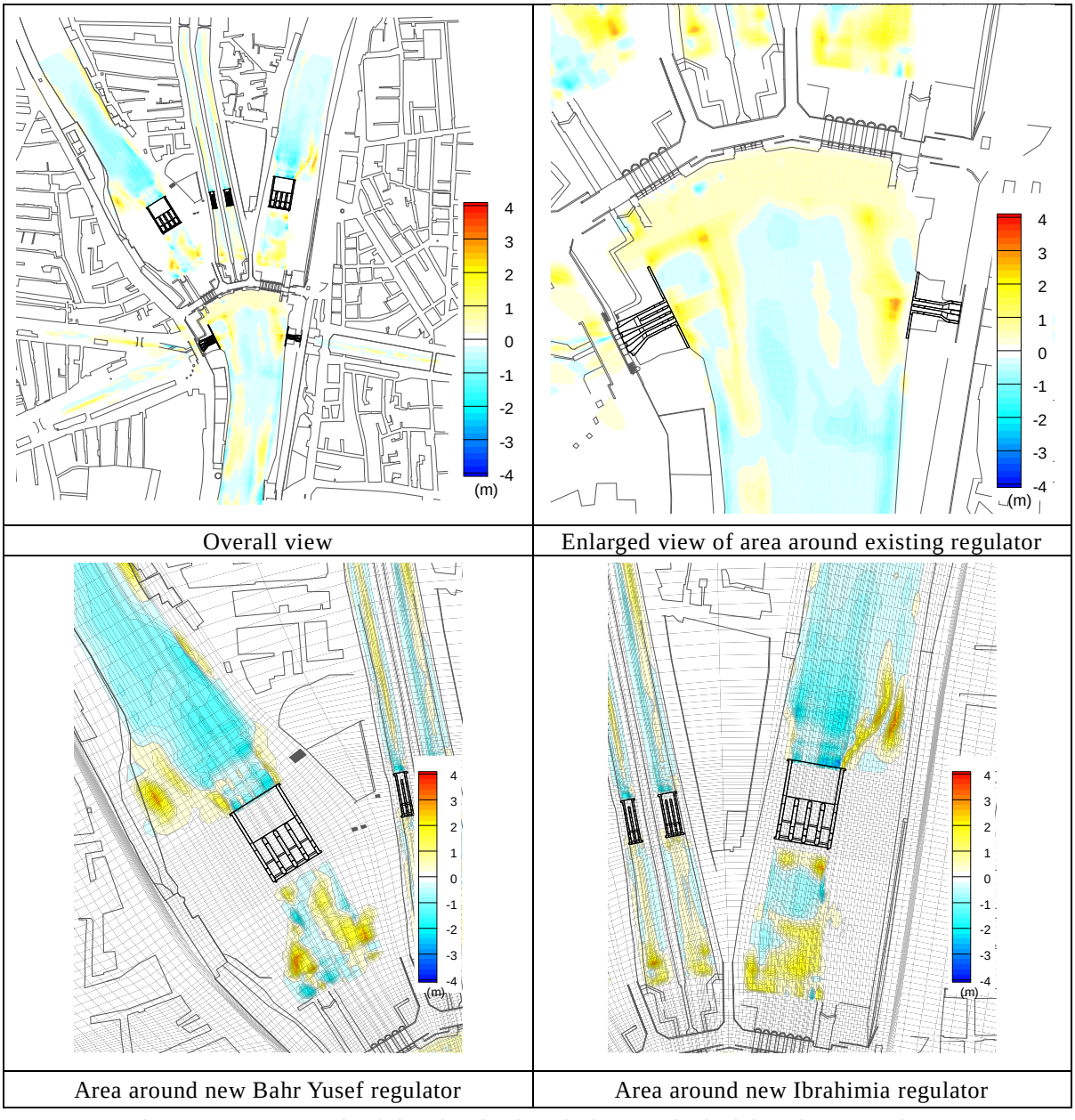

Overall view | Enlarged view of area around existing regulator

Area around new Bahr Yusef regulator | Area around new Ibrahimia regulator

Figure 2-2.58 Result of the riverbed variation analysis (planning stage)

b) Evaluation

From the analysis of riverbed variation, the following statements can be made.

1) New Bahr Yusef regulator

There is the possibility of local scouring directly downstream of the new Bahr Yusef regulator.

2) New Ibrahimia regulator

There is the possibility of local scouring directly downstream, as well as slight deposition directly upstream of the new Ibrahimia regulator.

3) New Abo Gabal regulator and new Sahelyia regulator

Regardless of the existence of the new regulators, there is a possibility of deposition occurring on the left bank side upstream of the existing Abo Gabal regulator, in the upper reaches of the Ibrahimia canal, and in front of the Sahelyia regulator. However, the new Abo Gabal and Sahelyia regulators jut out the existing canal banks, which is reducing the slow-flowing area on upstream area of the existing regulators and the amount of deposition in front of the new small regulators compared with the present conditions. From this, it is assumed that there is less impact on intake.

Interpretation on the riverbed change in front of the central part of DGRs at calibration stage

Figure 2-2.54 titled "Result of the riverbed variation analysis (calibration stage)," takes the data surveyed between November 2015 and January 2016 as the reference data of the calibration, which indicates that more sedimentation occurs than previously considered.

The captioned area is supposed to display reverse sedimentation/erosion. The natural assumption was that the sedimentation in the area was the result of natural deposition that occurred from November 2015 to January 2016. The calculation results at the calibration stage also showed sedimentation patterns in the area, even though its extent was different. This means that actual survey results and calculated results are generally matched.

This reverse phenomenon was observed because most of the excavation work was carried out during the survey period (the beginning of January 2016), when there was no data collected on the excavated area. This problem made the evaluation much harder because the reason for the change in bed level remained unknown. Therefore, no evaluation of bed transport can be made in the design of NDGRs.

However, a model has been constructed that can show future trends in bed level changes. This model was built based on all the available data during the project period, even without data on actual sediment discharge volume, and actual particle size distribution.

In the future, to improve the accuracy of the model, more detailed topographical data and time series data of flow discharge, water level, and the operating state of each canal regulator are required.